

THE UNIVERSITY OF CALGARY

**Low Complexity Code Shift Keying
Over The Wireless Channel**

by

Mable Man Chee Chow

A THESIS

**SUBMITTED TO THE FACULTY OF GRADUATE STUDIES
IN PARTIAL FULFILLMENT OF THE REQUIREMENTS FOR THE
DEGREE OF MASTER OF SCIENCE**

**DEPARTMENT OF ELECTRICAL AND
COMPUTER ENGINEERING**

CALGARY, ALBERTA

DECEMBER, 1998

© Mable Man Chee Chow 1998



National Library
of Canada

Acquisitions and
Bibliographic Services

395 Wellington Street
Ottawa ON K1A 0N4
Canada

Bibliothèque nationale
du Canada

Acquisitions et
services bibliographiques

395, rue Wellington
Ottawa ON K1A 0N4
Canada

Your file Votre référence

Our file Notre référence

The author has granted a non-exclusive licence allowing the National Library of Canada to reproduce, loan, distribute or sell copies of this thesis in microform, paper or electronic formats.

The author retains ownership of the copyright in this thesis. Neither the thesis nor substantial extracts from it may be printed or otherwise reproduced without the author's permission.

L'auteur a accordé une licence non exclusive permettant à la Bibliothèque nationale du Canada de reproduire, prêter, distribuer ou vendre des copies de cette thèse sous la forme de microfiche/film, de reproduction sur papier ou sur format électronique.

L'auteur conserve la propriété du droit d'auteur qui protège cette thèse. Ni la thèse ni des extraits substantiels de celle-ci ne doivent être imprimés ou autrement reproduits sans son autorisation.

0-612-38623-6

Abstract

A new Code Shift Keying (CSK) system which belongs to the class of Spread Spectrum (SS) signals is investigated. The conventional Direct Sequence Spread Spectrum (DSSS) system uses only one PN sequence for spreading the data signal while the CSK system chooses one out of M possible PN sequences for spreading. Hence, the CSK system increases the system throughput over the DSSS system.

The classical CSK system requires M correlators in the receiver while this low complexity CSK system requires only one correlator. This is achieved through the design of proper spreading codes such as the TRLabs codes. However, there is a trade off between receiver complexity and system performance.

The performance of the low complexity CSK system over the wireless channel is also examined. Three techniques are considered to improve system performance over the multipath channel. They are the DFE, the RAKE receiver and the Viterbi Algorithm.

Acknowledgments

I would like to express my sincere thanks to Dr. M. Fattouche for his guidance, support, understanding and proofreading of this thesis. I would also thank Dr. A. Sesay for his guidance and support.

I would like to thank The University of Calgary, Telecommunications Research Laboratories, and the Natural Sciences and Engineering Research Council of Canada for providing financial support as well as a comfortable working environment.

Most of all, I would like to thank my parents, my sister and brother for the support and caring they have given me throughout my life.

Table of Contents

Approval Page	ii
Abstract.....	iii
Acknowledgments	iv
Table of Contents	v
List of Tables	viii
List of Figures	ix
List of Symbols and Abbreviations.....	xiv
Chapter 1 Introduction to Code Shift Keying (CSK)	1
1.1 Introduction to Wireless Communication Systems.....	1
1.2 Why use Spread Spectrum (SS) ?	1
1.3 What is Spread Spectrum ?.....	2
1.4 Direct-Sequence Spread Spectrum (DSSS).....	5
1.5 What is Code-Shift-Keying (CSK)?.....	9
Chapter 2 Conventional and Low Complexity CSK System	11
2.1 A Conventional CSK System	11
2.2 Reasons for a CSK System with Low Receiver Complexity	13
2.3 Requirements of the CSK System with Low Receiver Complexity	14
2.4 Outline of the Thesis	16
Chapter 3 Benchmark Models: DSSS, Conventional CSK and Low Complexity CSK Systems	17
3.1 $\pi/4$ DQPSK Modulation Scheme	17
3.2 DSSS System using Barker Code.....	19
3.3 A CSK System using the Barker Code (Conventional CSK)	22
3.4 A CSK System using the Wi-LAN Codes (Low Complexity CSK)	26
3.5 Summary of SS Systems	33

Chapter 4	Increase the Bit Rate using CSK	34
4.1	Increase the Number of PN Sequences in a Set.....	34
4.1.1	A CSK System using $M = 16$ Wi-LAN Codes with 8-DPSK	35
4.1.2	A CSK System using $M = 16$ Wi-LAN Codes with 8-QAM	42
4.2	Introduction to TRLabs Codes (Low Complexity CSK)	52
Chapter 5	Improve the BER Performance of CSK System Over an AWGN Channel	62
5.1	Use Longer PN Sequences (Increase Processing Gain)	62
5.1.1	Barker Code with 7 Chips	63
5.1.2	Barker Code with 11 Chips	67
Chapter 6	CSK System Over Multipath Channel.....	70
6.1	Multipath Channel Model	70
6.2	DSSS System using Barker Code.....	71
6.3	CSK System using Wi-LAN Codes	73
6.3.1	$M = 2$ Wi-LAN Codes	73
6.3.2	$M = 16$ Wi-LAN Codes	75
6.4	CSK System using TRLabs Codes.....	77
Chapter 7	Improve the Performance of a CSK System Over the Multipath Channel using Different Algorithms in the Receiver	80
7.1	Decision-Feedback-Equalizer (DFE)	80
7.1.1	Background.....	80
7.1.2	Simulations and Results.....	82
7.2	RAKE Receiver	90
7.2.1	Background.....	90
7.2.2	Simulations and Results.....	92
7.3	Viterbi Algorithm (VA)	100
7.3.1	Background.....	100
7.3.2	Simulations and Results.....	102

Chapter 8 Conclusion and Future Work 105

8.1 Conclusion..... 105

8.2 Future Work..... 107

References 108

Appendix A TRILabs Codes Generation and C Programs

List of Tables

Table 3.5-1	Summary of bit rate and receiver complexity of the SS systems (I)	33
Table 4.1.1-7	Summary of bit rate and receiver complexity of the SS systems (II)	41
Table 4.2-7	Summary of bit rate and receiver complexity of the SS systems (III) ...	60
Table 5.1-1	Barker Synchronization Codewords	63
Table 5.1.2-4	Summary of bit rate and improvement in SNR for different N chip Wi-LAN/CSK systems	69

List of Figures

Fig 1.3-1	The model of a spread spectrum digital communication system	3
Fig 1.4-1	The PN sequence and data signal of a DSSS system	5
Fig 1.4-2	The transmitter of a DSSS system.....	6
Fig 1.4-3	The power spectrum of data signal (a) before and (b) after spreading.....	7
Fig 1.4-4	The receiver of a DSSS system	7
Fig 1.4-5	The power spectrum of the despreaded data signal	8
Fig 2.1-1	The transmitter of a conventional CSK system.....	11
Fig 2.1-2	The receiver of a conventional CSK system	12
Fig 3.1-1	The signal constellations showing differential phases of DQPSK.....	18
Fig 3.2-1	The auto-correlation of the 11 chip Barker Code	19
Fig 3.2-2	The transmitter of a DSSS system using the Barker Code	20
Fig 3.2-3	The receiver of a DSSS system using the Barker Code	20
Fig 3.2-4	The BER for the Barker/DSSS system over an AWGN channel	21
Fig 3.2-5	The cross-correlation of the two 11 chip Barker Codes	23
Fig 3.2-6	The transmitter of a CSK system using two Barker Codes	23
Fig 3.2-7	The receiver of a CSK system using two Barker Codes	24
Fig 3.2-8	The BER for the Barker/DSSS and the Barker/CSK systems over an AWGN channel	25
Fig 3.4-1	The auto-correlation of the 10 chip Wi-LAN Code	26
Fig 3.4-2	The cross-correlation of the two 10 chip Wi-LAN Codes	27

Fig 3.4-3	The relationship between data bits and the Wi-LAN/CSK symbols ($M = 2$)	28
Fig 3.4-4	The transmitter of a CSK system using the Wi-LAN Codes	28
Fig 3.4-5	The receiver of a CSK system using the Wi-LAN Codes	29
Fig 3.4-6	The BER for the Barker/DSSS, the Barker/CSK and the Wi-LAN/CSK systems over an AWGN channel	31
Fig 4.1.1-1	The relationship between data bits and the Wi-LAN/CSK symbols ($M = 16$)	35
Fig 4.1.1-2	The 8-DPSK signal constellations.....	35
Fig 4.1.1-3	The transmitter of a CSK system using the $M = 16$ Wi-LAN Codes.....	37
Fig 4.1.1-4	The receiver of a CSK system using the $M = 16$ Wi-LAN Codes	38
Fig 4.1.1-5	The BER for the Barker/DSSS, the Barker/CSK, the $M=2$ Wi-LAN/CSK and the $M=16$ Wi-LAN/CSK systems over an AWGN channel.....	40
Fig 4.1.1-6	The signal constellations of DQPSK and 8-DPSK	41
Fig 4.1.2-1	The four possible signal constellations for 8-QAM	42
Fig 4.1.2-2	The signal constellation and demodulator for signal set (a).....	45
Fig 4.1.2-3	The signal constellation and demodulator for signal set (b)	45
Fig 4.1.2-4	The demodulators for signal set (c)	46
Fig 4.1.2-5	The demodulators for signal set (d).....	46
Fig 4.1.2-6	The BER for the 8-PSK, 8-DPSK and 8-QAM over an AWGN channel	47
Fig 4.1.2-7	The BER for the $M = 16$ Wi-LAN/CSK systems with 8-DPSK and 8-QAM over an AWGN channel	49
Fig 4.1.2-8	The BER for the $M = 16$ Wi-LAN/CSK system with 8-QAM signal set (c) over an AWGN channel	49

Fig 4.1.2-9	The BER for the $M = 16$ Wi-LAN/CSK system with 8-QAM signal set(d) over an AWGN channel.....	51
Fig 4.1.2-10	The BER for the Barker/DSSS, the $M = 16$ Wi-LAN/CSK with QAM and 8-DPSK over an AWGN channel	51
Fig 4.2-1	The relationship between data bits and the TRLabs/CSK symbols ($M = 4$)	53
Fig 4.2-2	The auto-correlations of the $M = 4$ TRLabs Codes	55
Fig 4.2-3	The cross-correlations of the $M = 4$ TRLabs Codes	56
Fig 4.2-4	The transmitter of a CSK system using the $M = 4$ TRLabs Codes	57
Fig 4.2-5	The receiver of a CSK system using the $M = 4$ TRLabs Codes	58
Fig 4.2-6	The BER for the Barker/DSSS, the Barker/CSK, the Wi-LAN/CSK and the TRLabs/CSK systems over an AWGN channel	60
Fig 5.1.1-1	The auto-correlation of the 14 chip Wi-LAN Code	64
Fig 5.1.1-2	The cross-correlation of the two 14 chip Wi-LAN Codes	64
Fig 5.1.2-1	The auto-correlation of the 22 chip Wi-LAN Code	67
Fig 5.1.2-2	The cross-correlation of the 22 chip Wi-LAN Codes	68
Fig 6.1-1	The multipath model	71
Fig 6.1-2	The BER for the Barker/DSSS over the multipath channel	72
Fig 6.3.1-1	The BER for the $M = 2$ Wi-LAN/CSK over the multipath channel.....	74
Fig 6.3.2-1	The BER for the $M = 16$ Wi-LAN/CSK over the multipath channel.....	76
Fig 6.4-1	The BER for the TRLabs/CSK over the multipath channel (1 and 2 chips delay)	77
Fig 6.4-2	The BER for the TRLabs/CSK over the multipath channel (3 to 5 chips delay)	78

Fig 7.1.1-1	The structure of a Decision-Feedback Equalizer (DFE)	82
Fig 7.1.2-1	The BER for the Barker/DSSS using DFE over the multipath channel	83
Fig 7.1.2-2	The BER for the $M = 2$ Wi-LAN/CSK using DFE over the multipath channel	84
Fig 7.1.2-3	The BER for the $M = 16$ Wi-LAN/CSK using DFE over the multipath channel	85
Fig 7.1.2-4	The BER for the TRLabs/CSK using DFE over the multipath channel (1 chip)	86
Fig 7.1.2-5	The BER for the TRLabs/CSK using DFE over the multipath channel (2 chips)	87
Fig 7.1.2-6	The BER for the TRLabs/CSK using DFE over the multipath channel (3 chips)	88
Fig 7.1.2-7	The BER for the TRLabs/CSK using DFE over the multipath channel (4 chips)	88
Fig 7.1.2-8	The BER for the TRLabs/CSK using DFE over the multipath channel (5 chips)	89
Fig 7.2.1-1	A RAKE demodulator for DPSK signals	91
Fig 7.2.2-1	The BER for the Barker/DSSS using a RAKE receiver over the multipath channel	94
Fig 7.2.2-2	The BER for the $M=2$ Wi-LAN/CSK using a RAKE receiver over the multipath channel	94
Fig 7.2.2-3	The BER for the TRLabs/CSK with a RAKE receiver over the multipath channel (1 chip, phase 0)	96
Fig 7.2.2-4	The BER for the TRLabs/CSK with a RAKE receiver over the multipath channel (1 chip, phase 180)	96
Fig 7.2.2-5	The BER for the TRLabs/CSK with a RAKE receiver over the multipath channel (2 chips)	97

Fig 7.2.2-6	The BER for the TRLabs/CSK with a RAKE receiver over the multipath channel (3 chips)	97
Fig 7.2.2-7	The BER for the TRLabs/CSK with a RAKE receiver over the multipath channel (4 chips)	98
Fig 7.2.2-8	The BER for the TRLabs/CSK with a RAKE receiver over the multipath channel (5 chips)	99
Fig 7.3.1-1	One stage of trellis diagram for a $M = 4$ symbol alphabet signal	100
Fig 7.3.2-1	The BER for the Barker/DSSS system over an AWGN channel and the multipath channel ($\pi/4$ QPSK, coherent detection)	102
Fig 7.3.2-2	The BER for the Barker/DSSS using VA over the multipath channel	103
Fig 7.3.2-3	The BER for the $M = 2$ Wi-LAN/CSK using VA over the multipath channel	104

List of Symbols and Abbreviations

Symbols

$\sigma, \theta, \phi, \xi$	phases
$\hat{\sigma}, \hat{\theta}, \hat{\phi}, \hat{\xi}$	estimated phases
ρ	partial correlation
ξ_b	signal energy per bit
ξ_k	kth DQPSK symbol
γ_b	signal to noise ratio per bit
$ae^{j\theta}$	complex gain of the multipath component
(a_{re}, a_{im})	coordinate of a signal point on the complex plane
B_e	bandwidth expansion factor
C	spreading code
c_n	tap gains for the FFF of a DFE
D	normalized minimum distance between pair of signal points
d_k	detected signal of a DFE
d_{min}	minimum distance between pair of signal points
F_i	tap gains for the FBF of a DFE
j	imaginary part of a complex signal
J_{av}	average jamming power
J_o	power spectral density of a jamming signal
K	stage in the trellis
L	number of multipath components
L_c	processing gain
M	number of spreading code

N	length of a spreading code
$P(t)$	repetition code
P_e	probability of error
P_{av}	average signal power
R	bit rate
$R_{ij}(k)$	cross-correlation value
$S(t)$	signal waveform
S_k	CSK symbol
S_r^2	received signal power
T_b	symbol duration
T_c	chip duration
T_{ex}	Excess Delay in time
W	channel bandwidth
y_n	inputs for the FFF of a DFE
$Z(t)$	interference

Abbreviations

AWGN	Additive White Gaussian Noise
BER	Bit Error Rate
BPSK	Binary Phase Shift Keying
CD	Coherent Detection
CDMA	Code Division Multiple Access
CSK	Code Shift Keying
$\pi/4$ DQPSK	$\pi/4$ Differential Quadrature Phase Shift Keying
8-DPSK	8 - Differential Phase Shift Keying
DD	Differential Detection
DFE	Decision Feedback Equalizer
DSP	Digital Signal Processing
DSSS	Direct Sequence Spread Spectrum
FBF	Feedback Filter
FCC	Federal Communications Commission
FFF	Feedforward Filter
FH	Frequency Hopping
FPGA	Field Programmable Gate Array
FSK	Frequency Shift Keying
ICI	Interchip Interference
IM	Intermodulation
ISI	Intersymbol Interference
LOS	Line of Sight
LPI	Low Probability of Intercept

MLSE	Maximum Likelihood Sequence Estimation
PN	Pseudo-noise
PSK	Phase Shift Keying
QAM	Quadrature Amplitude Modulation
SJR	Signal to Jamming Ratio
SNR	Signal to Noise Ratio
SS	Spread Spectrum
VA	Viterbi Algorithm

Chapter 1

Introduction to Code Shift Keying (CSK)

1.1 Introduction to Wireless Communication Systems

In wireless communication systems, the transmission channel is always changing from time to time, and from place to place with a number of users sharing the same wireless channel. Therefore, there are various kinds of interferences encountered over such a channel, such as jamming signals and interferences arising from other users over the same channel, as well as self-interference due to multipath. In this thesis, we investigate Code Shift Keying (CSK) which belongs to the class of Spread Spectrum signals. More specifically, we examine the performance of high bit rate CSK over the wireless channel using low complexity receiver.

1.2 Why use Spread Spectrum (SS) ?

Spread Spectrum (SS) signals are used in digital communications because of their ability in interference rejection. The unique characteristic of a SS signal is that its bandwidth is much greater than the minimum bandwidth necessary to send its information. This can be achieved by spreading the signal with coding. A large redundancy in coding can overcome the severe levels of interference due to jamming and multipath propagation.

Moreover, SS signals are transmitted at low power so they can be hidden in the background noise. Because of their low power level, it is sometimes difficult for an unintended listener to detect the SS signals. Thus, SS signals are also called low-probability-of-intercept (LPI) signals.

SS signals have another important application in multiple-access communication systems. In such systems, a number of users share a common channel bandwidth while being able to transmit information simultaneously to their corresponding receivers. SS signals make use of the pseudo-random pattern in their spreading codes, so that each transmitter has its own unique spreading code and transmitted signals can be distinguished from one another in this common spectrum. Thus, a particular receiver can recover a given transmitter's information by knowing the spreading code used by the corresponding transmitter. This type of communication technique is called code division multiple access (CDMA). CDMA is not considered in this research thesis.

1.3 What is Spread Spectrum ?

As previously mentioned, SS signals are characterized by their bandwidth which is in excess of the minimum necessary to transmit its information. Therefore, the bandwidth expansion factor for a SS signal is much greater than unity. This is achieved by spreading each symbol of the signal with a pseudo-random or pseudo-noise (PN) pattern known as a PN sequence or spreading code. The spreading code is independent of the transmitting data.

The block diagram shown in Fig 1.3-1 illustrates the basic elements of a SS digital communication system. The system is divided into three parts: transmitter, channel and receiver.

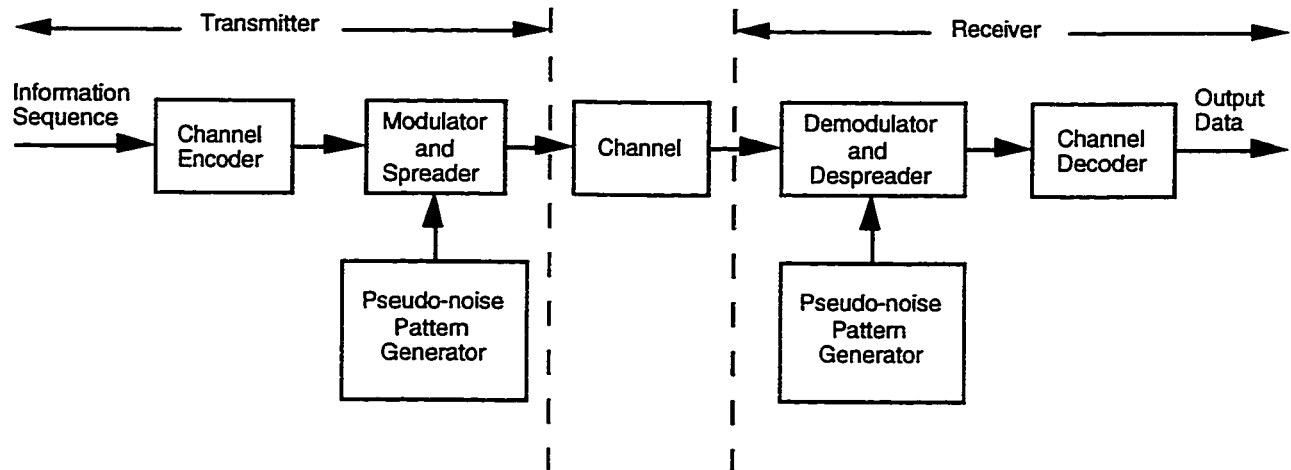


Fig 1.3-1 The model of a spread spectrum digital communication system

At the transmitter, a binary information sequence is encoded and modulated before being passed through the channel. There is an additional element in the system, the pseudo-noise (PN) pattern generator which interfaces with the modulator at the transmitting end. The spreading of a SS signal is simply done by multiplying the PN sequence with the transmitted signal at the modulator.

Two types of channels have been considered in this thesis: they are the Additive White Gaussian Noise Channel (AWGN) and the multipath channel. Computer simulations are used to investigate the performances of the SS signals over these two channels. The AWGN and multipath channels are discussed in detail in later chapters. Note that all computer simulations are done at baseband.

Finally, the receiver contains a demodulator and a channel decoder. Again, a binary sequence is the output of the system. A pseudo-noise (PN) pattern generator interfaces with the demodulator at the receiving end. The PN pattern generator in the transmitter and the one in the receiver must be identical. Otherwise, the desired transmitted signal may not be detected in the receiver.

Synchronization of the PN sequence at the receiver with the PN sequence in the incoming received signal is required in order to despread the received signal. Usually, prior to the transmission of information, synchronization is achieved by transmitting a fixed PN sequence that the receiver will recognize in the presence of interference with a high probability [1]. This PN sequence is also known as a training sequence. Throughout this thesis, synchronization of the PN sequences are always assumed. Moreover, it is assumed that the first incoming received signal in a multipath channel is the strongest received signal.

Two types of SS signals are commonly used in practice. They are the Frequency-Hopping (FH) spread spectrum signals and the Direct-Sequence spread spectrum (DSSS) signals. In a FHSS system, the available channel bandwidth is subdivided into a large number of contiguous frequency slots. The pseudo-random sequence generated from a PN generator selects one or more frequency slots for signal transmission within a signaling interval. This research thesis focuses on DSSS only which is discussed in detail in the next section.

1.4 Direct-Sequence Spread Spectrum (DSSS)

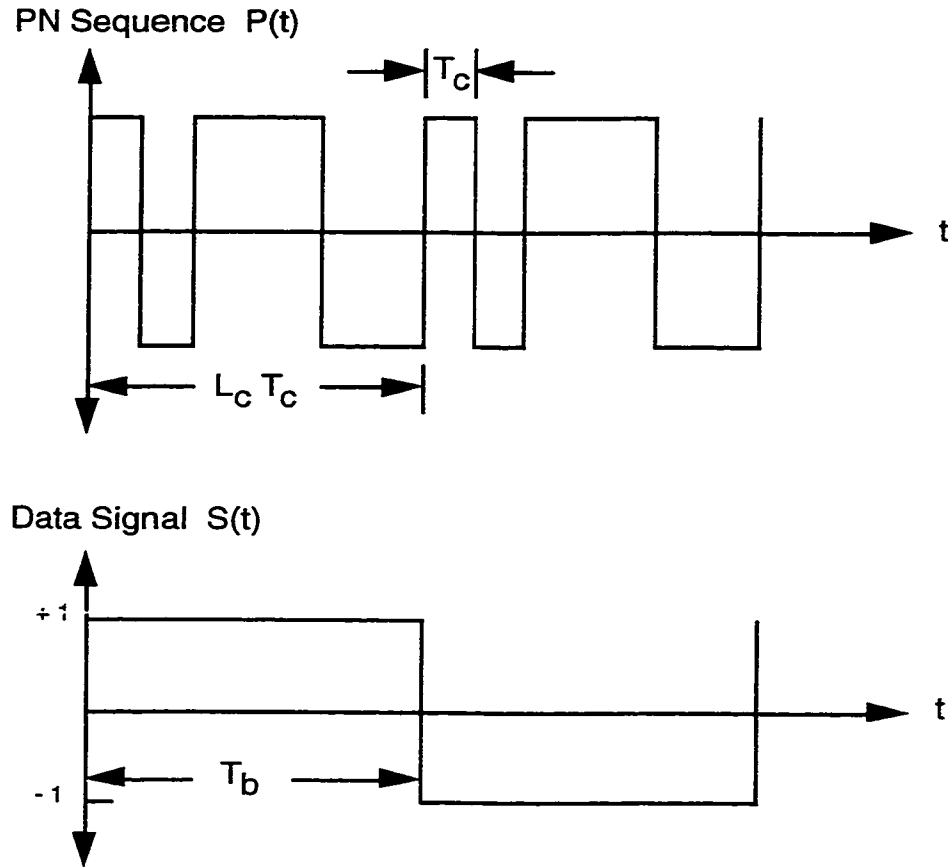


Fig 1.4-1 The PN sequence and data signal of a DSSS system

The data signal has a bit rate at the input to the encoder of R bit/s and the available channel bandwidth is W Hz. The reciprocal of W , denoted by T_c , defines the duration of a rectangular pulse, which is called a chip. A chip is the basic element in a DSSS signal. The reciprocal of R , denoted by T_b , defines the rectangular pulse duration of a data signal. Fig 1.4-1 illustrates the relationships between the PN sequence and the data signal. Thus, we have a bandwidth expansion factor, Be , of W / R , which may also be expressed as

$$Be = \frac{W}{R} = \frac{T_b}{T_c} = L_c \quad (1.1)$$

This ratio L_c denotes the number of chips per information bit and is also known as the processing gain of the DSSS system. It represents the advantage gained over the jammer that is obtained by expanding the bandwidth of the transmitted signal. The larger the processing gain, the better the performance in the presence of the jammer.

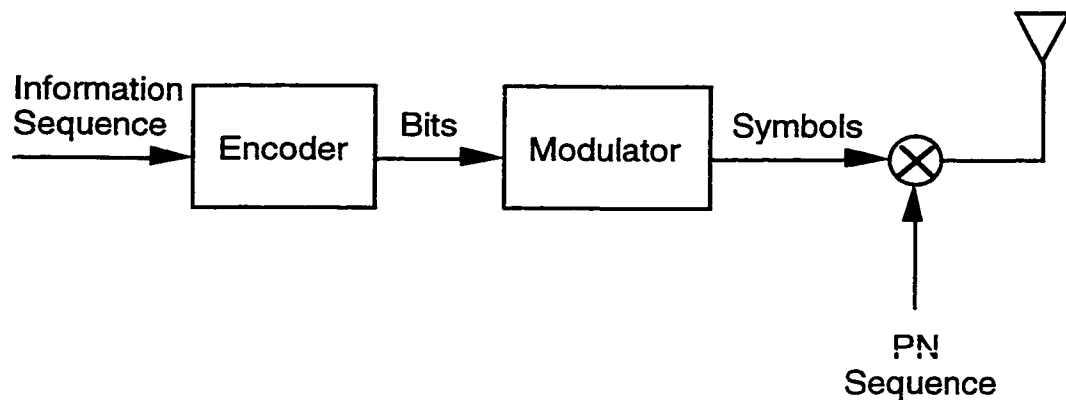


Fig 1.4-2 The transmitter of a DSSS system

Fig 1.4-2 shows the transmitter of a DSSS system. The information sequence is encoded into the data sequence, which is then modulated with both PN sequence and conventional modulation schemes such as Phase-Shift-Keying (PSK) or Frequency-Shift-Keying (FSK). All encoders in the thesis use repetition codes. Fig 1.4-1 illustrates the signal waveform $S(t)$ corresponding to the information bits [0 1] as well as the repetition code $P(t)$. The resulting modulated signal $P(t)S(t)$ is a DSSS signal. The spreading process consists simply of multiplying the data signal $S(t)$ with the PN sequence $P(t)$ in the time domain, that is, spreading the data signal's bandwidth in the frequency domain. All data signals use the same PN sequence for spreading.

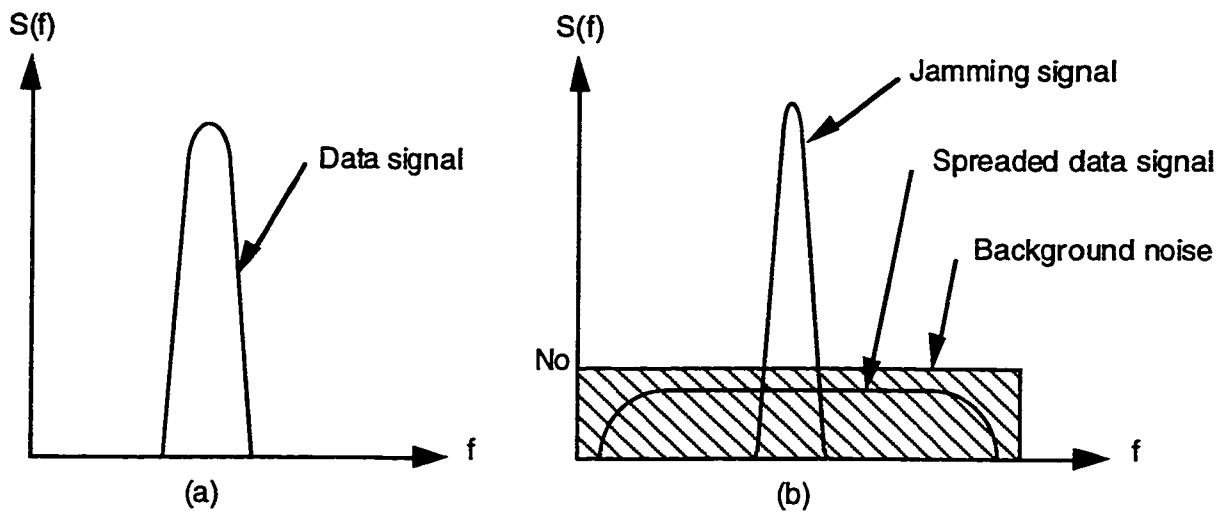


Fig 1.4-3 The power spectrum of data signal (a) before and (b) after spreading

The spreading process of a DSSS system is shown in Fig 1.4-3. The power spectrum of the original data signal is shown in Fig 1.4-3 (a). It can be seen that the data signal is a narrowband signal. Moreover, the power spectrum of the data signal after spreading is shown in Fig 1.4-3 (b). The narrowband jamming signal and the background noise present in the communication channel are also shown in this figure. The SS signal power is reduced due to spreading, and so, it is clear that the SS signal is hidden in the background noise. The jamming signal is present only over a short portion of the entire bandwidth.

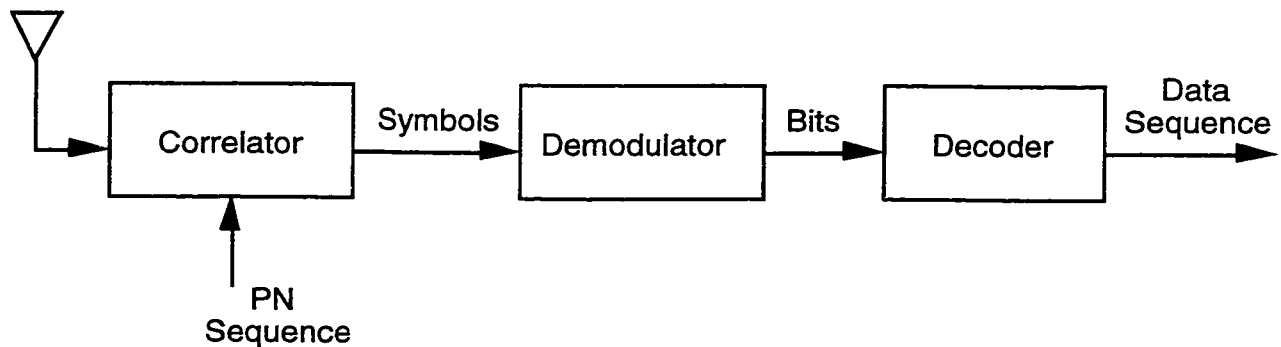


Fig 1.4-4 The receiver of a DSSS system

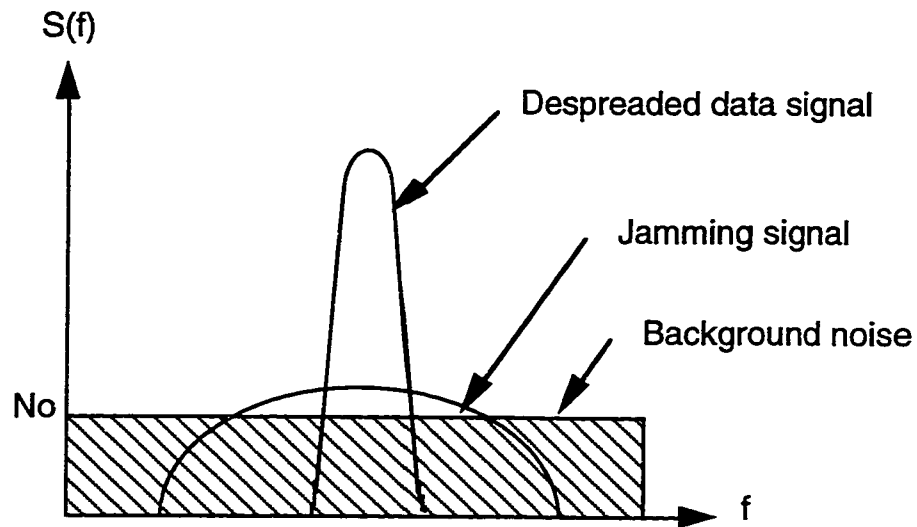


Fig 1.4-5 The power spectrum of the despreaded data signal

At the receiver, the received signal is despread before demodulation using the same PN sequence used in the transmitter. The despreading process for the repetition code is carried out using a correlator. The correlator contains an integrator having an integration interval of a bit interval, T_b . The block diagram of the receiver is shown in Fig 1.4-4. The despreading process aims at removing the pseudo-noise (PN) pattern from the received signal. The despreaded signal is shown in Fig 1.4-5. As a result, the received wideband signal becomes a high-energy narrowband signal again. This narrowband signal is then demodulated to retrieve its information. It is noted that only one correlator is needed in the receiver because there is only one PN sequence ever used in the transmitter.

The effect of the despreading process on the interference $Z(t)$ of the channel can be explained as follows. The multiplication of $Z(t)$ by the PN sequence $P(t)$ in the time domain, is simply the convolution of the two corresponding spectra in the frequency domain. The effect of convolving the two spectra is to spread the power of $Z(t)$ in bandwidth. Since the bandwidth of $P(t)$ occupies the available channel bandwidth W , the

result of the convolution of the two spectra is to spread the power spectral density of $Z(t)$ over the frequency band of width W . The integrator used in the correlator has a bandwidth of $1/T_b$. Since $1/T_b \ll W$, only a fraction of the total interference power appears at the output of the correlator. This fraction is equal to the ratio of bandwidth $1/T_b$ to W .

That is:

$$\frac{1/T_b}{W} = \frac{T_c}{T_b} = \frac{1}{L_c} \quad (1.2)$$

In other words, the multiplication of the interference with the PN sequence $P(t)$ spreads the interference to the signal bandwidth W , and the narrowband integration of the correlator sees only a fraction $1/L_c$ of the total interference. Thus, the performance of the DSSS system using a repetition code is enhanced by the processing gain L_c . The repetition code is used for coding throughout the thesis.

1.5 What is Code-Shift-Keying (CSK) ?

Code Shift Keying is not a new research topic. It has been suggested for several communication systems such as in the reverse link in IS-95, the North American CDMA Digital Cellular standard developed by Qualcomm Inc. [2], whereby the transmitter in the portable selects one out of 64 Walsh codes to spread the BPSK information symbol.

In contrast to a DSSS system (with a repetition code) which uses only one PN sequence for spreading the data signal, a CSK system chooses one out of M possible PN sequences from a pre-selected set for spreading the data signal. The selection of the PN

sequence is dependent on the binary information data. One or more bits of information data are used to select the PN sequence for spreading at the transmitter. Thus, in addition to the modulated bits, one or more bits are transmitted over to the receiver through the selection of the spreading code. In this way, CSK can increase the bit rate of a system over the DSSS system.

Chapter 2

Conventional and Low Complexity CSK System

In this chapter, a conventional CSK system is discussed in detail in Section 2.1. It is necessary to have a low complexity CSK receiver for reasons discussed in Section 2.2. The requirements for such a low complexity CSK receiver are included in Section 2.3. Finally, the outline of the thesis is in Section 2.4.

2.1 A Conventional CSK System

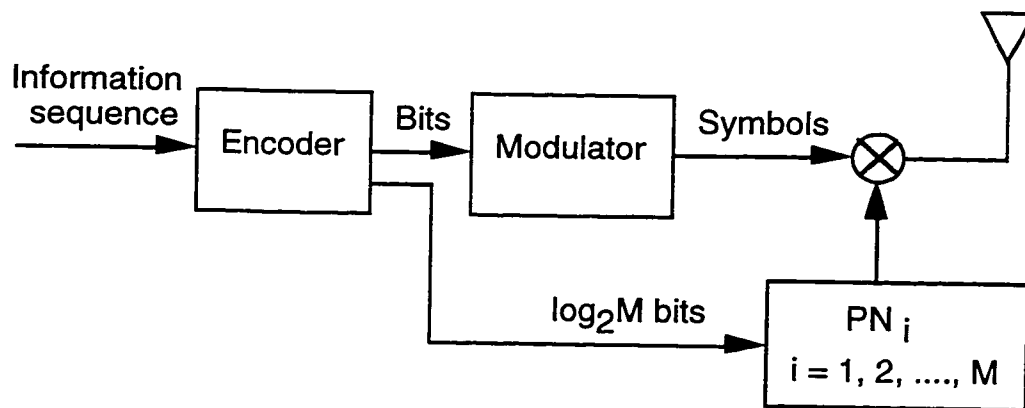


Fig 2.1-1 The transmitter of a conventional CSK system

In the transmitter of a conventional CSK system, certain bits of data are used to choose one out of M possible PN sequences as the spreading code. The block diagram of a transmitter for a conventional CSK system is shown in Fig 2.1-1. The encoded sequence is

then modulated and spread before passing through the channel. The M possible PN sequences must be known in both transmitter and receiver before the transmission of data over the wireless communication channel.

At the receiver, the despreading process requires M matched filters or correlators to recover the transmitted signal. The block diagram of a receiver for a conventional CSK system is shown in Fig 2.1-2. The M correlation outputs will be compared, and the one with largest magnitude will be demodulated and decoded to recover the information data.

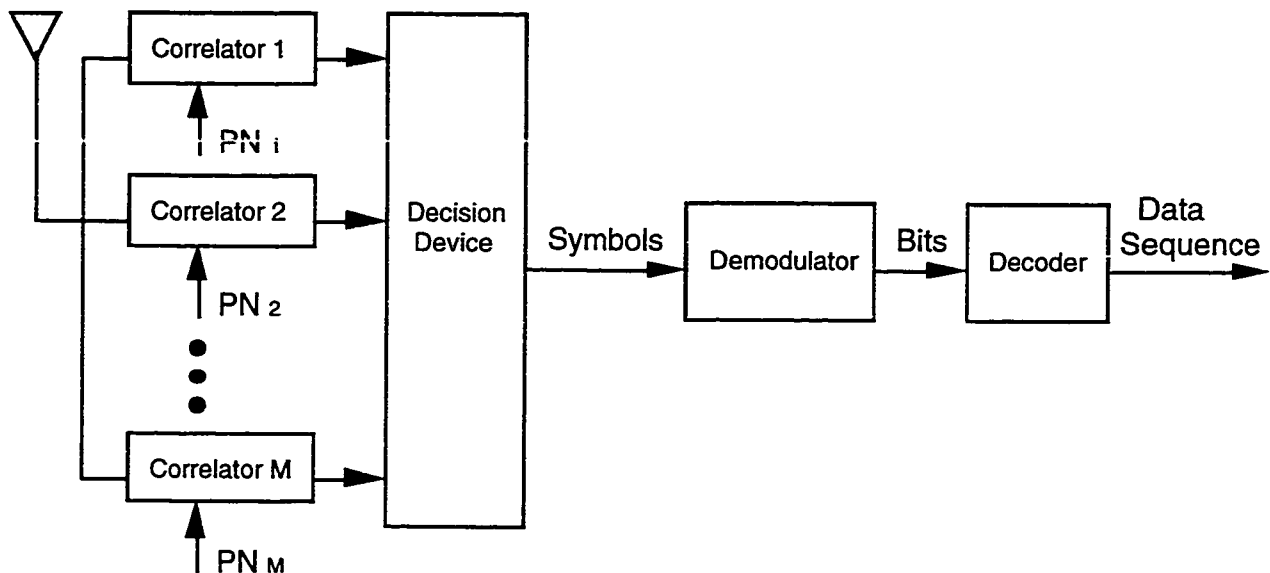


Fig 2.1-2 The receiver of a conventional CSK system

Since the particular PN sequence used for spreading in the transmitter is detected as the one producing the largest correlation output, the bits used for the PN sequence selection can be recovered. In this way, CSK can transmit extra bits over a fixed bandwidth. Thus, it can increase the bit rate of a conventional DSSS system. However, CSK requires M correlators in the receiver. This is an M -fold increase in receiver complexity over conventional DSSS.

2.2 Reasons for a CSK System with Low Receiver Complexity

Any communication system focuses on three main design factors: they are signal power, channel bandwidth and system complexity. Signal power is dependent on the modulation scheme used in the transmitter. The transmitted signal power is normalized to one throughout the thesis for both DSSS and CSK systems. Thus, the performances of the two systems can be compared easily.

Moreover, without loss of generality the channel bandwidth throughout this thesis is chosen as 8Mchips/s. This particular bandwidth is used in Wi-LAN's Hopper+ system, which in turn, will be used as the benchmark model in this thesis. Wi-LAN's Hopper+ is a DSSS system which will be covered in chapter 3.

Finally, as it is stated in the previous section, DSSS requires only one correlator in the receiver while CSK requires M correlators.

Therefore, the aim of this thesis is to find a new CSK system which uses only one correlator in the receiver regardless of the number of possible PN sequences used. This can be achieved through the design of proper spreading codes for the CSK system. The details of the coding requirements are discussed in the next section.

2.3 Requirements of the CSK System with Low Receiver Complexity

The M possible PN sequences used for spreading should be chosen as distinct as possible. Ideally, this can be achieved by choosing them to be orthogonal. However, the orthogonality is often lost over the wireless communication channel. There are several reasons [3]:

- The non-linearities in the transceiver such as amplifiers and mixers, can introduce Intermodulation (IM) products.
- When the transmitting antenna and the receiving antenna are not in clear Line-Of-Sight (LOS), the channel is in multipath which introduces Interchip Interference (ICI) and also Intersymbol Interference (ISI).
- A single tone interferer interferes with the despread signal as it has often non-zero coordinates along the orthogonal codes.

A constant envelope SS signal can reduce the effect of non-linearities. For this reason, constant energy codes are used over non-linear channels. On the other hand, non-constant energy codes will be used over those channels which can tolerate some IM distortion. In the thesis, only constant energy codes will be considered.

The effect of multipath is to create a delayed version of the original SS signal. The amount of relative delay is measured using the excess delay T_{ex} which is a function of the separation between the transmitting antenna and the receiving antenna. The separation in the indoor wireless channel is typically below 100 m while in the outdoor channel it is above 100 m. The excess delay T_{ex} for the Non-LOS indoor channel ranges from 20 ns to 250 ns while for the LOS outdoor channel it ranges from 250 ns to up to 7 μ s.

The Hopper+ system uses an 11-chip Barker Code as the spreading code and Differential Quadrature Phase Shift Keying (DQPSK) as the modulation scheme. It has a bit rate of $(2/11) \text{ bits/chips} \times 8 \text{ Mchips/s} = 1.454 \text{ Mbps}$, where the chip rate is 8 Mchips/s, it transmits 11 chips/symbol, and 2 bits/symbol. It is robust against an excess delay of up to 11 chips with a 8 Mchips/s chip rate, that is $11 \text{ chips} / 8 \text{ Mchips/s} = 1.375 \mu\text{s}$. On the other hand, CSK is designed in this thesis to have a bit rate greater than 1.454 Mbps over a multipath channel with a T_{ex} of up to 500 ns. This choice of channel covers every indoor channel and a portion of the outdoor channels. It allows for a maximum ICI of 4 chips with 8 Mchips/s chip rate ($4 \text{ chips} / 8 \text{ Mchips/s} = 500 \text{ ns}$). For the outdoor channels, where T_{ex} is larger than 500 ns, either an equalizer or a RAKE receiver is required. An equalizer is needed when the ISI dominates the ICI, while a RAKE receiver is needed when the ICI dominates the ISI. Both equalization and RAKE reception are considered in the thesis, in addition to the Viterbi algorithm.

According to part-15 rules of the FCC, SS codes must have at least a 10 dB jamming margin in the presence of a single tone interferer [4]. The jamming margin is measured as:

$$\text{Jamming margin} = \text{SNR} - \text{SJR} \text{ dB}$$

where SNR is the Signal-to-Noise Ratio required to achieve a specific Bit Error Rate (BER) over an AWGN channel without interference while SJR is the Signal-to-Jamming Ratio required to achieve the same specific BER over a narrowband interference channel without noise.

In summary, the goal of this thesis is to find a new class of CSK codes which has a bit rate larger than 1.454 Mbps with a 8 Mchips/s chip rate, and is able to have a reduced complexity receiver with the same performance as DSSS over the AWGN channel. For the

multipath channel, the new class of CSK codes should have a comparable performance as DSSS with an equalizer, a RAKE receiver or a Viterbi algorithm implemented in the receiver. Synchronization of the PN sequences is assumed throughout the thesis.

2.4 Outline of the Thesis

In Chapter 3, the basic structures and performances of a DSSS system and a conventional CSK system are discussed. These two systems are used as benchmarks throughout the thesis. A class of low complexity CSK codes, referred to as the Wi-LAN codes, and their performances are also included in Chapter 3.

In Chapter 4, various coding methods and modulation schemes for further increasing the system bit rate are reviewed. This gives way to the discovery of a new class of CSK codes referred to as the TRLabs codes.

In Chapter 5, the method used to improve the BER performance of a CSK system over the AWGN channel is discussed. The simulation results are also included.

In Chapter 6, the performance of a DSSS system and a CSK system using different spreading codes are also investigated over the multipath channel.

In Chapter 7, three algorithms for improving the BER performance of a CSK system over the multipath channel are discussed. The three algorithms are the Decision Feedback Equalizer (DFE), the RAKE receiver and the Viterbi algorithm (VA). The BER performances of a CSK system using different receivers are plotted for comparison.

Finally, the conclusion and future work are discussed in Chapter 8.

Chapter 3

Benchmark Models: DSSS, Conventional CSK and Low Complexity CSK Systems

In this chapter, we first introduce $\pi/4$ DQPSK modulation as it is primarily used in all the SS systems considered in the thesis. Secondly, the basic structure and performance of a DSSS system is discussed in Section 3.2, while a conventional CSK system is discussed in Section 3.3 and a low receiver complexity CSK system is discussed in Section 3.4. The conventional DSSS and CSK systems are both used as benchmarks throughout the thesis. According to reference [3], a new class of CSK codes named the Wi-LAN Codes are capable of increasing the bit rate of conventional DSSS, reducing the receiver complexity of conventional CSK, and having the same performance as DSSS over the AWGN channel. This CSK system does not have either an equalizer or a RAKE receiver in the receiving end. Therefore, it has a comparable performance to DSSS only over multipath channels with a maximum ICI of 4 chips only. In order to search for other new classes of CSK codes, these three SS systems are investigated and understood first. A new class of CSK codes is researched based on these ideas too. Finally, a brief summary of the SS systems concludes this chapter.

3.1 $\pi/4$ DQPSK Modulation Scheme

As mentioned before, DSSS uses modulation schemes such as PSK and FSK, which require the estimation of the carrier phase and carrier frequency respectively in the receiver. Ideally, the demodulator of a PSK signal has available a perfect estimate of the carrier phase. In practice, the carrier phase is extracted from the received signal by performing

some non-linear operation that introduces a phase ambiguity. Consequently, it is not possible to have an absolute estimate of the carrier phase for demodulation [5].

The phase ambiguity problem resulting from the estimation of the carrier phase can be overcome by encoding the information in phase differences between successive signal transmissions. This is known as Differential PSK (DPSK). The demodulation of DPSK does not require the estimation of the carrier phase. Instead, the received signal in any given signaling interval is compared to the phase of the received signal from the preceding signaling interval.

In this thesis, $\pi/4$ Differential Quadrature PSK (DQPSK) is used. The signal constellation showing the differential phases of DQPSK is illustrated in Fig 3.1-1 (not to be confused with the absolute phase). All four points have the same amplitude and are separated by the same distance because the probability of detection error is dominated by the minimum distance between pairs of signal points. The signal power is normalized to one, so all four points lie on the unit circle.

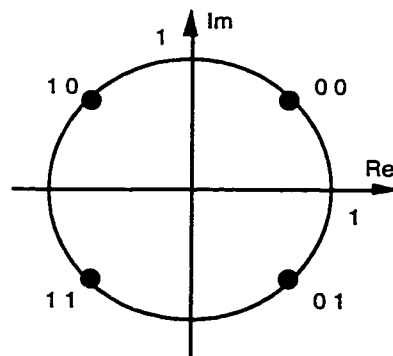


Fig 3.1-1 The signal constellation showing differential phases of DQPSK

Bits assignment to the signal points are according to Gray Code. The Gray coding ensures that adjacent signal points differ by only one binary digit. This is important in the

demodulation of the signal because the most likely errors caused by noise involve the erroneous selection of a signal point adjacent to the transmitted signal point. In such a case, only a single bit error occurs.

3.2 DSSS System using Barker Code

The Hopper+ is considered as a benchmark here. It is a DSSS system using an 11 chip Barker Code for spreading a DQPSK signal with a 8 Mchips/s chip rate. The Hopper+ has an architecture that consists of an FPGA which performs one correlation every set of 11 chips and a DSP chip which performs the differential detection on each correlation value in order to extract the DQPSK information [3]. The Barker Code considered is:

$$\text{Barker Code} = [1 \ -1 \ 1 \ 1 \ -1 \ 1 \ 1 \ 1 \ -1 \ -1 \ -1]$$

The Barker Code $\{ C_1, C_2, \dots, C_N \}$ of length $N = 11$ chips takes values of 1 and -1 only. The characteristics of this Barker Code can be viewed through the cyclic Barker Code auto-correlation, $R(k)$, of which is defined as:

$$R(k) = \sum_{n=1}^N C_n \cdot C_{n-k}^* \quad \text{for } 0 \leq k \leq N-1 \quad (3.1)$$

$$\text{where } C_{N+k} = C_k, \quad 1 \leq k \leq N.$$

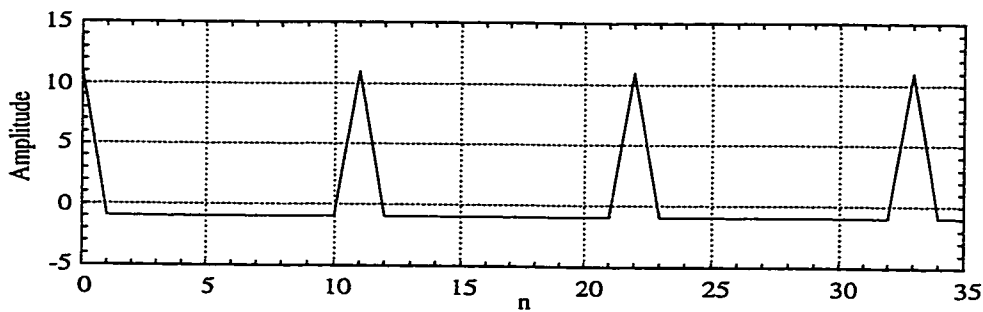


Fig 3.2-1 The auto-correlation of the 11 chip Barker Code

The auto-correlation of the Barker Code is plotted in Fig 3.2-1. The Barker Code sequence exhibits a periodic auto-correlation $R(k)$ with values $R(k) = N$ for $k = 0, \pm N, \pm 2N, \dots$, and $R(k) = -1$ for all other k 's. This impulse-like auto-correlation implies that the power spectrum is nearly white and the sequence resembles white noise. Thus, the Barker Code is used as the PN sequence for spreading in the SS system.

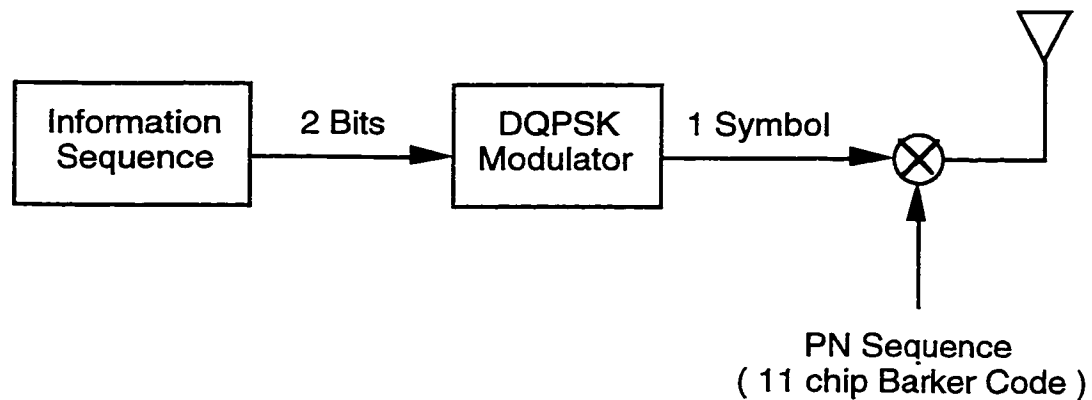


Fig 3.2-2 The transmitter of a DSSS system using the Barker Code

At the transmitter, two bits of information data are modulated by the DQPSK modulator according to the signal constellation mentioned in the previous section. The resulting signal symbol is then multiplied by the 11 chip Barker Code before sending out to the channel through the transmitting antenna.

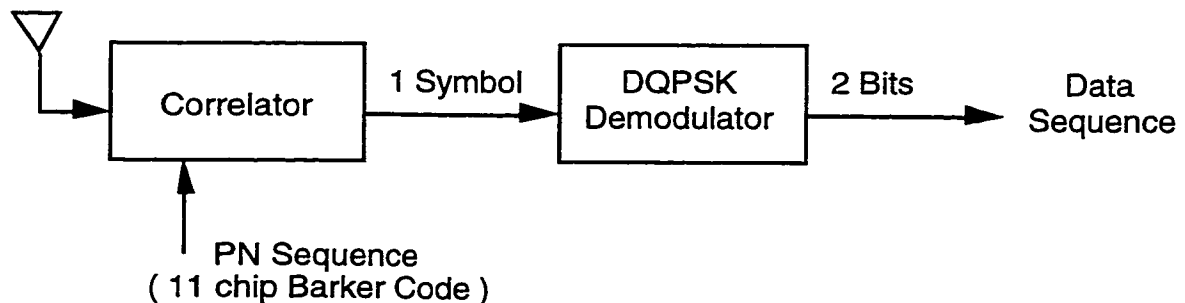


Fig 3.2-3 The receiver of a DSSS system using the Barker Code

At the receiver, the received signal is despread by the correlator using the same 11 chip Barker Code. The resulting signal symbol is then demodulated by the DQPSK demodulator. As a result, two bits of data are recovered. In conclusion, the Barker/DSSS system can transmit two bits of data with a 8 Mchips/s chip rate. Its bit rate is $\frac{8 \text{ Mchips} / \text{s}}{11 \text{ chips} / \text{symbol}} \times 2 \text{ bits} / \text{symbol} = 1.454 \text{ Mbps}$, where the chip rate is 8 Mchips/s, with 11 chips/symbol, and 2 bits/symbol.

A Matlab™ program has been written to simulate the BER performance of the Barker/DSSS system over an Additive White Gaussian Noise (AWGN) channel. The simulation results are plotted in Fig 3.2-4. It is clear that the BER curve has a waterfall shape. The BER decreases as the SNR per symbol increases. This BER for the Barker/DSSS will be used as a benchmark for other systems.

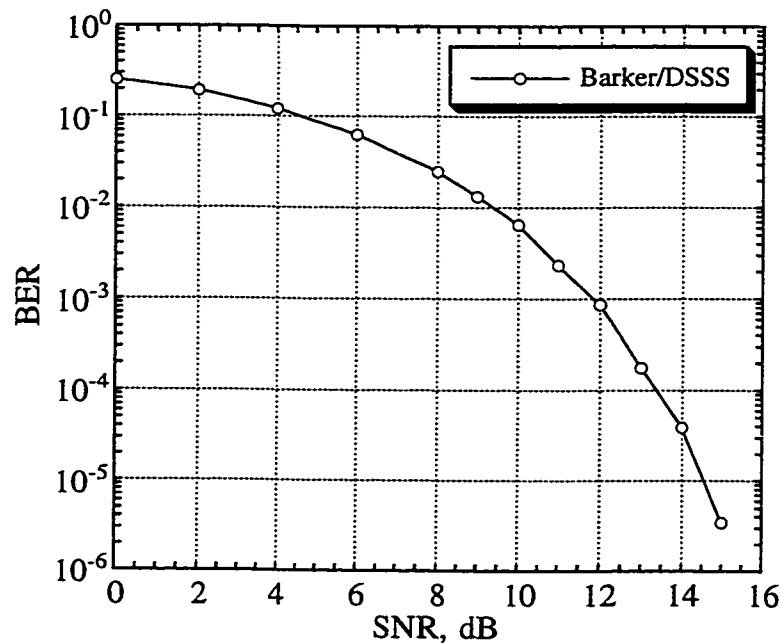


Fig 3.2-4 The BER for the Barker/DSSS system over an AWGN channel

3.3 A CSK System using the Barker Code (Conventional CSK)

In this section, a CSK system using $N = 11$ chip Barker Code is investigated. For simplicity, only $M = 2$ Barker Codes are used (M denotes the number of possible PN sequences used in a CSK system). The performance of the conventional CSK system is considered here, therefore, there are two correlators in the receiver. The two Barker Codes used are in this format:

$$\begin{aligned}\vec{C1} &= [c_1 \ c_2 \ c_3 \ c_4 \ c_5 \ c_6 \ c_7 \ c_8 \ c_9 \ c_{10} \ c_{11}] \\ \vec{C2} &= [c_7 \ c_8 \ c_9 \ c_{10} \ c_{11} \ c_1 \ c_2 \ c_3 \ c_4 \ c_5 \ c_6]\end{aligned}$$

The two Barker Codes, $\vec{C1}$ and $\vec{C2}$, are exactly the same except that $\vec{C2}$ is shifted by 5 chips compared to $\vec{C1}$. The auto-correlations of the two codes are the same. The periodic auto-correlation $R_{i,i}(k)$ has values $R_{i,i}(k) = N$ for $k = 0, \pm N, \pm 2N, \dots$, and $R_{i,i}(k) = -1$ for all other k 's. The cross-correlation $R_{i,j}(k)$ of $\vec{C1}$ and $\vec{C2}$ is defined as follows:

$$R_{i,j}(k) = \sum_{n=1}^N C_{i,n} \cdot C_{j,n-k}^* \quad \text{for } 0 \leq k \leq N-1 \text{ and } 1 \leq i, j \leq M \quad (3.2)$$

where $\vec{Ci} = [C_{i,1} \ C_{i,2} \ \dots \ C_{i,N}]$ and $C_{i,N+k} = C_{i,k} \quad 1 \leq k \leq N \text{ and } 1 \leq i \leq M$

The actual Barker Codes used for the computer simulation are:

$$\begin{aligned}\vec{C1} &= [1 \ -1 \ 1 \ 1 \ -1 \ 1 \ 1 \ 1 \ -1 \ -1 \ -1] \\ \vec{C2} &= [1 \ 1 \ -1 \ -1 \ -1 \ 1 \ -1 \ 1 \ 1 \ -1 \ 1]\end{aligned}$$

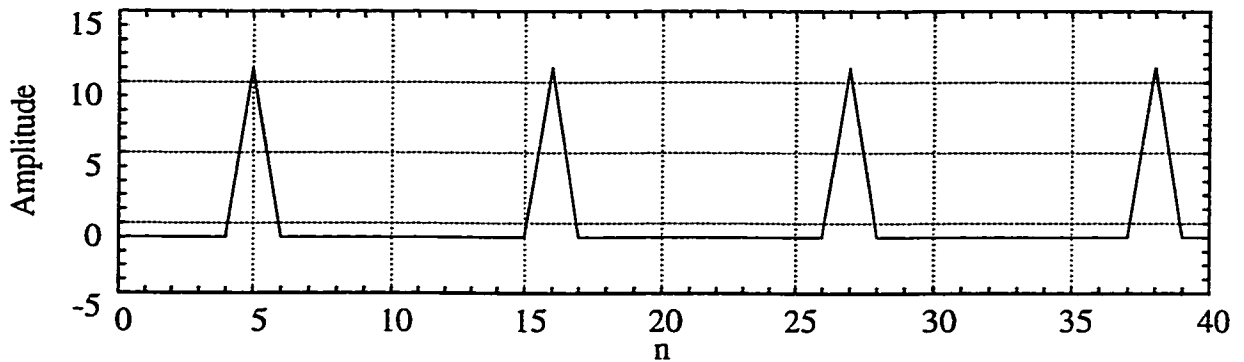


Fig 3.2-5 The cross-correlation of the two 11 chip Barker Codes

The cross-correlation between the two codes \bar{C}_1 and \bar{C}_2 is plotted in Fig 3.2-5. Again, the Barker Codes exhibit a periodic cross-correlation $R_{i,j}(k)$, but with values $R_{i,j}(k) = N$ for $k = 5, \pm(N+5), \pm(2N+5), \dots$, and $R_{i,j}(k) = -1$ for all other k 's. Since \bar{C}_2 is shifted by 5 chips compared to \bar{C}_1 , the peak cross-correlation values will occur at $k = 5$ instead of $k = 0$. In other words, there will be a distortion to the received signal when there is a multipath coming delayed by 5 chips. This means that the maximum ICI allowed for the Barker/CSK system is 4 chips. In this section, only the AWGN channel is considered, so, only the auto-correlations of the Barker Codes are of importance.

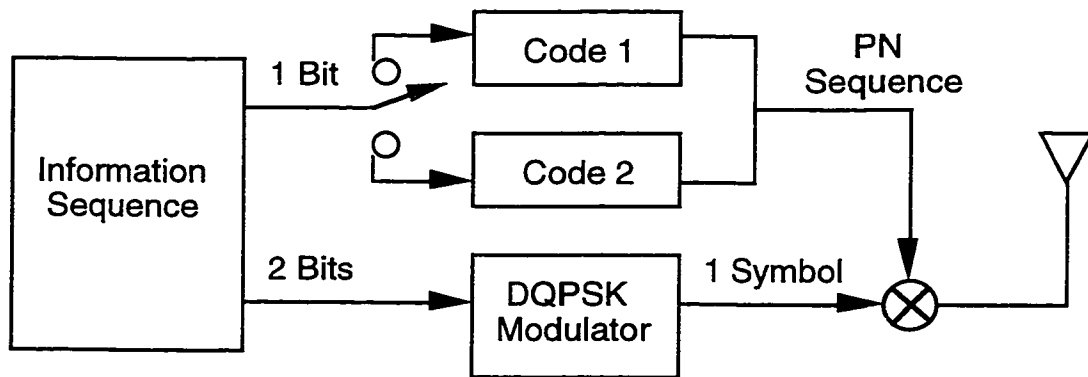


Fig 3.2-6 The transmitter of a CSK system using two Barker Codes

At the transmitter, one bit of information is used to choose one out of the two Barker Codes as the spreading code. Another two bits of information are modulated by the DQPSK modulator. The resulting signal is then multiplied by the chosen Barker Code before sending it out to the communication channel.

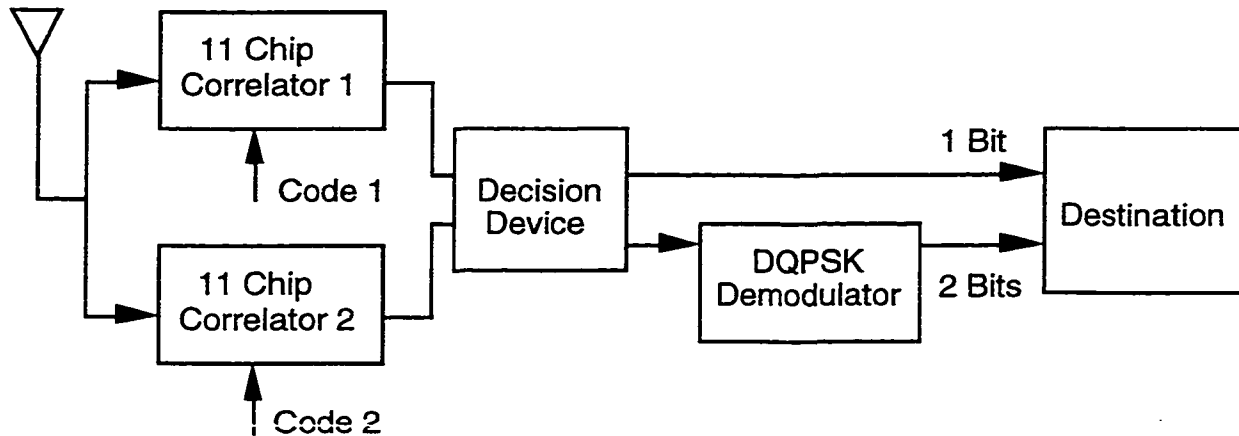


Fig 3.2-7 The receiver of a CSK system using two Barker Codes

At the receiver, the received signal is despread by both correlators with 11 chip Barker Codes \bar{C}_1 and \bar{C}_2 respectively. The results are compared in the decision device. The one with the largest magnitude will be selected and demodulated by the DQPSK demodulator. As a result, two bits of data are recovered from the DQPSK demodulator. At the same time, when the decision is made on the correlation results in the decision device, the bit used for code selection can be recovered. In conclusion, the Barker/CSK system can transmit three bits of data with a 8 Mchips/s chip rate. Its chip rate is 8 Mchips/s, with 11 chips/symbol and 3 bits/symbol. Therefore, its bit rate is

$$\frac{8 \text{ Mchips / s}}{11 \text{ chips / symbol}} \times (2 + 1) \text{ bits / symbol} = 2.182 \text{ Mbps.}$$

A Matlab™ program has been written to simulate the BER performance of the Barker/ CSK system over an AWGN channel. The simulation results are plotted in

Fig 3.2-8. The BER for the Barker/DSSS system is also plotted on the same graph for comparison. It is clear that the BER curves for both systems have the same shape and they are almost the same at high SNR. It is concluded that the Barker/CSK system has a similar performance as the Barker/DSSS, but it requires $M = 2$ correlators in the receiver, which is twice as complicated as that of the Barker/DSSS system.

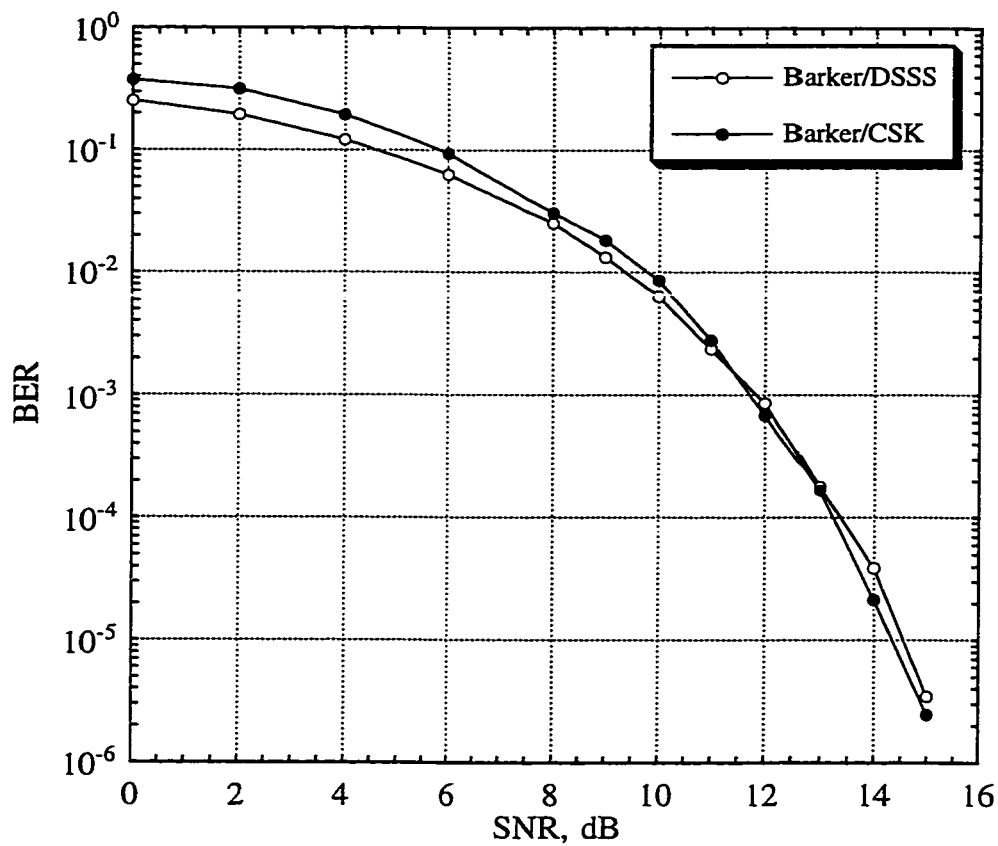


Fig 3.2-8 The BER for the Barker/DSSS and the Barker/CSK systems over an AWGN channel

3.4 A CSK System using the Wi-LAN Codes (Low Complexity CSK)

In this section, a CSK system using $N = 10$ chip Wi-LAN Code is investigated. For simplicity, only $M = 2$ Wi-LAN Codes are considered. The Wi-LAN Codes are in this format [3]:

$$\begin{aligned}\vec{C1} &= [c_1 \ c_2 \ c_3 \ c_4 \ c_5 \ c_6 \ c_7 \ c_8 \ c_9 \ c_{10}] \\ \vec{C2} &= [c_1 \ c_2 \ c_3 \ c_4 \ c_5 \ -c_6 \ -c_7 \ -c_8 \ -c_9 \ -c_{10}]\end{aligned}$$

The two Wi-LAN Codes, $\vec{C1}$ and $\vec{C2}$, are exactly the same except that their second halves are of opposite polarity. This special characteristic of the Wi-LAN Codes allows it to use only one correlator in the receiver. This will be explained later using a block diagram.

First of all, the auto-correlation and cross-correlation of the Wi-LAN Codes are discussed. The definitions for both correlations are the same as for the Barker Codes. The actual codes used for computer simulations are:

$$\begin{aligned}\vec{C1} &= [1 \ -1 \ 1 \ 1 \ 1 \ -j \ j \ -j \ -j \ -j] \\ \vec{C2} &= [1 \ -1 \ 1 \ 1 \ 1 \ j \ -j \ j \ j \ j]\end{aligned} \quad \text{where } j = \sqrt{-1}$$

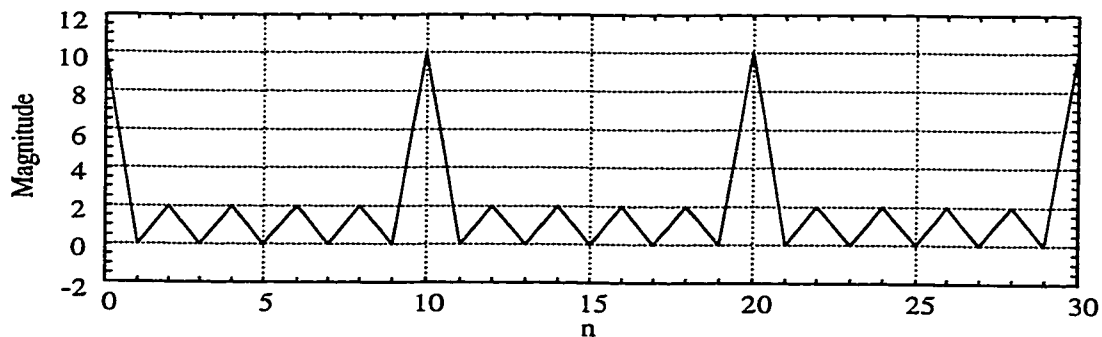


Fig 3.4-1 The auto-correlation of the 10 chip Wi-LAN Code

The auto-correlations of the two Wi-LAN Codes are the same. The auto-correlation for one of the Wi-LAN Codes is plotted in Fig 3.4-1. Since the codes contain the complex value j , the magnitude of the correlations are considered here. The Wi-LAN Codes exhibit a periodic auto-correlation $R_{i,j}(k)$ with values $|R_{i,j}(k)| = N$ for $k = 0, \pm N, \pm 2N, \dots$, and $|R_{i,j}(k)| = 0$ or 2 for all other k 's, where $i = 1$ or 2 . It is clear that the maximum out-of-phase auto-correlation of the Wi-LAN Codes is smaller than $N/2$.

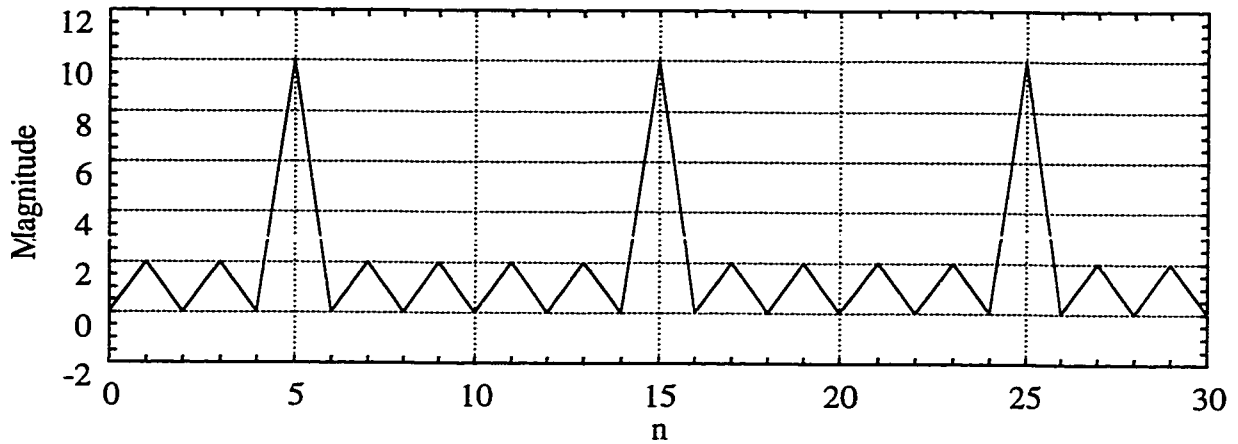


Fig 3.4-2 The cross-correlation of the two 10 chip Wi-LAN Codes

The cross-correlation of the two codes is shown in Fig 3.4-2. The Wi-LAN Codes exhibit a periodic cross-correlation $R_{i,j}(k)$, but with values $|R_{i,j}(k)| = N$ for $k = \pm 5, \pm(N+5), \pm(2N+5), \dots$, and $|R_{i,j}(k)| = 0$ or 2 for all other k 's. Since the second halves of \bar{C}_1 and \bar{C}_2 are of opposite polarity, the peak cross-correlation values occur at $k = 5, N+5, 2N+5, \dots$, instead of $k = 0, N, 2N$. This means that the maximum ICI allowed for the Wi-LAN/CSK system is 4 chips. The CSK system requires either a RAKE receiver or an equalizer in the receiving end when the ICI of the channel is larger than 4 chips.

The transmitting CSK symbol can be expressed as follows:

$$\bar{S}_k = \xi_k [\bar{C}_{1,1} \quad \bar{C}_{1,2} e^{j\theta_k}] = [\bar{S}_{k,1} \quad \bar{S}_{k,2}] \quad (3.3)$$

where $\bar{C}_{1,1} = [c_1 \ c_2 \ c_3 \ c_4 \ c_5]$ and $\bar{C}_{1,2} = [c_6 \ c_7 \ c_8 \ c_9 \ c_{10}]$, ξ_k is the k th DQPSK symbol, θ_k is either 0 or π depending on the choice of code \bar{C}_1 or \bar{C}_2 respectively, and $\bar{S}_{k,1}$ and $\bar{S}_{k,2}$ are the parts of \bar{S}_k corresponding to subcodes $\bar{C}_{1,1}$ and $\bar{C}_{1,2}$ respectively. The relationship between the data bits and the corresponding CSK symbols is illustrated in Fig 3.4-3. The θ_k is treated as an extra DBPSK symbol inside the information symbol ξ_k .

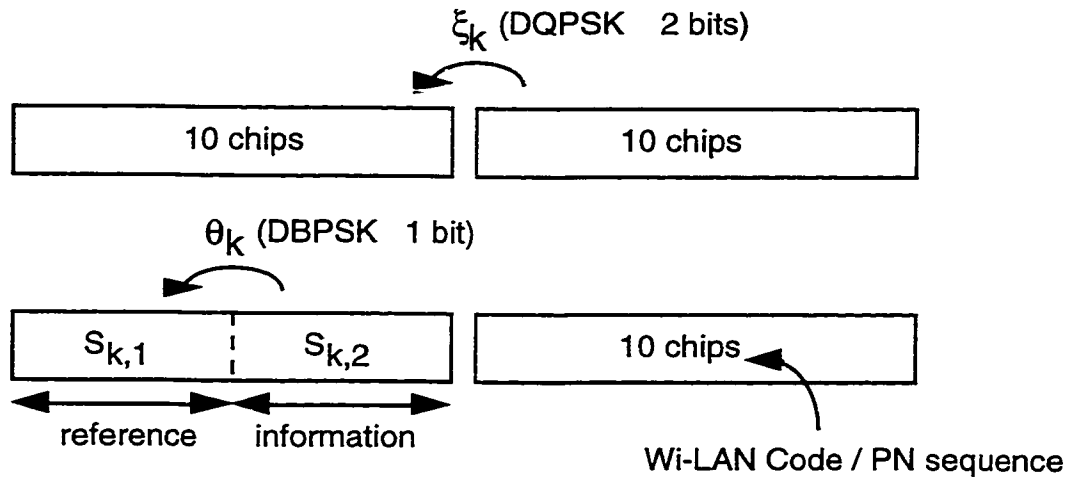


Fig 3.4-3 The relationship between data bits and the Wi-LAN/CSK symbols ($M = 2$)

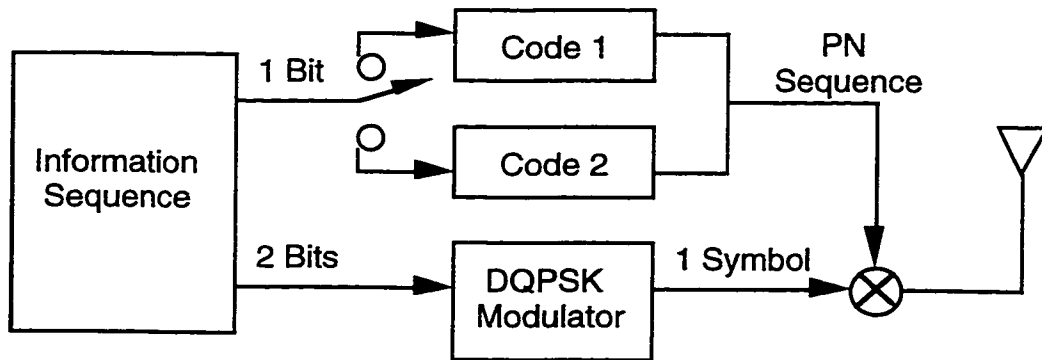


Fig 3.4-4 The transmitter of a CSK system using the Wi-LAN Codes

The transmitters for a CSK system using either the Wi-LAN Codes or the Barker Codes are the same. The transmitter for a CSK system using the Wi-LAN Codes is shown in Fig 3.4-4. Two bits of information are modulated by the DQPSK modulator producing the symbol, ξ_k . Another bit of data is used to decide on θ_k , which in turns, chooses one out of $M = 2$ Wi-LAN Codes for spreading the modulated signal. The resulting signal symbol, \bar{S}_k , is then passed on to the channel through the transmitting antenna.

Since the two Wi-LAN Codes have identical first halves and have opposite polarity on their second halves, only one $N/2$ chip correlator is necessary to perform an initial-partial correlation on the first half of the received signal and another $N/2$ chip correlator to perform a second partial correlation on the second half of the received signal.

The Wi-LAN Codes considered are $N = 10$ chip long. Therefore, there are two 5-chip correlators in the receiver. Each 5-chip correlator performs 5 complex additions. There are 10 complex additions in total for a received symbol. In terms of receiver complexity, it is the same as if there were a single 10-chip correlator in the receiver.

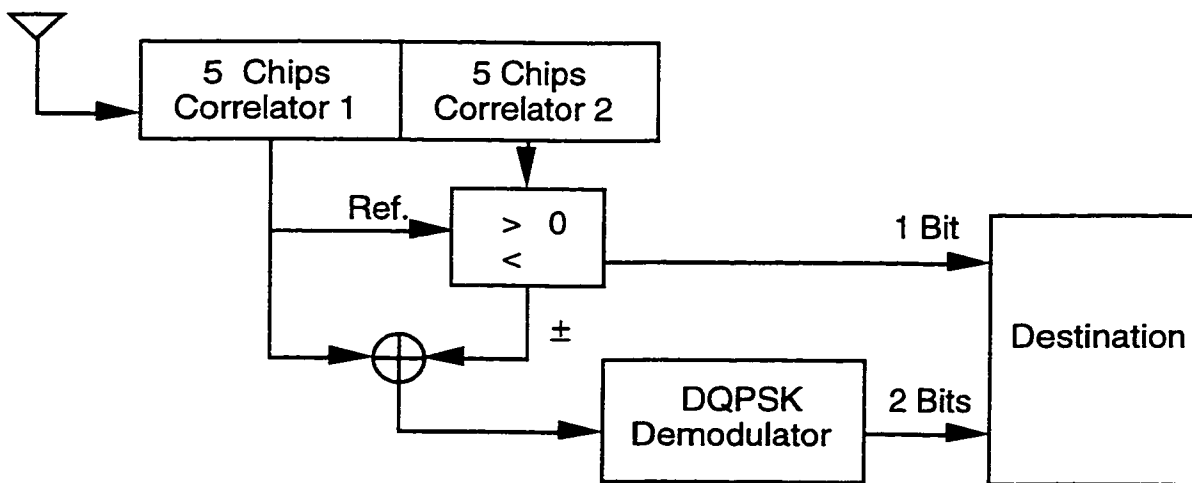


Fig 3.4-5 The receiver of a CSK system using the Wi-LAN Codes

The block diagram of a receiver for the Wi-LAN/CSK system is shown in Fig 3.4-5. Once the partial correlations are computed as $\rho_1 = \bar{S}_{k,1} \bullet \bar{C}_{1,1}^*$ and $\rho_2 = \bar{S}_{k,2} \bullet \bar{C}_{1,2}^*$ where \bullet denotes an inner product, it is easy to make a decision on $\hat{\theta}_k$, and know whether \bar{C}_1 or \bar{C}_2 was used for spreading according to this rule:

$$\hat{\theta}_k = \begin{cases} 0 & \text{if } \operatorname{Re}(\rho_1 \rho_2^*) \geq 0 \\ \pi & \text{if } \operatorname{Re}(\rho_1 \rho_2^*) < 0 \end{cases} \quad \text{where } \hat{\theta}_k \text{ is the estimated } \theta_k \quad (3.4)$$

Thus, one bit of information is recovered. The total correlation can be obtained by either adding or subtracting the two partial correlations depending on $\hat{\theta}_k$. The total correlation is then demodulated by the DQPSK demodulator, recovering two bits of information. These can all be done in a DSP chip. As a result, the Wi-LAN/CSK system can transmit three bits of data with a 8 Mchips/s chip rate. Its bit rate is $\frac{8 \text{ Mchips/s}}{10 \text{ chips/symbol}} \times (2+1) \text{ bits/symbol} = 2.4 \text{ Mbps}$, where the chip rate is 8 Mchips/s, and transmits 10 chips/symbol and 3 bits/symbol.

A Matlab™ program was written to simulate the BER performance of the Wi-LAN/CSK system over an AWGN channel. The simulation results are plotted in Fig 3.4-6. The BER for the Barker/DSSS and the Barker/CSK systems are also plotted on the same graph for comparison. It is clear that the BER curves for all three systems have the same shape and they are lying closely to each other.

The Wi-LAN Codes are only 10 chips long with a processing gain L_c of 10 while the Barker Codes are 11 chips long with a processing gain L_c of 11. Thus the SS systems using the Barker Codes will have a slightly better performance than that using the Wi-LAN

Codes over the same bandwidth. It can be seen that the Wi-LAN/CSK system has a slightly higher BER than the Barker/DSSS and the Barker/CSK systems for the same SNR per symbol. Since the Barker Codes are only 1 chip longer than the Wi-LAN Codes, the difference in BER for the two systems is relatively small.

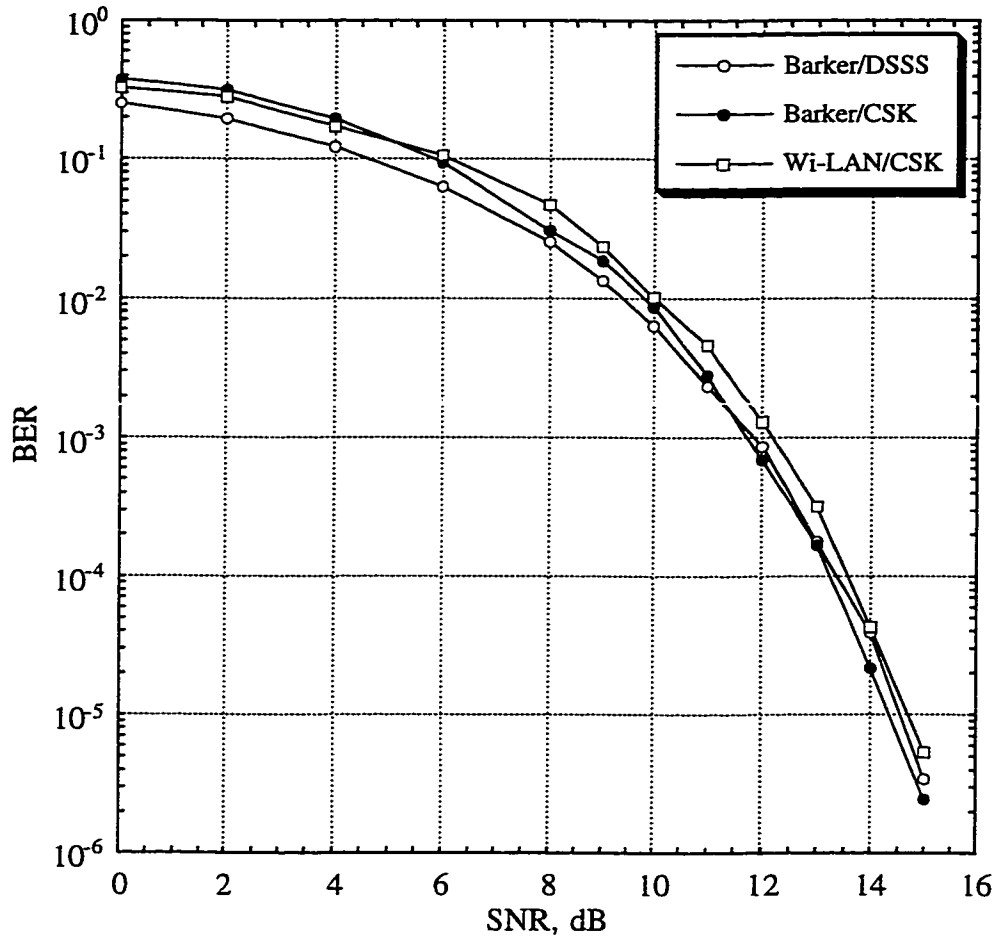


Fig 3.4-6 The BER for the Barker/DSSS, the Barker/CSK and the Wi-LAN/CSK systems over an AWGN channel

According to the simulation results, it is found that almost all of the errors encountered at high SNR are coming from the detection of the DQPSK symbol between adjacent received signals rather than from the DBPSK symbol embedded within the PN

sequence of the received signal. This can be explained as the probability of error being dominated by the minimum distance between pairs of signal points, and the DQPSK symbols, having a smaller minimum distance between pairs of signal points than the DBPSK symbols, will dominate in BER even after taking into consideration their corresponding processing gains. We will refer to such a minimum distance as the normalized minimum distance. This important characteristic may be manipulated to transmit more important bits of information through the DBPSK symbols while transmitting less important bits through the DQPSK symbols.

It is concluded that the Wi-LAN/CSK system has almost the same performance as the Barker/DSSS and the Barker/CSK systems. Since the Wi-LAN/CSK system requires only one N chip correlator in the receiver (the system architecture is kept the same as the Barker/DSSS system), its receiver complexity is comparable to that of the Barker/DSSS and is less complicated than that of the Barker/CSK system i.e. the conventional CSK system. As a result, the selection of the spreading codes in a CSK system is very important. Low complexity CSK can be achieved using specially selected codes such as the Wi-LAN Codes.

3.5 Summary of the SS systems

The structure and performance of the three SS systems: the DSSS system using a Barker Code, the CSK system using two Barker Codes (conventional CSK) and the CSK system using the Wi-LAN Codes (low complexity CSK) have been discussed. The following table, Table 3.5, is a summary of the bit rate and receiver complexity of these SS systems.

SS systems	Bit Rate in bits/symbol	Receiver Complexity	Bit Rate in bits/sec
Barker / DSSS	2 bits / symbol	1 correlator	1.454 Mbps
Barker / CSK	3 bits / symbol	2 correlators	2.182 Mbps
Wi-LAN / CSK	3 bits / symbol	1 correlator	2.400 Mbps

Table 3.5-1 Summary of bit rate and receiver complexity of the SS systems (I)

According to the above table, it can be concluded that the Wi-LAN/CSK system can increase the bit rate of a transceiver over a DSSS system. It can also reduce the receiver complexity over a conventional CSK system. Finally, the Wi-LAN/CSK system has a comparable performance to the DSSS system over an AWGN channel.

A higher speed CSK system can be achieved by manipulating the codes for spreading. This is discussed in Chapter 4. Furthermore, in order to complete the investigation of low complexity CSK systems, the performance of DSSS and CSK systems over multipath channels is discussed in Chapters 6 and 7.

Chapter 4

Increase the Bit Rate using CSK

Low complexity CSK can be used to further increase the bit rate of a SS system over a fixed bandwidth. As mentioned in chapter 3, a CSK system using $M = 2$ Wi-LAN Codes can transmit 3 bits/symbol, with a 8 Mchips/s chip rate, has a bit rate of 2.4 Mbps, and only requires one N chip correlator in the receiver. In the following two sections, methods that can increase the bit rate of a CSK system to more than 2.4 Mbps are discussed. The first solution is to increase the number of PN sequences available for spreading code selection. This can be achieved using $M = 16$ Wi-LAN Codes in a CSK system. There are two kinds of modulation schemes used here with $M = 16$ Wi-LAN/CSK. They are 8-DPSK and 8-QAM. They are discussed in Section 4.1. The second solution is to use a new class of CSK codes, which we refer to as the TRLabs Codes. They are introduced in detail in Section 4.2.

4.1 Increase the Number of PN Sequences in a Set

In this section, the number of possible PN sequences available for spreading code selection of a CSK system is increased from $M = 2$ to $M = 16$. They are the $M = 16$ Wi-LAN Codes. As the number of PN sequences in a set is increased, more data bits are required for code selection. Therefore, a larger number of data bits can be transmitted over a fixed bandwidth.

4.1.1 A CSK System using $M = 16$ Wi-LAN Codes with 8-DPSK

In this section, the structure and performance of a CSK system using $M = 16$ Wi-LAN Codes with 8-DPSK are investigated. Each Wi-LAN Code is still $N = 10$ chips long. The Wi-LAN Code will be the basic unit of the 16 possible PN sequences for this CSK system. The mechanism for this CSK system is well illustrated in Fig 4.1.1-1. The 'ref' represents the reference signal, while the 'info' denotes the information.

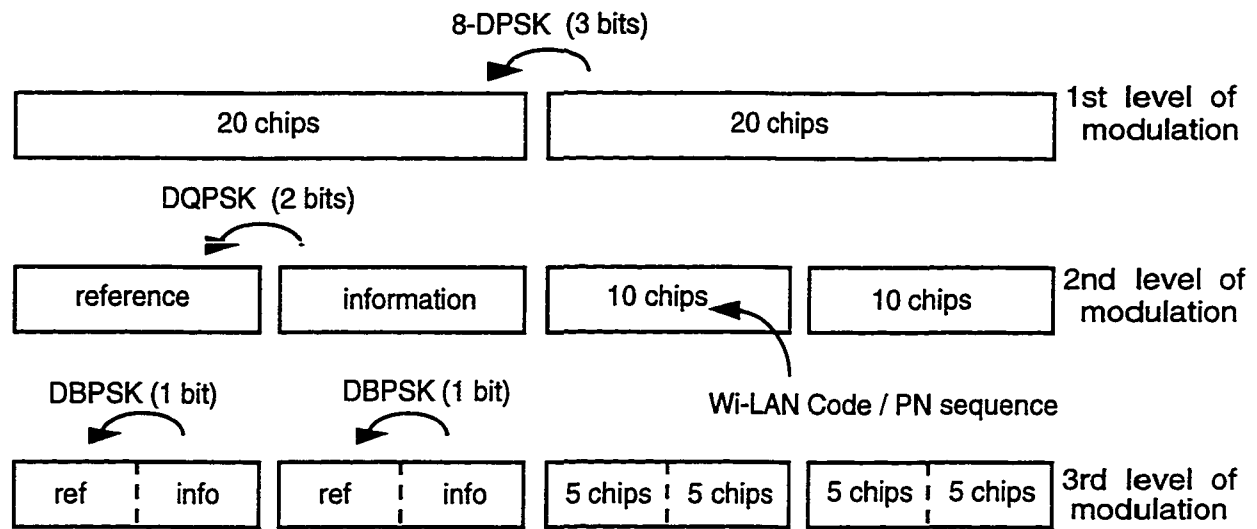


Fig 4.1.1-1 The relationship between data bits and the Wi-LAN/CSK symbols ($M = 16$)

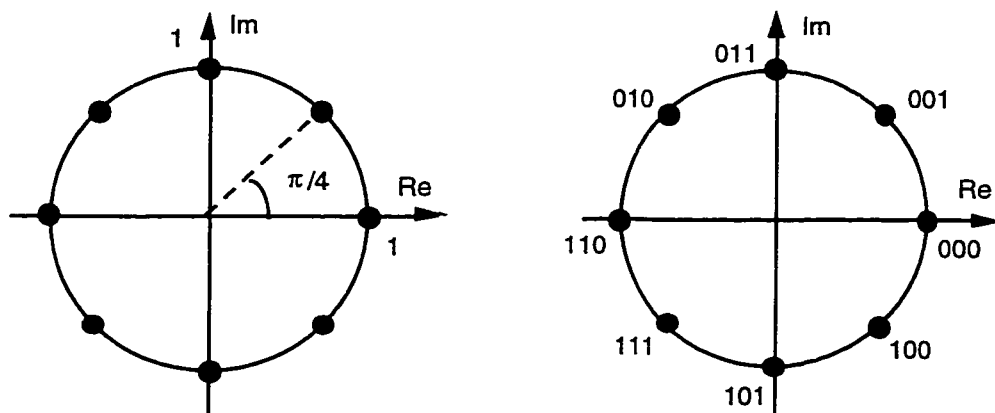


Fig 4.1.1-2 The 8-DPSK signal constellations

There are three different levels of modulations. The first modulation level is made up of 20 chip PN sequences, which in turn, are made up of 10 chip Wi-LAN Codes. The modulation scheme used on the first modulation level is Differential 8-PSK (8-DPSK). The signal constellation for 8-DPSK is shown in Fig 4.1.1-2 on the previous page. Bit assignment to the signal points are according to Gray Code. All the signal points lie on the unit circle. The DQPSK is embedded within each 20 chip PN sequence producing the second modulation level. Furthermore, each 10 chip Wi-LAN Code is subdivided into two halves, five chips in each half. The DBPSK is embedded within every 10 chips to form the third modulation level.

This Wi-LAN/CSK system has $M = (2^2 \times 2^1 \times 2^1) = 16$ possible 20 chip long PN sequences. Since each 20 chip PN sequence is made up of two 10 chip Wi-LAN Codes, it has a similar periodic auto-correlation and cross-correlation as the Wi-LAN Codes. The $M = 16$ Wi-LAN/CSK system can transmit $(3+2+1+1)$ bits per 20 chips. Its bit rate is $\frac{8 \text{ Mchips / s}}{20 \text{ chips / symbol}} \times (3+2+1+1) \text{ bits / symbol} = 2.8 \text{ Mbps}$, where the chip rate is 8 Mchips/s, with 20 chips/symbol and 7 bits/symbol.

The transmitting CSK symbol can be expressed as follows:

$$\begin{aligned} \bar{S}_k &= \xi_k \begin{bmatrix} \bar{C}_{1,1} & \bar{C}_{1,2} e^{j\theta_k} & \bar{C}_{1,1} & \bar{C}_{1,2} e^{j\phi_k} \end{bmatrix} e^{j\sigma_k} \\ &= \xi_k [\bar{C}_{1,1} \quad \bar{C}_{1,2} e^{j\theta_k} \quad \bar{C}_{1,1} e^{j\sigma_k} \quad \bar{C}_{1,2} e^{j\sigma_k} e^{j\phi_k}] \\ &= [\bar{S}_{k,1} \quad \bar{S}_{k,2} \quad \bar{S}_{k,3} \quad \bar{S}_{k,4}] \end{aligned} \quad (4.1)$$

where $\bar{C}_{1,1} = [c_1 \ c_2 \ c_3 \ c_4 \ c_5]$ and $\bar{C}_{1,2} = [c_6 \ c_7 \ c_8 \ c_9 \ c_{10}]$, ξ_k is the k th 8-DPSK symbol, σ_k is either $\pi/4$, $3\pi/4$, $5\pi/4$ or $7\pi/4$ depending on the k th DQPSK phase, θ_k and ϕ_k are either 0 or π depending on the choices of code \bar{C}_1 or \bar{C}_2 respectively.

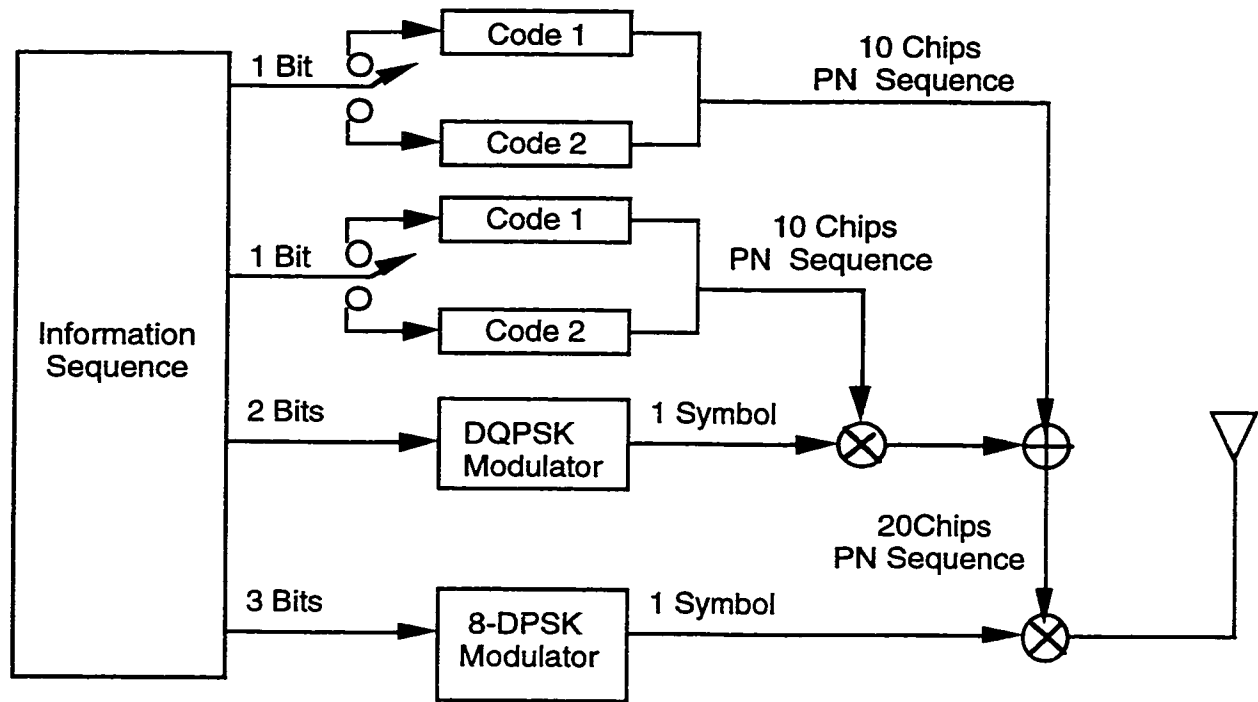


Fig 4.1.1-3 The transmitter of a CSK system using the $M = 16$ Wi-LAN Codes

The block diagram of a CSK transmitter using $M = 16$ Wi-LAN Codes is shown in Fig 4.1.1-3. First of all, three bits of information are modulated by the 8-DPSK modulator producing the symbol, ξ_k . Another bit of data is used to decide on θ_k , which in turn, chooses one out of the two 10 chip Wi-LAN Codes, \bar{C}_1 or \bar{C}_2 , to form the first half of the 20 chip PN sequence. Another two bits of data are modulated by the DQPSK modulator producing the symbol, σ_k . Then, another bit of data is used to decide on ϕ_k , which in turn, chooses either the 10 chip Wi-LAN Code \bar{C}_1 or \bar{C}_2 for spreading the modulated DQPSK signal, σ_k . The resulting 10 chip sequence forms the second half of the 20 chip PN sequence. At this time, the resulting 20 chip PN sequence is used for spreading the modulated 8-DPSK signal, ξ_k . Finally, the spreaded signal, \bar{S}_k , is passed on to the transmitting antenna for transmission.

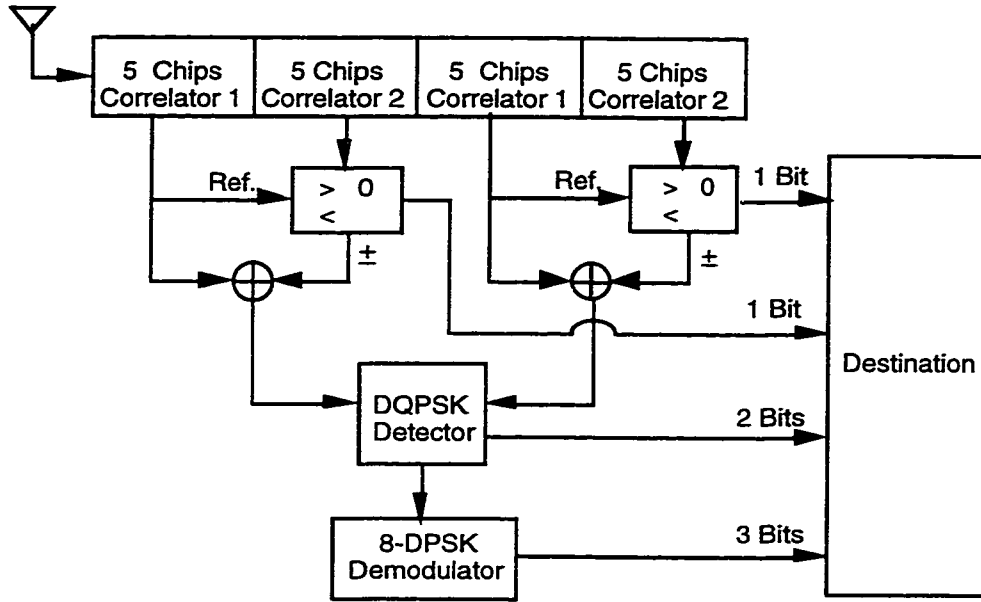


Fig 4.1.1-4 The receiver of a CSK system using the $M = 16$ Wi-LAN Codes

Since each 20 chip PN sequence is made up of 10 chip Wi-LAN Codes, which have identical first halves and have opposite polarity on their second halves, only two 5 chip correlators are necessary in the receiver. The reasons for this simplification is the same as that for the $M = 2$ Wi-LAN/CSK system. The receiver complexity is the same as if there were only a single 10-chip correlator in the receiver.

The block diagram of a receiver for $M = 16$ Wi-LAN/CSK system is shown in Fig 4.1.1-4. Every 20 chips of received signal are grouped and demodulated together, in order to recover the transmitted information data. Initially, the first 10 chips of received sequence are correlated with the 10 chip PN sequence in the receiver, forming two partial correlations: $\rho_1 = \bar{S}_{k,1} \cdot \bar{C}_{1,1}^*$ and $\rho_2 = \bar{S}_{k,2} \cdot \bar{C}_{1,2}^*$. The decision made on $\hat{\theta}_k$ is according to the following rule (same as rule (3.4) in chapter 3):

$$\hat{\theta}_k = \begin{cases} 0 & \text{if } \text{Re}(\rho_1 \rho_2^*) \geq 0 \\ \pi & \text{if } \text{Re}(\rho_1 \rho_2^*) < 0 \end{cases} \quad \text{where } \hat{\theta}_k \text{ is the estimated } \theta_k \quad (4.2)$$

Thus, one bit of information is recovered. The total correlation $\rho_{12} = \rho_1 \pm \rho_2$ is obtained by either adding or subtracting the two partial correlations depending on $\hat{\theta}_k$. The second 10 chips of received signal are then correlated with the 10 chip PN sequence in the receiver, forming another two partial correlations $\rho_3 = \bar{S}_{k,3} \cdot \bar{C}_{1,1}^*$ and $\rho_4 = \bar{S}_{k,4} \cdot \bar{C}_{1,2}^*$. The decision made on $\hat{\phi}_k$ is according to the following rule:

$$\hat{\phi}_k = \begin{cases} 0 & \text{if } \operatorname{Re}(\rho_3 \rho_4^*) \geq 0 \\ \pi & \text{if } \operatorname{Re}(\rho_3 \rho_4^*) < 0 \end{cases} \quad \text{where } \hat{\phi}_k \text{ is the estimated } \phi_k \quad (4.3)$$

Another bit of information is recovered. Again, the second total correlation $\rho_{34} = \rho_3 \pm \rho_4$ is obtained by either adding or subtracting the two partial correlations depending on $\hat{\phi}_k$. The next step is to recover the DQPSK signal embedded between these two total correlations ρ_{12} and ρ_{34} . The two total correlations ρ_{12} and ρ_{34} is compared according to the following rules, and two bits of information can be recovered.

$$\hat{\sigma}_k = \begin{cases} \frac{\pi}{4} & \text{if } \operatorname{Re}(\rho_{12} \rho_{34}^*) \geq 0 \text{ \& } \operatorname{Im}(\rho_{12} \rho_{34}^*) \geq 0 \\ \frac{3\pi}{4} & \text{if } \operatorname{Re}(\rho_{12} \rho_{34}^*) < 0 \text{ \& } \operatorname{Im}(\rho_{12} \rho_{34}^*) \geq 0 \\ \frac{5\pi}{4} & \text{if } \operatorname{Re}(\rho_{12} \rho_{34}^*) < 0 \text{ \& } \operatorname{Im}(\rho_{12} \rho_{34}^*) < 0 \\ \frac{7\pi}{4} & \text{if } \operatorname{Re}(\rho_{12} \rho_{34}^*) \geq 0 \text{ \& } \operatorname{Im}(\rho_{12} \rho_{34}^*) < 0 \end{cases} \quad (4.4)$$

where $\hat{\sigma}_k$ is the estimated σ_k .

The two total correlations ρ_{12} and ρ_{34} can be combined to form ρ_{total} according to the estimated $\hat{\sigma}_k$ and the following rule:

$$\rho_{total} = \rho_{12} + \rho_{34} \cdot e^{-j\hat{\sigma}_k} \quad (4.5)$$

Finally, the total correlation ρ_{total} can be demodulated by the 8-DPSK demodulator, recovering three bits of information. All of these complex-number computations can be accomplished using a DSP chip. As a result, $M = 16$ Wi-LAN/CSK system can transmit seven bits of data with a 8 Mchips/s chip rate. The bit rate is 2.8 Mbps again.

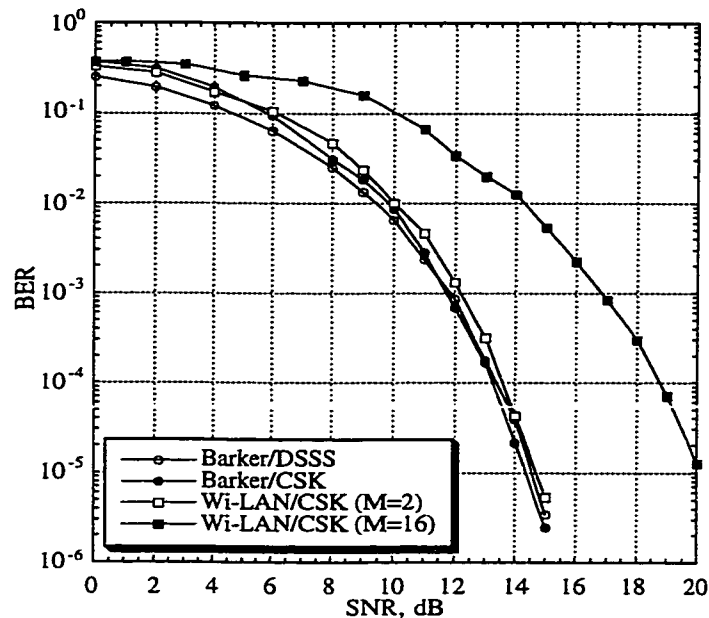


Fig 4.1.1-5 The BER for the Barker/DSSS, the Barker/CSK, the $M=2$ Wi-LAN/CSK and the $M=16$ Wi-LAN/CSK systems over an AWGN channel

A Matlab™ program has been written to simulate the BER performance of the $M = 16$ Wi-LAN/CSK system over an AWGN channel. The result is plotted in Fig 4.1.1-5. The BER for the Barker/DSSS, the Barker/CSK and the $M = 2$ Wi-LAN/CSK are also plotted for comparison. The BER curve for the $M = 16$ Wi-LAN/CSK system is about 5.3 dB worse than that for the $M = 2$ Wi-LAN/CSK system. This can be explained as the normalized minimum distance between pairs of signal points for 8-DPSK ($2xD_2$) being smaller than that for DQPSK (D_1). See Fig 4.1.1-6 on the next page. However, the processing gain of the $M = 16$ Wi-LAN Codes offers an extra 3 dB gain in SNR over the $M = 2$ Wi-LAN Codes. In addition, differential detection causes roughly a 3 dB

degradation in 8-DPSK while it causes only 2.1 dB degradation in DQPSK over coherent detection. Thus, 8-DPSK phase detection results into a higher probability of error.

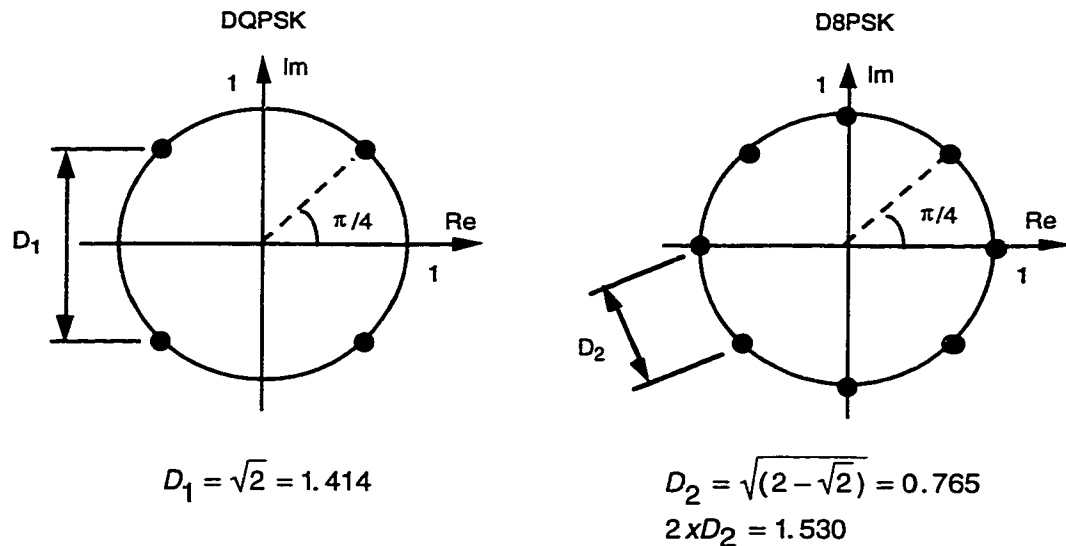


Fig 4.1.1-6 The signal constellations of DQPSK and 8-DPSK

SS systems	Bit Rate in bits/sec	Receiver Complexity
Barker / DSSS	1.454 Mbps	1 correlator
Barker / CSK	2.182 Mbps	2 correlators
M=2 Wi-LAN / CSK	2.400 Mbps	1 correlator
M=16 Wi-LAN / CSK	2.800 Mbps	1 correlator

Table 4.1.1-7 Summary of bit rate and receiver complexity of the SS systems (II)

The summary of bit rate and receiver complexity for the SS systems considered is shown in Table 4.1.1. It can be seen that the M = 16 Wi-LAN/CSK system can further increase the bit rate to 2.8 Mbps. In terms of receiver complexity, the M = 16 Wi-LAN/CSK requires only one N-chip correlator which is the same as the Barker/DSSS. From the simulation results, the BER for M = 16 Wi-LAN/CSK system is about 5.3 dB worse than that for the DSSS and the M = 2 Wi-LAN/CSK systems over an AWGN channel. This represents a trade off between the bit rate and the performance of a SS system.

4.1.2 A CSK System using $M = 16$ Wi-LAN Codes with 8-QAM

The basic structure of the $M = 16$ Wi-LAN/CSK system stays the same. The 10 chip Wi-LAN Code is still the basic unit for the 16 possible PN sequences for this CSK system. There are again three levels of modulation in the transmitting end, but with the first level of modulation on the 20 chip PN sequence replaced by the 8-QAM instead of the 8-DPSK. Since $M = 16$, the Wi-LAN/CSK system with 8-QAM is still transmitting seven bits per 20 chips per symbol. Its bit rate is still 2.8 Mbps. The 8-DPSK modulator and demodulator of the CSK system are subjected to changes, they are replaced by the 8-QAM modulator and demodulator. Therefore, the first thing to look at is the signal constellations of the 8-QAM and the difference between it and the 8-DPSK constellation.

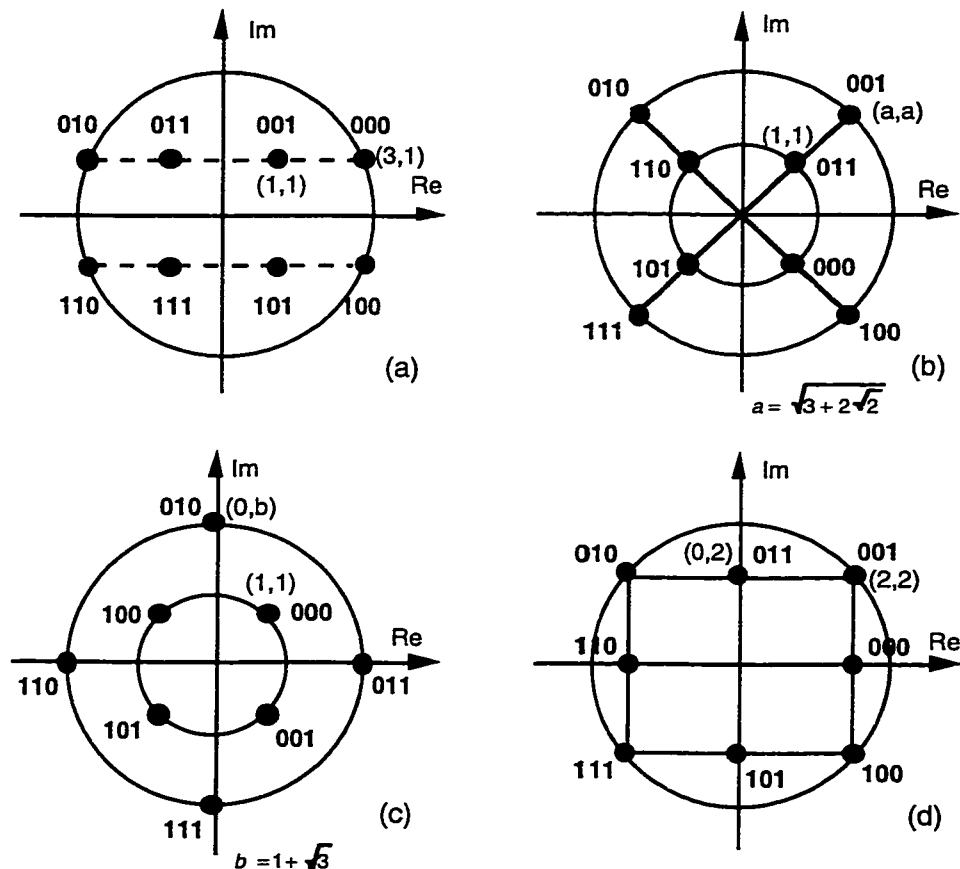


Fig 4.1.2-1 The four possible signal constellations for 8-QAM

Recall the signal constellation of 8-DPSK in Fig 4.1.1-2, where all the signal points are lying on the unit circle separated from each other by the same angle. Thus, the minimum distance between pairs of signal points are the same and the average signal power is $P_{av} = \frac{1}{8} \sum_{k=1}^8 P_k = \frac{1}{8} \sum_{k=1}^8 1^2 = 1$, where P_k is the power of each individual signal point. On the other hand, the minimum distance between pairs of signal points for 8-QAM are no longer constant. Fig 4.1.2-1 shows four possible signal constellations of 8-QAM [6]. The bit assignments according to Gray Code again are as shown in the figure. The coordinates (A_{re}, A_{im}) for each signal point, normalized by A , are given in the figure, too. The minimum distance between signal points for these signal constellations is always $2A$. If the signal points are equally probable, the average transmitted signal power is:

$$P_{av} = \frac{1}{8} \sum_{k=1}^8 (A_{re}^2 + A_{im}^2) = \frac{A^2}{8} \sum_{k=1}^8 (a_{re}^2 + a_{im}^2) \quad (4.6)$$

where (a_{re}, a_{im}) are the coordinates of the signal points, normalized by A . The signal sets (a) and (d) have the same average power $P_{av} = 6A^2$. Signal set (b) requires an average transmitted power $P_{av} = 6.83A^2$, and set (c) requires $P_{av} = 4.73A^2$. Therefore, for the same probability of error, signal set (c) requires less power than the other three sets. This signal constellation is known to be the best eight-point QAM constellation because it requires the least power for a given minimum distance between signal points.

In order to compare the performance of the 8-DPSK system with the 8-QAM system, their average signal powers P_{av} is set equal to each other. Thus, P_{av} for all four 8-QAM signal sets is normalized to one. As a result, the signal sets (a) and (d) have the same minimum distance $d_{\min} = 0.816$ between pairs of signal points. Signal set (b) has $d_{\min} = 0.765$, and set (c) has $d_{\min} = 0.919$. Recall that 8-DPSK has $d_{\min} = 0.765$. The

performance for the $M = 16$ Wi-LAN Codes is investigated by simulating the CSK system using 8-QAM over an AWGN channel.

As previously mentioned, the transmitting CSK symbol can be expressed as follows:

$$\begin{aligned}
 \bar{S}_k &= \xi_k \left[[\bar{C}_{1,1} \quad \bar{C}_{1,2}e^{j\theta_k}] [\bar{C}_{1,1} \quad \bar{C}_{1,2}e^{j\phi_k}]e^{j\sigma_k} \right] \\
 &= \xi_k [\bar{C}_{1,1} \quad \bar{C}_{1,2}e^{j\theta_k} \quad \bar{C}_{1,1}e^{j\sigma_k} \quad \bar{C}_{1,2}e^{j\sigma_k}e^{j\phi_k}] \\
 &= [\bar{S}_{k,1} \quad \bar{S}_{k,2} \quad \bar{S}_{k,3} \quad \bar{S}_{k,4}]
 \end{aligned} \tag{4.7}$$

where $\bar{C}_{1,1} = [c_1 \ c_2 \ c_3 \ c_4 \ c_5]$ and $\bar{C}_{1,2} = [c_6 \ c_7 \ c_8 \ c_9 \ c_{10}]$, ξ_k is the k th 8-QAM symbol, σ_k is either $\pi/4$, $3\pi/4$, $5\pi/4$ or $7\pi/4$ depending on the k th DQPSK phase, θ_k and ϕ_k are either 0 or π depending on the choices of code \bar{C}_1 or \bar{C}_2 respectively.

As it was stated before, the 8-DPSK modulator at the transmitter is simply replaced by an 8-QAM modulator. At the receiver, the received signal is demodulated as discussed in the previous section. The demodulation is done in the reverse order to the modulation process. Firstly, the 5-chip partial correlations ρ_1 , ρ_2 , ρ_3 and ρ_4 are obtained by correlating the received sequence with the PN sequence at the receiver for every 20 chips. Then, the total correlations ρ_{12} and ρ_{34} are obtained by either adding or subtracting the two corresponding partial correlations depending on the estimated phases $\hat{\theta}_k$ and $\hat{\phi}_k$ respectively. After that, the total correlation ρ_{total} is obtained as the sum of ρ_{12} and $\rho_{34} \cdot e^{-j\hat{\sigma}_k}$. Finally, ρ_{total} can be demodulated by the 8-QAM demodulator according to the signal constellations in Fig 4.1.2-1.

There are four 8-QAM demodulators corresponding to the four signal sets. Since QAM involves amplitude and phase modulation, a demodulator is divided into two halves,

one for amplitude detection, the other for phase detection. Fig 4.1.2-2 to Fig 4.1.2-5 show the demodulators for 8-QAM in detail. They may not be the optimal demodulators. However, all the complex-number computations can be accomplished in a DSP chip.

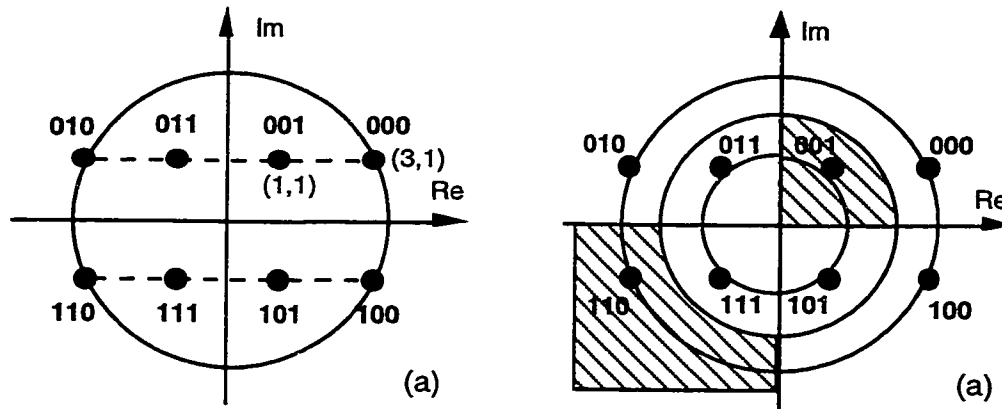


Fig 4.1.2-2 The signal constellation and demodulator for signal set (a)

Fig 4.1.2-2 shows the signal constellation and the corresponding demodulator for signal set (a). In the demodulator, each shaded region represents the area belonging to a bit pattern. For example, one of the shaded regions belongs to bit pattern 001 and the other belongs to 110. The circle separating the two shaded regions is in the middle of the inner and the outer circle. This demodulation involves both amplitude and phase detection.

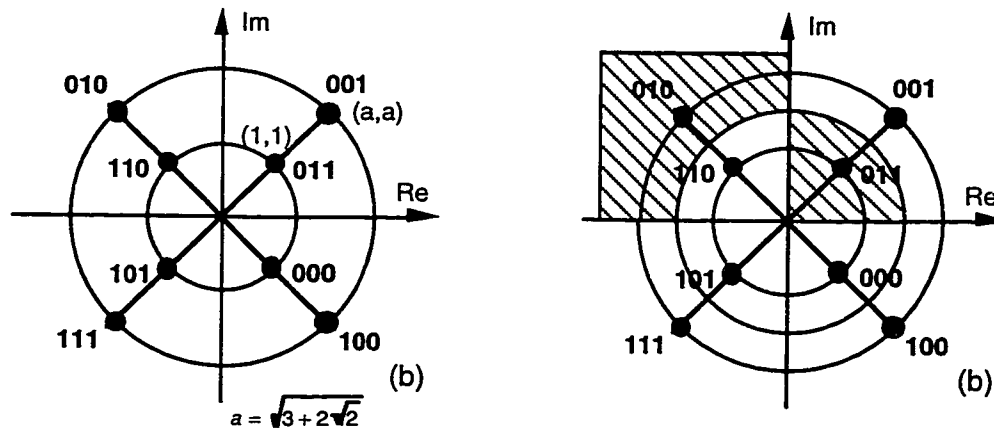


Fig 4.1.2-3 The signal constellation and demodulator for signal set (b)

Fig 4.1.2-3 shows the signal constellation and the corresponding demodulator for signal set (b). The demodulator involves both amplitude and phase detection. The circle separating the two shaded regions is also in the middle of the inner and the outer circle.

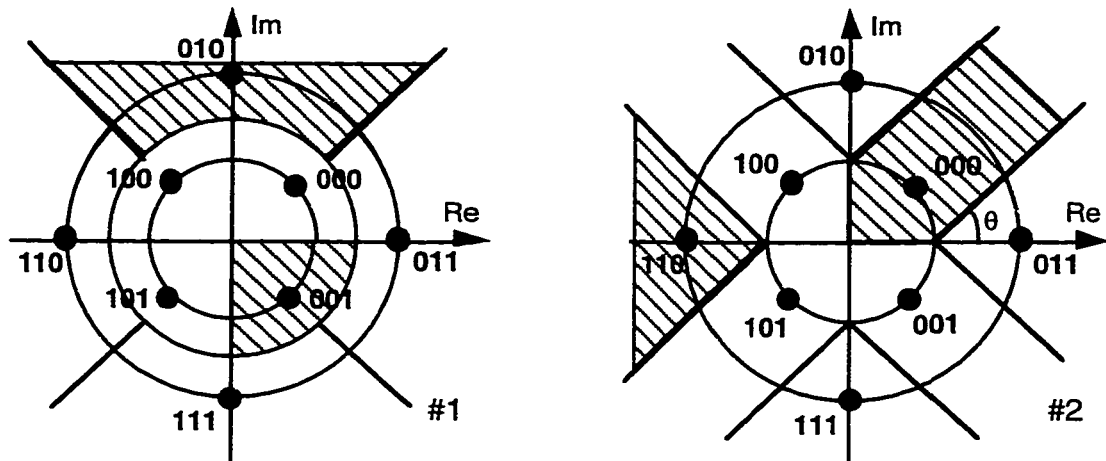


Fig 4.1.2-4 The demodulators for signal set (c)

Fig 4.1.2-4 shows two possible demodulators for signal set (c). The angle θ is set to $\pi/4$ for demodulator #2. Both demodulations involve amplitude and phase detection. This kind of demodulation is more effective and should produce better performance than amplitude or phase detection alone.

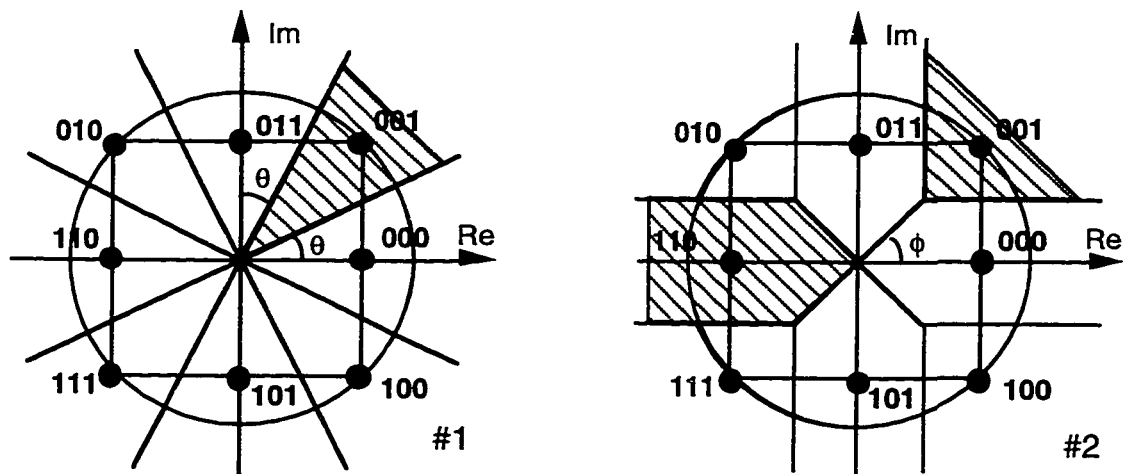


Fig 4.1.2-5 The demodulators for signal set (d)

Fig 4.1.2-5 shows two possible demodulators for signal set (d). Demodulator #1 involves phase detection only and its angle θ is equal to $\pi/8$. Demodulator #2 involves both amplitude and phase detection and its angle ϕ is equal to $\pi/4$. Thus, in terms of receiver complexity, demodulator #1 is less complicated than #2. However, the performance of demodulator #2 is slightly better than that of #1. There is a trade off between system's receiver complexity and its BER performance. The simulation results are discussed later in the section.

It is important to note that the demodulation of 8-QAM requires the estimation of the carrier phase as the information is encoded with the exact phase at the transmitter. Thus, a coherent receiver is necessary. As it is stated in Chapter 3, it is impossible to have an absolute estimate of the carrier phase for demodulation in practice. However, the computer simulation assumes a perfect estimate of the carrier phase for demodulation. The effect of the differences in signal constellations between 8-DPSK and 8-QAM is the main concern here.

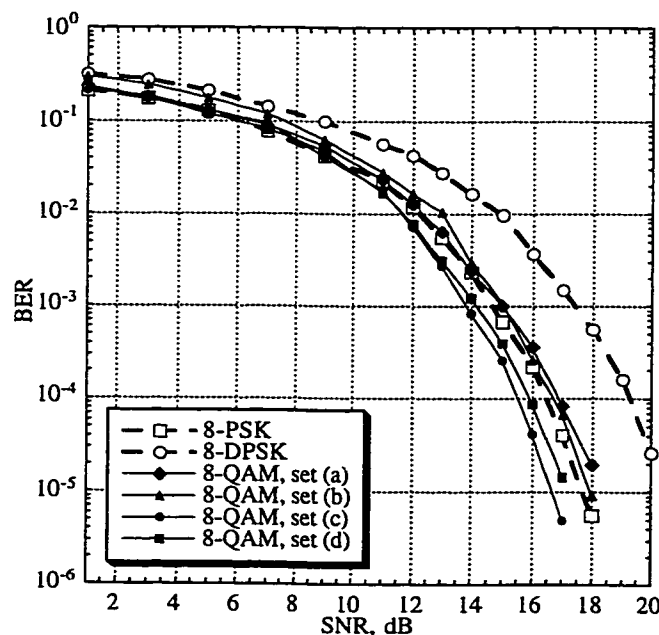


Fig 4.1.2-6 The BER for the 8-PSK, 8-DPSK and 8-QAM over an AWGN channel

A Matlab™ program was written to simulate the performance of the 8-PSK, 8-DPSK and 8-QAM without SS. In theory, the best eight-point QAM constellation, that is signal set (c) here, should have a better performance than 8-PSK by about 1-2 dB. Also, 8-PSK should have a better performance than 8-DPSK by about 3 dB. As a result, the 8-QAM, signal set (c), should have a better performance than 8-DPSK by about 4-5 dB totally. Fig 4.1.2-6 on the previous page shows that 8-QAM, signal set (c), is about 4 dB better than 8-DPSK, as predicted.

Another four Matlab™ programs corresponding to the four signal sets of 8-QAM have been written to simulate the BER performance of the $M = 16$ Wi-LAN/CSK system over an AWGN channel. The simulation results are plotted in Fig 4.1.2-7 on the next page. The BER for the $M = 16$ Wi-LAN/CSK system with 8-DPSK are also plotted for comparison. It is clear that signal set (d) has the lowest BER among the four signal sets for 8-QAM for the same SNR per symbol. Thus, signal set (d) has the best performance among the four 8-QAM signal sets. In addition, only signal set (d) has a lower BER than 8-DPSK for the same SNR per symbol. It is concluded that Wi-LAN/CSK system using signal set (d) in 8-QAM has a better performance than that using 8-DPSK. The reason for the discrepancy between the results in Fig 4.1.2-6 and Fig 4.1.2.7 is believed to be due to the fact that when the amplitude of the 8-QAM signal is lower than that for the 8-DPSK signal, the sub-symbols in the 8-QAM signal have a lower SNR than for the 8-DPSK signal which causes a degradation in performance.

Fig 4.1.2-8 on the next page shows the BER for the $M = 16$ Wi-LAN/CSK system using 8-QAM with signal set (c). The curves corresponding to the two demodulators #1 and #2 have almost the same BER. However, the BER for demodulator #2 is slightly smaller than demodulator #1.

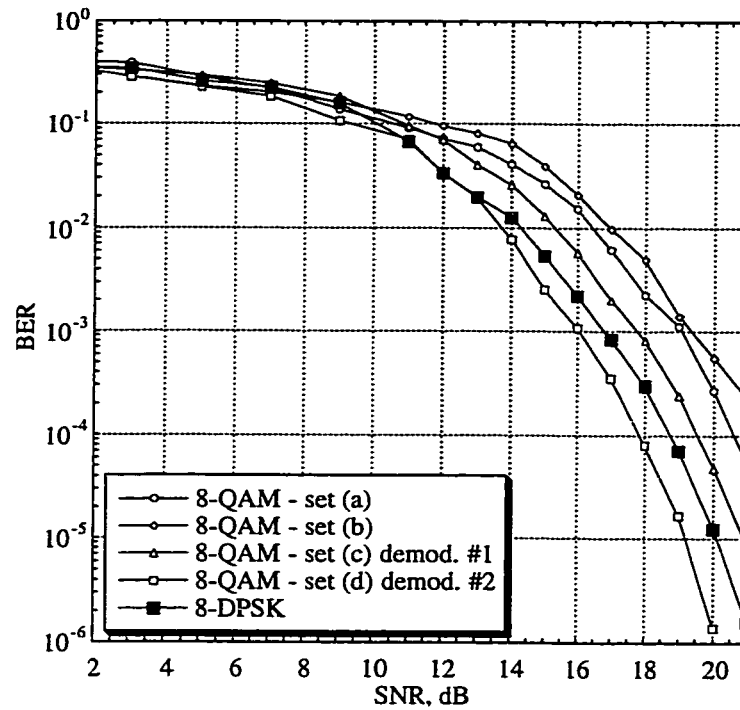


Fig 4.1.2-7 The BER for the $M = 16$ Wi-LAN/CSK systems with 8-DPSK and 8-QAM over an AWGN channel

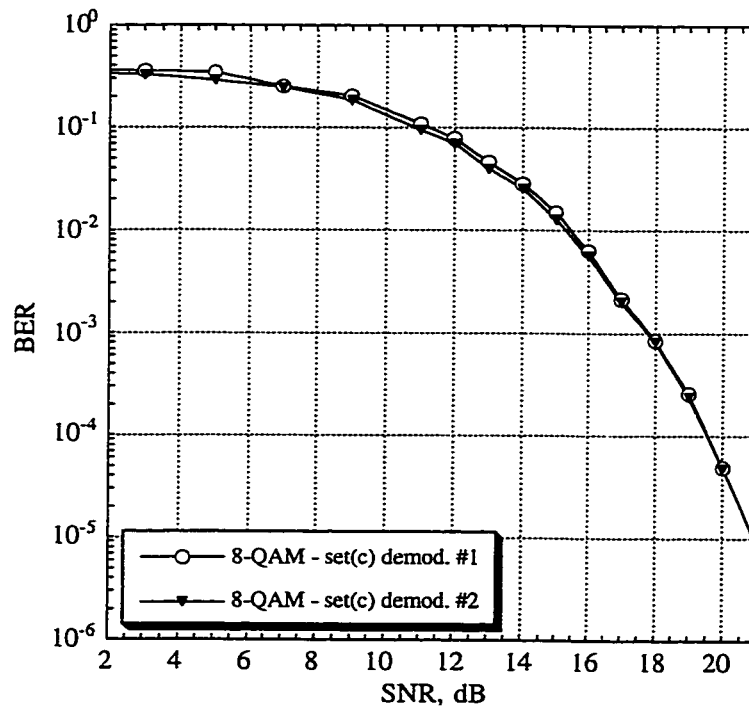


Fig 4.1.2-8 The BER for the $M = 16$ Wi-LAN/CSK system with 8-QAM signal set (c) over an AWGN channel

Fig 4.1.2-9 on the next page shows the BER for the $M = 16$ Wi-LAN/CSK system using 8-QAM with signal set (d). The curves corresponding to the two demodulators #1 and #2 mentioned have similar BER. However, the BER of demodulator #2 is a little bit lower than #1. Recall that demodulator #1 involves phase detection only while demodulator #2 involves both amplitude and phase detection. In terms of receiver complexity, they both require only one correlator in the receiver. However, demodulator #2 involves larger number of complicated computations than demodulator #1 although they can be done in a DSP chip.

Fig 4.1.2-10 on the next page shows the BER for the Barker/DSSS system, the $M = 16$ Wi-LAN/CSK systems with 8-QAM and the 8-DPSK over an AWGN channel. The BER for CSK system using 8-QAM is about 1 dB better than that using 8-DPSK. This is significantly different from the theoretical value, 4 dB. The reason is that the $M = 16$ Wi-LAN/CSK system now employs three modulation levels totally. Despite the 8-QAM gains 4 dB in SNR over the 8-DPSK in the first modulation level, the DBPSK and DQPSK in the second and the third modulation levels respectively become the weakest links now. Whenever the detected DBPSK symbol has an error, the DQPSK and the 8-QAM most likely have errors too. This causes a degradation in performance. Therefore, the $M = 16$ Wi-LAN/CSK system using 8-QAM offers only 1 dB improvement in SNR over that using 8-DPSK. Moreover, the CSK system using 8-QAM requires a coherent receiver and the phase ambiguity problem still exists. Consideration of a differential receiver for the 8-QAM signal is outside the scope of this thesis. Therefore, the 8-QAM is not recommended here and this thesis will focus on 8-DPSK rather than 8-QAM from now on.

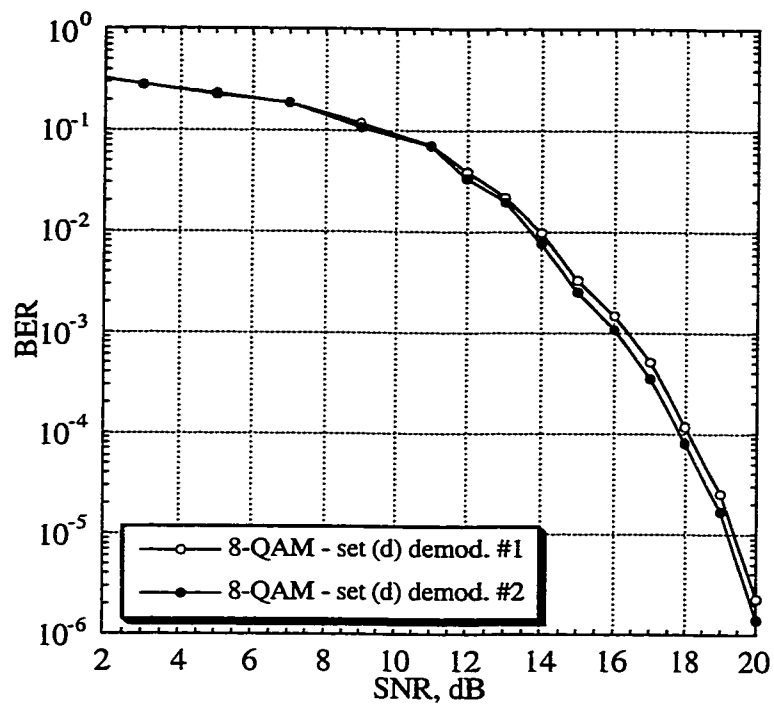


Fig 4.1.2-9 The BER for the $M = 16$ Wi-LAN/CSK system with 8-QAM signal set(d) over an AWGN channel

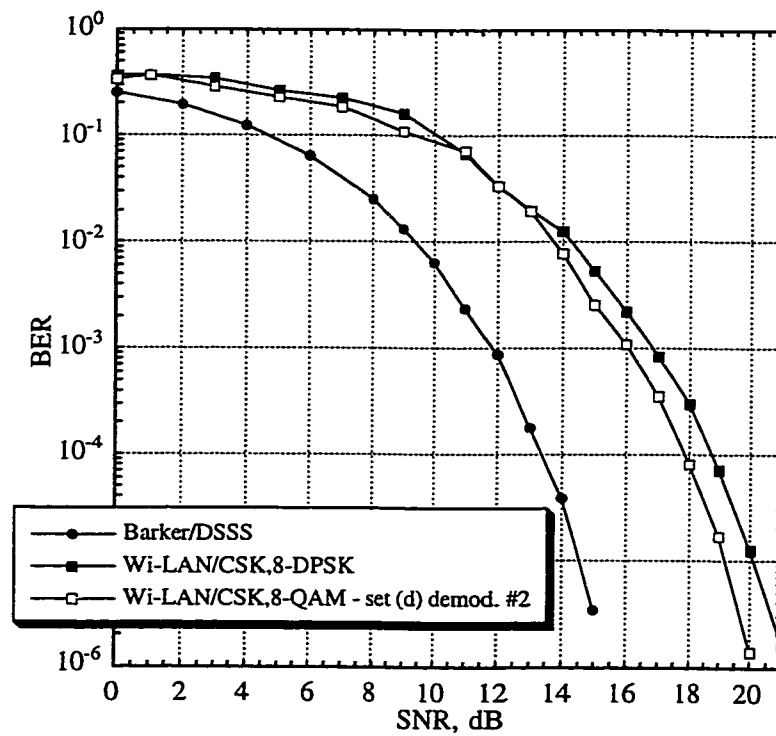


Fig 4.1.2-10 The BER for the Barker/DSSS, the $M = 16$ Wi-LAN/CSK with QAM and 8-DPSK over an AWGN channel

4.2 Introduction to TRLabs Codes (Low Complexity CSK)

Another way to increase the bit rate of a CSK system is to use a new class of CSK codes we introduce in this section and refer to as the TRLabs Codes. The TRLabs Codes are obtained through an exhaustive computer search over all possible combinations of codes within certain constraints. To be comparable to the Barker/DSSS and to the Wi-LAN/CSK, each of the TRLabs Codes is also $N = 10$ chips long.

The Wi-LAN/CSK system embeds extra data bits within the 10 chips spreading sequence by means of differential PSK phases. Each Wi-LAN Code is divided into two halves, the second half carries a binary differential phase while the first half is the reference. The TRLabs Codes are thus obtained based on this idea. However, each TRLabs Code is divided into three sections. Recall the simulation result in section 3.4, it is found that most of the bit errors encountered originate from the detection of the DQPSK symbol between adjacent PN sequences rather than the DBPSK symbol that is embedded within a PN sequence. That means the DBPSK symbol has better error protection than the DQPSK symbol. Therefore, the number of chips within each spreading sequence that is designated for the DBPSK can be reduced. As a result, each new TRLabs Code is divided into three segments with the following format:

$$\begin{aligned}\vec{C1} &= [c_1 \ c_2 \ c_3 \ \ c_4 \ c_5 \ c_6 \ c_7 \ \ c_8 \ c_9 \ c_{10}] \\ \vec{C2} &= [c_1 \ c_2 \ c_3 \ -c_4 \ -c_5 \ -c_6 \ -c_7 \ \ c_8 \ c_9 \ c_{10}] \\ \vec{C3} &= [c_1 \ c_2 \ c_3 \ \ c_4 \ c_5 \ c_6 \ c_7 \ \ -c_8 \ -c_9 \ -c_{10}] \\ \vec{C4} &= [c_1 \ c_2 \ c_3 \ -c_4 \ -c_5 \ -c_6 \ -c_7 \ \ -c_8 \ -c_9 \ -c_{10}]\end{aligned}$$

In this case, the CSK system using the TRLabs Codes has $M = 4$ possible spreading sequences $\{\vec{C1}, \vec{C2}, \vec{C3}, \vec{C4}\}$.

The CSK symbol \bar{S}_k can be expressed as follows:

$$\bar{S}_k = \xi_k [\bar{C}_{1,1} \quad \bar{C}_{1,2}e^{j\theta_k} \quad \bar{C}_{1,3}e^{j\phi_k}] = [\bar{S}_{k,1} \quad \bar{S}_{k,2} \quad \bar{S}_{k,3}] \quad (4.8)$$

where $\bar{C}_{1,1} = [c_1 \ c_2 \ c_3]$, $\bar{C}_{1,2} = [c_4 \ c_5 \ c_6 \ c_7]$ and $\bar{C}_{1,3} = [c_8 \ c_9 \ c_{10}]$, ξ_k is the k th DQPSK symbol, θ_k and ϕ_k take the value 0 or π depending on the choices of the sequences $\bar{C}_1, \bar{C}_2, \bar{C}_3$ or \bar{C}_4 , and $\bar{S}_{k,1}$, $\bar{S}_{k,2}$ and $\bar{S}_{k,3}$ are the parts of \bar{S}_k corresponding to subcodes $\bar{C}_{1,1}$, $\bar{C}_{1,2}$ and $\bar{C}_{1,3}$ respectively.

The TRLabs Codes $\{\bar{C}_1, \bar{C}_2, \bar{C}_3, \bar{C}_4\}$ are identical except that some sections are of opposite polarity according to the phases θ_k and ϕ_k . There are two levels of modulation for the CSK system using the TRLabs Codes. The relationship between the data bits and the TRLabs/CSK symbol is shown in Fig 4.2-1.

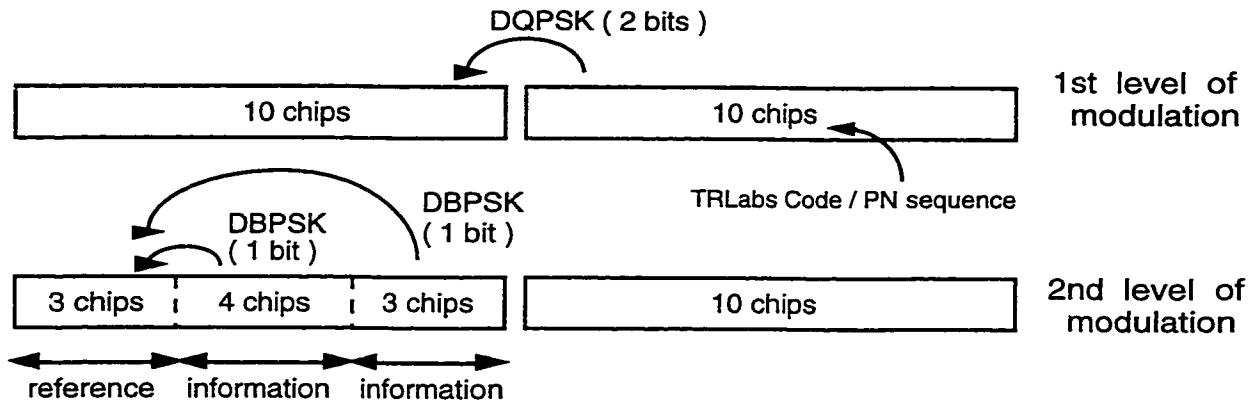


Fig 4.2-1 The relationship between data bits and the TRLabs/CSK symbols ($M = 4$)

The first level of modulation is made up of 10 chip PN sequences, which are the TRLabs Codes. The modulation scheme used here is DQPSK as it is mentioned previously. After that, each 10 chip TRLabs Code is divided into three sections as shown in Fig 4.2-1, carrying two DBPSK symbols, hence, forming the second level of modulation.

As it is stated before, the TRLabs Codes are obtained through a computer search over all possible combinations of $\bar{C}_{1,1}$, $\bar{C}_{1,2}$ and $\bar{C}_{1,3}$. Since a binary constant energy SS signal is preferred, the elements of the TRLabs Code must have a unit amplitude. For simplicity, we choose them from the set $\{1, -1, j, -j\}$ only.

Recall the definition of cross-correlation $R_{i,j}(k)$ between any two sequences C_i and C_j in section 3.3, equation (3.2) as:

$$R_{i,j}(k) = \sum_{n=1}^N C_{i,n} \cdot C_{j,n-k}^* \quad \text{for } 0 \leq k \leq N-1 \text{ and } 1 \leq i, j \leq M \quad (4.9)$$

where $\bar{C}_i = [C_{i,1} \ C_{i,2} \ \dots \ C_{i,N}]$ and $C_{i,N+k} = C_{i,k} \quad 1 \leq k \leq N, \ 1 \leq i \leq M$.

A C program was written to search for the $M = 4$ TRLabs Codes according to the following two constraints:

- (1) $R_{i,j}(0), R_{i,j}(1), \dots, R_{i,j}(4)$ are minimized for all $1 \leq i \neq j \leq M$, under the condition that $\max_{1 \leq i \neq j \leq M} \{R_{i,j}(0), R_{i,j}(1), \dots, R_{i,j}(4)\} < N/2$.
- (2) $R_{i,j}(1), R_{i,j}(2), \dots, R_{i,j}(N-1)$ are minimized for all $1 \leq i \leq M$, under the condition that the jamming margin ≥ 10 dB.

The first constraint ensures that the effects of the ICI that exist on the chosen class of channels are minimized. The chosen class of channels has a maximum ICI of 4 chips in this case. The second constraint ensures that the jamming margin dictated by part-15 rules is achieved or surpassed.

One of the TRLabs Codes that satisfies both constraints listed above is:

$$\vec{C_1} = \begin{bmatrix} -j & -j & -j & -1 & 1 & -1 & -1 & -j & -j & j \end{bmatrix}$$

where $\vec{C}_{1,1} = [-j \ -j \ -j]$, $\vec{C}_{1,2} = [-1 \ 1 \ -1 \ -1]$ and $\vec{C}_{1,3} = [-j \ -j \ j]$. Other corresponding sequences $\{\vec{C}_2, \vec{C}_3, \vec{C}_4\}$ are obtained according to the following rule:

$$\begin{aligned}\vec{C}_2 &= [\vec{C}_{1,1} \quad -\vec{C}_{1,2} \quad \vec{C}_{1,3}] \\ \vec{C}_3 &= [\vec{C}_{1,1} \quad \vec{C}_{1,2} \quad -\vec{C}_{1,3}] \\ \vec{C}_4 &= [\vec{C}_{1,1} \quad -\vec{C}_{1,2} \quad -\vec{C}_{1,3}]\end{aligned}\quad (4.10)$$

The auto-correlations and cross-correlations of the TRLabs sequences $\{\vec{C}_1, \vec{C}_2, \vec{C}_3, \vec{C}_4\}$ are shown in Fig 4.2-2 and Fig 4.2-3.

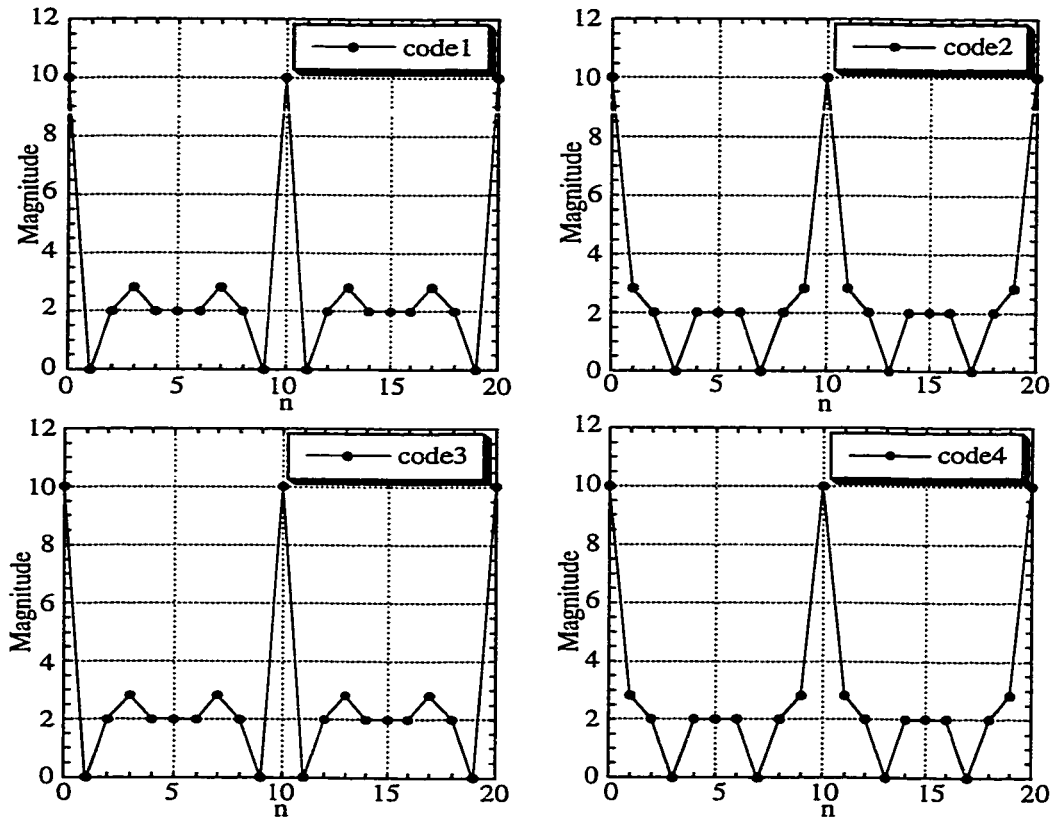


Fig 4.2-2 The auto-correlations of the M = 4 TRLabs Codes

According to Fig 4.2-2, $|R_{i,i}(1)|$, $|R_{i,i}(2)|$, ..., $|R_{i,i}(N-1)|$ for $i = 1, 2, 3, 4$ and $N = 10$ are $< N/2$ for all four TRLabs Codes. The auto-correlation $R_{i,i}(k)$ has a maximum peak

correlation value of 10 for $k = 0, \pm N, \pm 2N, \dots$ etc. Since the TRLabs Codes contain complex elements, the magnitude of the auto-correlations are considered here.

Fig 4.2-3 shows the magnitudes of cross-correlations of the $M = 4$ TRLabs Codes. It is clear that $\{|R_{i,j}(0)|, |R_{i,j}(1)|, \dots, |R_{i,j}(4)|\} < N/2$ for all $1 \leq i \neq j \leq M$. Hence, the cross-correlations between the $M = 4$ TRLabs Codes are minimized over the chosen class of channels where the maximum ICI is 4 chips only. The condition that the maximum cross-correlation between codes be smaller than $N/2$, is necessary for receivers without a RAKE nor an equalizer, otherwise the codes are indistinguishable.

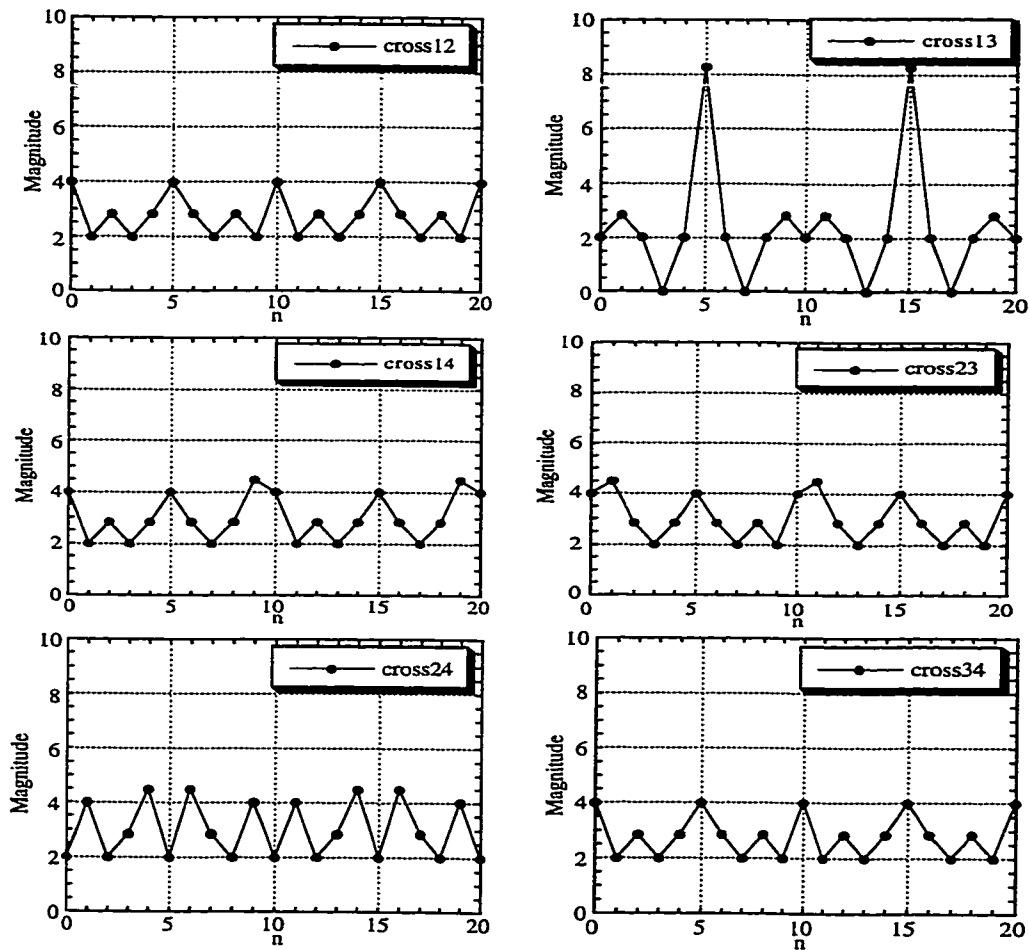


Fig 4.2-3 The cross-correlations of the $M = 4$ TRLabs Codes

The C programs which generate the TRLabs Codes and a list of the TRLabs Codes can be found in Appendix A.

The next thing to discuss is the modulation process at the transmitting end and the demodulation process at the receiving end of the CSK system. First of all, the block diagram of a transmitter for the CSK system using TRLabs Codes is shown in Fig 4.2-4.

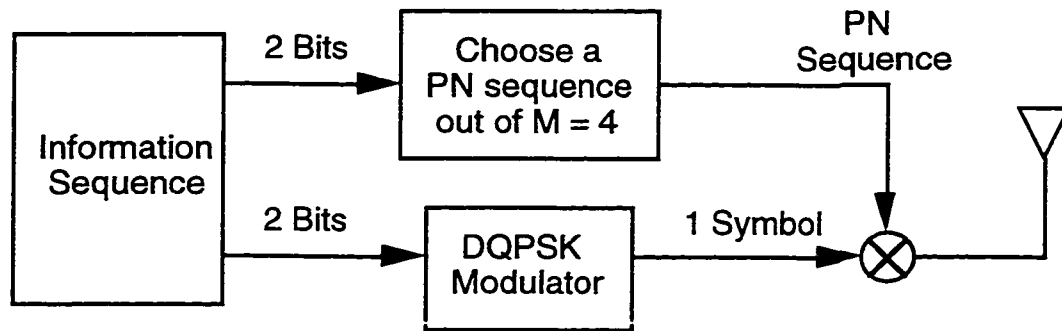


Fig 4.2-4 The transmitter of a CSK system using the $M = 4$ TRLabs Codes

At the transmitter, two bits of information are modulated by the DQPSK modulator producing a symbol, ξ_k . Another two bits of data are used to decide on the phases θ_k and ϕ_k according to the DBPSK modulation scheme, which in turn, choose one out of the $M = 4$ TRLabs Codes for spreading the modulated DQPSK symbol, ξ_k . Finally, the resulting signal, \tilde{S}_k , is then passed on to the channel through the transmitting antenna.

Since the four TRLabs Codes have identical first sections (the first 3 chips) and may have opposite polarity on their second (the following 4 chips) and third sections (the last 3 chips), only a 3-chip correlator is necessary to perform an initial-partial correlation on the first 3-chips of the received signal sequence, a 4-chip correlator to perform a second-partial correlation on the following 4-chips of the received signal sequence and another 3-chip correlator to perform a third-partial correlation on the last 3-chips of the received signal sequence.

Recall that the CSK system using the Wi-LAN Codes requires two 5-chip correlators in the receiver, performing 10 complex additions in total for each received signal sequence. In this case, the CSK system using the TRLabs Codes requires two 3-chip correlators and a 4-chip correlator, performing 10 complex additions in total for each received signal, too. Hence, in terms of receiver complexity, the CSK system using the TRLabs Codes is the same as if there were a single 10-chip correlator in the receiver.

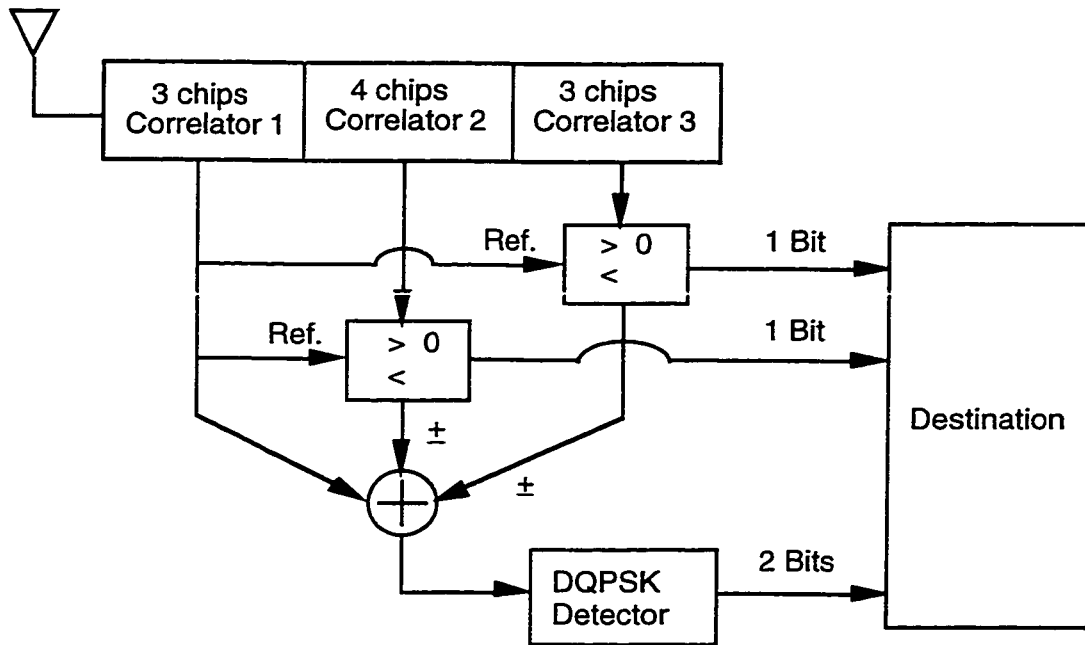


Fig 4.2-5 The receiver of a CSK system using the $M = 4$ TRLabs Codes

The block diagram of a receiver for the TRLabs/CSK system is shown in Fig 4.2-5. As soon as the partial correlations are computed as $\rho_1 = \bar{S}_{k,1} \cdot \bar{C}_{1,1}^*$, $\rho_2 = \bar{S}_{k,2} \cdot \bar{C}_{1,2}^*$ and $\rho_3 = \bar{S}_{k,3} \cdot \bar{C}_{1,3}^*$, it is easy to make a decision on $\hat{\theta}_k$ and $\hat{\phi}_k$ in order to tell which code was used for spreading the transmitted signal according to these rules:

$$\hat{\theta}_k = \begin{cases} 0 & \text{if } \text{Re}(\rho_1 \rho_2^*) \geq 0 \\ \pi & \text{if } \text{Re}(\rho_1 \rho_2^*) < 0 \end{cases} \quad \text{where } \hat{\theta}_k \text{ is the estimated } \theta_k \quad (4.11)$$

$$\hat{\phi}_k = \begin{cases} 0 & \text{if } \text{Re}(\rho_1 \rho_3^*) \geq 0 \\ \pi & \text{if } \text{Re}(\rho_1 \rho_3^*) < 0 \end{cases} \quad \text{where } \hat{\phi}_k \text{ is the estimated } \phi_k \quad (4.12)$$

Thus, two bits of data are recovered. The total correlation can be obtained by either adding or subtracting the second and the third partial-correlations to or from the first partial-correlation depending on $\hat{\theta}_k$ and $\hat{\phi}_k$ respectively. The total correlation is then demodulated by the DQPSK demodulator, recovering two bits of data. All of these complex number computations can be done in a DSP chip. As a result, the TRLabs/CSK system can transmit four bits of data in total with a 8 Mchips/s chip rate. Its bit rate is $\frac{8 \text{ Mchips/s}}{10 \text{ chips/symbol}} \times (2+1+1) \text{ bits/symbol} = 3.2 \text{ Mbps}$, where the chip rate is 8 Mchips/s with 10 chips/symbol and 4 bits/symbol.

A Matlab™ program has been written to simulate the BER performance of a CSK system using the TRLabs Codes over an AWGN channel. The simulation result is plotted in Fig 4.2-6 on the next page. The BER for the Barker/DSSS, the Barker/CSK and the Wi-LAN/CSK with $M = 2$ are also plotted on the same graph for comparison. It can be seen that the BER curve for the TRLabs/CSK system has the same waterfall shape as the other three SS systems and its BER is about 1 dB worse than that of other SS systems. This is because the number of chips for the DBPSK of the second level of modulation has been reduced. However, the bit rate for the TRLabs/CSK is now increased to 3.2 Mbps. Although there is a degradation in the BER performance, the system bit rate for a CSK system using TRLabs Codes has increased.

Since the TRLabs/CSK system requires only one N-chip correlator in the receiver, the system architecture is the same as the Barker/DSSS system. Hence, its receiver complexity

is comparable to that of the Barker/DSSS system and is less complicated than that of the conventional CSK system.

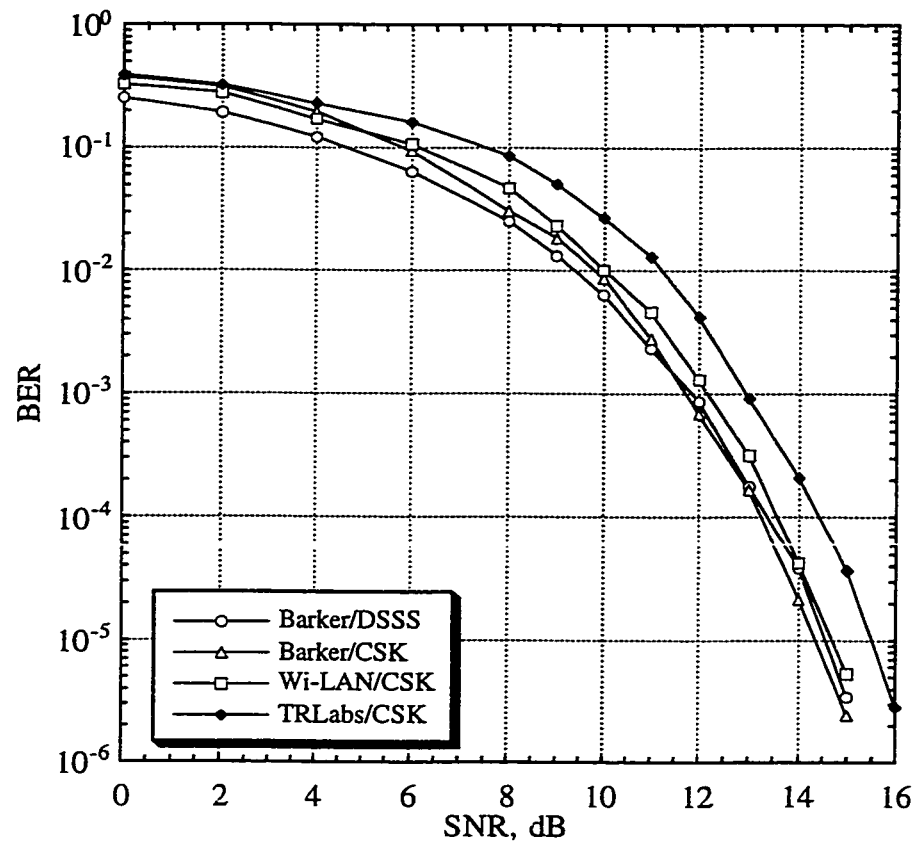


Fig 4.2-6 The BER for the Barker/DSSS, the Barker/CSK, the Wi-LAN/CSK and the TRLabs/CSK systems over an AWGN channel

SS System	Bit Rate in bits/sec	Receiver Complexity
Barker / DSSS	1.454 Mbps	1 correlator
Barker / CSK	2.182 Mbps	2 correlators
M=2 Wi-LAN / CSK	2.4 Mbps	1 correlator
M=16 Wi-LAN / CSK	2.8 Mbps	1 correlator
TRLabs / CSK	3.2 Mbps	1 correlator

Table 4.2-7 Summary of bit rate and receiver complexity of the SS systems (III)

The structure and performance of five SS systems: Barker/DSSS, Barker/CSK, $M = 2$ and $M = 16$ Wi-LAN/CSK and TRLabs/CSK have been investigated. A summary of the bit rate and receiver complexity of these SS systems is shown in Table 4.2-7 on the previous page. The system bit rates are calculated for a 8 Mc/s chip rate. An 11-chip correlator corresponds to the DSSS system while 10-chip correlator corresponds to the CSK systems.

Referring to Table 4.2-7, it can be concluded that the TRLabs/CSK system can further increase the bit rate of a transceiver over a DSSS system, it can also reduce the receiver complexity to only one N-chip correlator over the conventional CSK system which requires M N-chip correlators. Finally, the performance of a TRLabs/CSK system is still comparable to a DSSS system over an AWGN channel according to the simulation results previously shown.

A method that can improve the BER performance of a CSK system over an AWGN channel will be discussed in the next chapter.

Chapter 5

Improve the BER Performance of CSK System Over an AWGN Channel

The CSK system has proved to be capable of increasing the system bit rate. The receiver complexity can also be reduced by using a low complexity CSK system. Thus, it is important to focus on the improvement of the system performance for the low complexity CSK system over an AWGN channel.

5.1 Use Longer PN Sequences (Increase Processing Gain)

A method to improve the BER performance for a low complexity CSK system is to use longer spreading sequences. As the number of chips in a spreading sequence increases, the processing gain of the CSK system also increases, hence, the CSK system has a better performance against the jammer. Table 5.1-1 on the next page shows the existing Barker Codewords with different length [7]. The plus '+' denotes bit '1' and the minus '-' denotes bit '-1'.

Recall the CSK system using the $M = 2$ Wi-LAN Codes discussed in chapter 3, each Wi-LAN Code is $N = 10$ chips long consisting of two 5 chip subcodes. Each subcode is indeed a Barker Code. Therefore, in order to see the effect of a longer PN sequence on the performance of a CSK system, the $M = 2$ Wi-LAN/CSK systems using 7 chip and 11 chip Barker Codes as their subcodes are considered in Section 5.1.1 and 5.1.2 respectively.

N	Barker Sequence
1	+
2	++ or +-
3	++-
4	+++ - or +-+ -
5	+++ - +
7	+++ - - + -
11	+++ - - + - - + -
13	++++ + - - + + - + - +

Table 5.1-1 Barker Synchronization Codewords

5.1.1 Barker Code with 7 Chips

In this section, a CSK system using $N = 14$ chip Wi-LAN Codes is investigated. The $M = 2$ Wi-LAN Codes considered are in this format:

$$\vec{C1} = [c_1 \ c_2 \ c_3 \ c_4 \ c_5 \ c_6 \ c_7 \ c_8 \ c_9 \ c_{10} \ c_{11} \ c_{12} \ c_{13} \ c_{14}]$$

$$\vec{C2} = [c_1 \ c_2 \ c_3 \ c_4 \ c_5 \ c_6 \ c_7 \ -c_8 \ -c_9 \ -c_{10} \ -c_{11} \ -c_{12} \ -c_{13} \ -c_{14}]$$

The two Wi-LAN Codes $\{\vec{C1}, \vec{C2}\}$ are exactly the same except that the second halves of the codes are of opposite polarity. According to Table 5.1-1, each subcode of the Wi-LAN Codes $\{c_1 \ c_2 \ c_3 \ c_4 \ c_5 \ c_6 \ c_7\}$ corresponds to the 7 chip Barker Code $\{+++--+-\}$. Thus, the two actual Wi-LAN Codes used are:

$$\vec{C1} = [1 \ 1 \ 1 \ -1 \ -1 \ 1 \ -1 \ j \ j \ j \ -j \ -j \ j \ -j]$$

$$\vec{C2} = [1 \ 1 \ 1 \ -1 \ -1 \ 1 \ -1 \ -j \ -j \ -j \ j \ j \ -j \ j] \quad \text{where } j = \sqrt{-1}$$

It is important to check the auto- and cross-correlations of this type of Wi-LAN Codes. They are shown in Fig 5.1.1-1 and 5.1.1-2 on the next page.

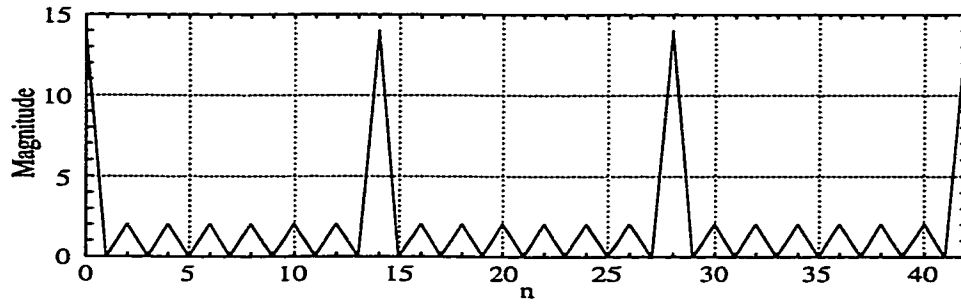


Fig 5.1.1-1 The auto-correlation of the 14 chip Wi-LAN Code

The auto-correlations of the two Wi-LAN Codes are the same. One of them is plotted in Fig 5.1.1-1. Since the code contains the complex value j , the magnitude of the correlations are considered here. The Wi-LAN Codes exhibit a periodic auto-correlation $R_{i,i}(k)$ with values $|R_{i,i}(k)| = N$ for $k = 0, \pm N, \pm 2N, \dots$, and $|R_{i,i}(k)| = 0$ or 2 for all other k 's, where $i = 1$ or 2 . It is clear that the maximum out-of-phase auto-correlation of the $N = 14$ chips Wi-LAN Codes is smaller than $N/2$.

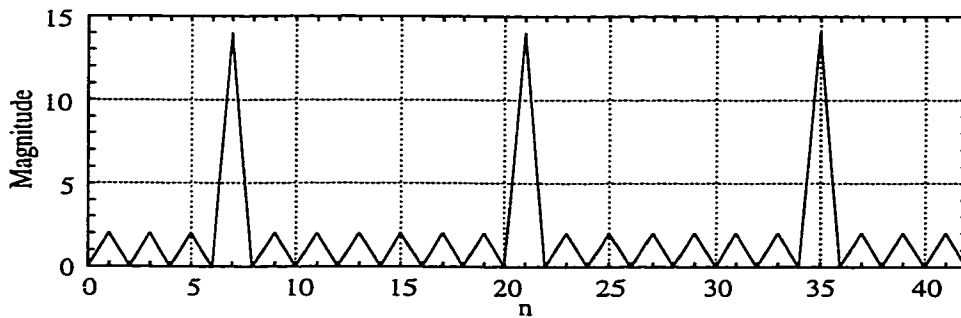


Fig 5.1.1-2 The cross-correlation of the two 14 chip Wi-LAN Codes

The cross-correlation between the two Wi-LAN Codes is plotted in Fig 5.1.1-2. The Wi-LAN Codes exhibit a periodic cross-correlation $R_{i,j}(k)$ again, but with values $|R_{i,j}(k)| = N$ for $k = 7, \pm(N+7), \pm(2N+7), \dots$, and $|R_{i,j}(k)| = 0$ or 2 for all other k 's. Since the subcodes are now 7 chips long, the peak cross-correlation values occur at $k = 7, N+7, 2N+7, \dots$, instead of $k = 0, N, 2N$. This means that the maximum ICI allowed for this

Wi-LAN/CSK system is 6 chips. The CSK system requires either a RAKE receiver or an equalizer in the receiving end when the ICI of the channel is larger than 6 chips.

The transmitter and receiver of a CSK system using the $N = 14$ chip Wi-LAN Codes are the same as that using the $N = 10$ chip Wi-LAN Codes, except the 5-chip correlators are now replaced by the 7-chip correlators at the receiver. Each 7-chip correlator performs 7 complex additions, thus, there are 14 complex additions in total for each received signal. It is the same as if there were a single 14-chip correlator in the receiver. In terms of receiver complexity, although correlators with a larger number of chips are required, two 7-chips correlators are necessary in total at the receiver no matter how many Wi-LAN Codes are used in the set. This is the characteristic of the low complexity CSK system where the receiver complexity is reduced from M N -chip correlators down to one N -chip correlator.

The CSK system using the $N = 14$ chip Wi-LAN Codes with $M = 2$ are transmitting three bits of information with a 8 Mchips/s chip rate. Thus, its bit rate is $\frac{8 \text{ Mchips/s}}{14 \text{ chips/symbol}} \times (2+1) \text{ bits/symbol} = 1.714 \text{ Mbps}$, where the chip rate is 8 Mchips/s, with 14 chips/symbol and 3 bits/symbol. Recall that the CSK system using the $N = 10$ chip Wi-LAN Codes with $M = 2$ are again transmitting three bits of information with a 8 Mchips/s chip rate. However, it has a bit rate of 2.4 Mbps. Hence, we would expect that the CSK system using the longer PN sequences as the spreading codes would result in a lower system bit rate.

In order to see the effect of the processing gain on a SS system, the performance of an N chip Wi-LAN/CSK system is analyzed. The SNR, γ_b , required to achieve a specified error rate performance is defined as:

$$\gamma_b = \frac{\xi_b}{J_o} = \frac{P_{av} / R}{J_{av} / W} = \frac{W / R}{J_{av} / P_{av}} \quad (5.1)$$

where ξ_b is the signal energy per bit, J_o is the power spectral density for the jamming signal, R is the information rate in bits/s, W is the channel bandwidth in Hz, P_{av} is the average signal power and J_{av} is the average jamming power. J_{av} / P_{av} is the jamming-to-signal power ratio and $W / R = T_b / T_c = B_e = L_c$ is just the bandwidth expansion factor, or, equivalently, the processing gain of the SS system.

The probability of error for a SS system is inversely proportional to the exponential function of its SNR, $P_e \propto \exp(-\gamma_b)$. Therefore, the improvement in BER performance can be expressed as the ratio of the SNRs of two CSK systems theoretically:

$$10 \log\left(\frac{\gamma_{b2}}{\gamma_{b1}}\right) = 10 \log\left(\frac{W / R_2}{W / R_1}\right) = 10 \log\left(\frac{N_2}{N_1}\right) \quad (5.2)$$

In this case, the Wi-LAN/CSK system using $N_1 = 10$ chips is compared to that using $N_2 = 14$ chips. The extra processing gain is predicted to be $10 \log(N_2/N_1) = 1.46$ dB.

5.1.2 Barker Code with 11 Chips

In this section, the CSK system using the $N = 22$ chip Wi-LAN Codes is investigated. The $M = 2$ Wi-LAN Codes considered are in this format:

$$\begin{aligned} \vec{C1} &= [c_1 \ c_2 \ c_3 \ c_4 \ c_5 \ c_6 \ c_7 \ c_8 \ c_9 \ c_{10} \ c_{11} \ c_{12} \ c_{13} \ c_{14} \ c_{15} \ c_{16} \ c_{17} \ c_{18} \ c_{19} \ c_{20} \ c_{21} \ c_{22}] \\ \vec{C2} &= [c_1 \ c_2 \ c_3 \ c_4 \ c_5 \ c_6 \ c_7 \ c_8 \ c_9 \ c_{10} \ c_{11} \ -c_{12} \ -c_{13} \ -c_{14} \ -c_{15} \ -c_{16} \ -c_{17} \ -c_{18} \ -c_{19} \ -c_{20} \ -c_{21} \ -c_{22}] \end{aligned}$$

The two Wi-LAN Codes $\{\bar{C}_1, \bar{C}_2\}$ are exactly the same except that the second halves of the codes are of opposite polarity. According to Table 5.1-1, each subcode of the $N = 22$ chip Wi-LAN Codes $\{C_1 C_2 C_3 C_4 C_5 C_6 C_7 C_8 C_9 C_{10} C_{11}\}$ corresponds to the 11 chip Barker Code $\{+ + + - - - + - - + -\}$.

The two Wi-LAN Codes are:

$$\begin{aligned}\vec{C}_1 &= [1 \ 1 \ 1 \ -1 \ -1 \ -1 \ 1 \ -1 \ -1 \ 1 \ -1 \ j \ j \ j \ -j \ -j \ -j \ j \ -j \ -j \ j \ -j] \\ \vec{C}_2 &= [1 \ 1 \ 1 \ -1 \ -1 \ -1 \ 1 \ -1 \ -1 \ 1 \ -1 \ -j \ -j \ -j \ j \ j \ j \ -j \ -j \ -j \ j \ j]\end{aligned}$$

where $j = \sqrt{-1}$.

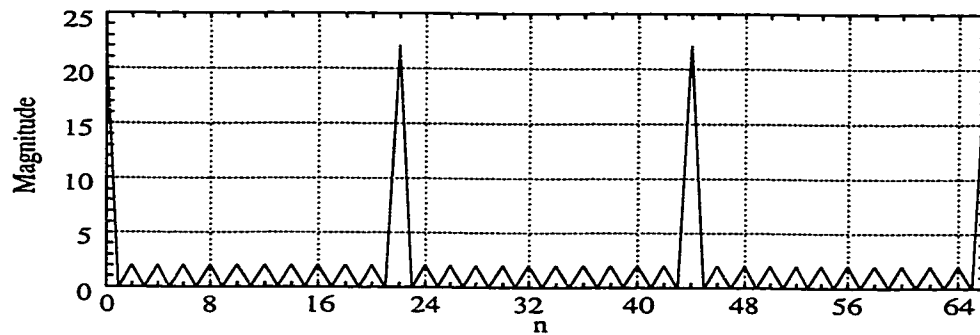


Fig 5.1.2-1 The auto-correlation of the 22 chip Wi-LAN Code

The auto-correlations of the two Wi-LAN Codes are the same. Again, one of them is plotted in Fig 5.1.2-1. The magnitude of the correlation is used here. The $N = 22$ chip Wi-LAN Code exhibits a periodic auto-correlation $R_{i,j}(k)$ with values $|R_{i,j}(k)| = N$ for $k = 0, \pm N, \pm 2N, \dots$, and $|R_{i,j}(k)| = 0$ or 2 for all other k 's, where $i = 1$ or 2 . The maximum out-of-phase auto-correlation of the $N = 22$ chip Wi-LAN Code is much smaller than $N/2$.

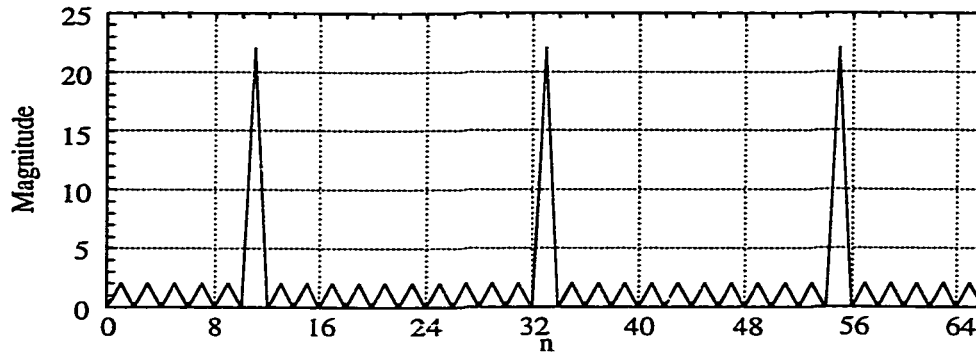


Fig 5.1.2-2 The cross-correlation of the 22 chip Wi-LAN Codes

The cross-correlation between the two Wi-LAN Codes is plotted in Fig 5.1.2-2. It is similar to that for the $N = 14$ chip Wi-LAN Codes, but with the peak values $|R_{i,j}(k)| = N$ for $k = 11, \pm(N+11), \pm(2N+11), \dots$, and $|R_{i,j}(k)| = 0$ or 2 for all other k 's. Since the subcodes are now 11 chips long, the peak cross-correlation values occur at $k = 11, N+11, 2N+11, \dots$, instead of $k = 0, N, 2N$. This means that the maximum ICI allowed for this Wi-LAN/CSK system is 10 chips. The CSK system requires either a RAKE receiver or an equalizer in the receiving end when the ICI of the channel is larger than 10 chips.

The transmitter and receiver of a CSK system using the $N = 22$ chip Wi-LAN Codes are the same as that using the $N = 10$ chip and the $N = 14$ chip Wi-LAN Codes, except that they use now 11-chip correlators at the receiver. Each 11-chip correlator performs 11 complex additions, thus, there are 22 complex additions in total for each received signal. It is the same as if there were a single 22-chip correlator in the receiver. In terms of receiver complexity, although correlators with a larger number of chips are used here, two 11-chip correlators are necessary in total at the receiver no matter how many Wi-LAN Codes are used in the set. The low complexity CSK system reduces the receiver complexity from M N -chip correlators down to one N -chip correlator.

The CSK system using the $N = 22$ chip Wi-LAN Codes with $M = 2$ is transmitting three bits of information with a 8 Mchips/s chip rate again. Thus, its bit rate is

$$\frac{8 \text{ Mchips / s}}{22 \text{ chips / symbol}} \times (2 + 1) \text{ bits / symbol} = 1.091 \text{ Mbps}, \text{ where the chip rate is 8 Mchips/s}$$

with 22 chips/symbol and 3 bits/symbol. Recall that the CSK system using the $N = 10$ chip Wi-LAN Codes with $M = 2$ has a bit rate of 2.4 Mbps while using the $N = 14$ chip Wi-LAN Codes has a bit rate of 1.714 Mbps. Hence, it is clear that the system bit rate is inversely proportional to the length of the spreading sequences used.

In this case, a $N_1 = 10$ chip Wi-LAN/CSK system is compared to a $N_2 = 22$ chip Wi-LAN/CSK system. The extra processing gain is predicted to be $10\log(N_2/N_1) = 3.42$ dB.

N chips Wi-LAN Codes	Bit rate in bits/ sec	Improvement in processing gain over $N = 10$ Wi-LAN Codes
10	2.4 Mbps	reference
14	1.714 Mbps	~ 1.5 dB
22	1.091 Mbps	~ 3.5 dB

Table 5.1.2-4 Summary of bit rate and improvement in SNR for different N chip Wi-LAN/CSK systems

In conclusion, a CSK system with longer spreading codes can increase its processing gain, which in turn, improves its BER performance over an AWGN channel. This is achieved at the expense of the system bit rate as it is shown in Table 5.1.2-4. A longer spreading code can be used in those applications where the performance of a CSK system is the main concern. However, there is always a trade off between the system bit rate and its performance.

Chapter 6

CSK System Over Multipath Channel

Upon this time, the structure and performance of the DSSS system and the CSK systems using different class of spreading codes over an AWGN channel have been investigated already. The performances of these SS systems over multipath channels are considered now. First, the model of a multipath channel is discussed in Section 6.1. Then, the performance of the DSSS system over the multipath channel is investigated in Section 6.2. The CSK system using the Wi-LAN Codes is discussed in Section 6.3 and the CSK system using the TRLabs Codes is discussed in Section 6.4.

6.1 Multipath Channel Model

In wireless communications, a single line-of-sight (LOS) path between the transmitting and receiving antennas rarely exists. Instead, the signal propagates through many different paths which include reflections from walls, ceilings, and other obstacles to get to the receiver. As a result, the received signal consists of many multipath components, each with a different phase and of a different amplitude. Since all propagation paths are not of the same length, each multipath signal will arrive with a certain time delay (forming the time delay spread) with respect to the shortest path. Fig 6.1.1 on the next page shows the two multipaths model.

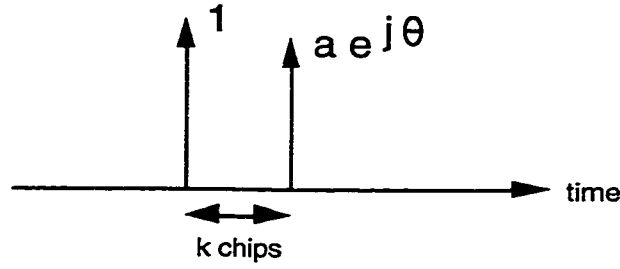


Fig 6.1-1 The multipath model

The multipath channel has an impulse response $h(t)$ defined as:

$$h(t) = \delta(t) + a e^{j\theta} \delta(t - \tau_{ex}) \quad (6.1)$$

where $a e^{j\theta}$ is the complex gain of the multipath component, τ_{ex} is the excess delay in time and k is the corresponding number of chips delay. In this thesis, two worst cases are considered where the multipath channels have values $a = 0.99$ and $\theta = 0$ or π in radian. The number of chip delay k is allowed to be equal to 1, 2, ..., N-1. The corresponding time excess delay, τ_{ex} , is kT_c where T_c is the chip duration of the SS system with a 8 Mchips/s chip rate ($T_c = 1 / 8 \text{ Mchips/s} = 125 \text{ ns}$). The performances of the SS systems without a RAKE receiver nor an equalizer are considered in the following section.

6.2 DSSS System using Barker Code

A Barker/DSSS system uses the same spreading sequence for all the transmitting SS signals. Recall that the 11 chip Barker Code used has a periodic auto-correlation $R(k)$ with values $R(k) = N$ for $k = 0, \pm N, \pm 2N, \dots$, and $R(k) = -1$ for all other k 's. This means that it is robust against an excess delay of up to $11 T_c = 11 \text{ chips} / 8 \text{ Mchips/s} = 1.375 \mu\text{s}$. This can be proved by simulating the Barker/DSSS system over the multipath channel.

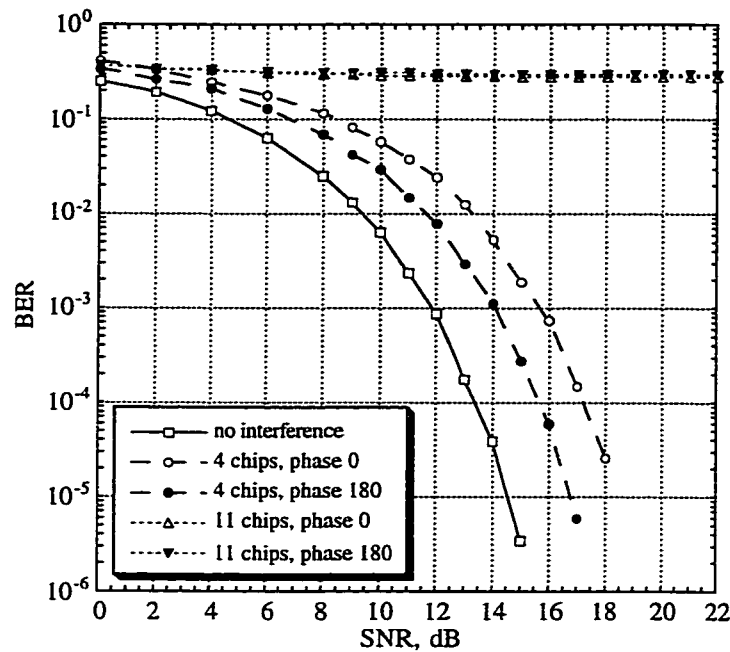


Fig 6.1-2 The BER for the Barker/DSSS over the multipath channel

In Fig 6.1-2, the BER for the DSSS system using the Barker Code over multipath channels are plotted. The BER for the Barker/DSSS over an AWGN channel without any interference is also plotted for comparison. Two types of multipath channels have been simulated. The first type of channel has the multipath delayed by 4 chips while the second type of channel has the multipath delayed by 11 chips. The chosen amplitude attenuation and phase are $a = 0.99$ and $\theta = 0^\circ$ or 180° respectively for both types of channels.

When the multipath is delayed by 4 chips, the current received SS signal contains not only the original SS signal, but also a portion of the previous SS signal and a portion of the delayed version of the current SS signal. Thus, both ICI and ISI are present in the received signal. The random-pattern introduced into the transmitted signal by the spreading process can remove parts of the undesired signals in the despreading process. However, the original signal and the resulting undesired signal may still add up either constructively or

destructively depending on the phase θ of the multipath channel and the DQPSK symbol between successive transmitted signals. Hence, the BER for the Barker/DSSS with multipath delayed by 4 chips with phase $\theta = 0^\circ$ is about 3.8 dB worse than that over AWGN channel while the BER with phase $\theta = 180^\circ$ is about 2 dB. The degradation in performance is still acceptable.

On the other hand, when the multipath is delayed by 11 chips, which is equal to the length of the spreading code, the received SS signal and its replica generated by the multipath channel are exactly one symbol off. It means that the received SS signal contains the original SS signal as well as the previous attenuated SS signal. The ISI is present in the received signal. Since the auto-correlation of the Barker Code has values $R(k) = N$ for $k = 0, \pm N, \pm 2N, \dots$ etc., it is impossible to remove the undesired signal from the received signal because it has the same random-pattern as the desired signal. Thus, there is no way to extract the correct data from the received signal. Hence, the BER is almost constant meaning that it will not change with increasing SNR. In this case, a RAKE receiver or an equalizer is necessary at the receiving end.

6.3 CSK System using Wi-LAN Codes

6.3.1 $M = 2$ Wi-LAN Codes

In Section 3.4, the auto- and cross-correlations of the $M = 2$ Wi-LAN Codes have been considered. Recall that its cross-correlation is periodic with values $|R_{i,j}(k)| = N$ for $k = 5, \pm(N+5), \pm(2N+5), \dots$, and $|R_{i,j}(k)| = 0$ or 2 for all other k 's. This means that the CSK system using the $M = 2$ Wi-LAN Codes is robust against a maximum ICI of 4 chips.

The CSK system requires a RAKE receiver or an equalizer when the ICI is larger than 4 chips.

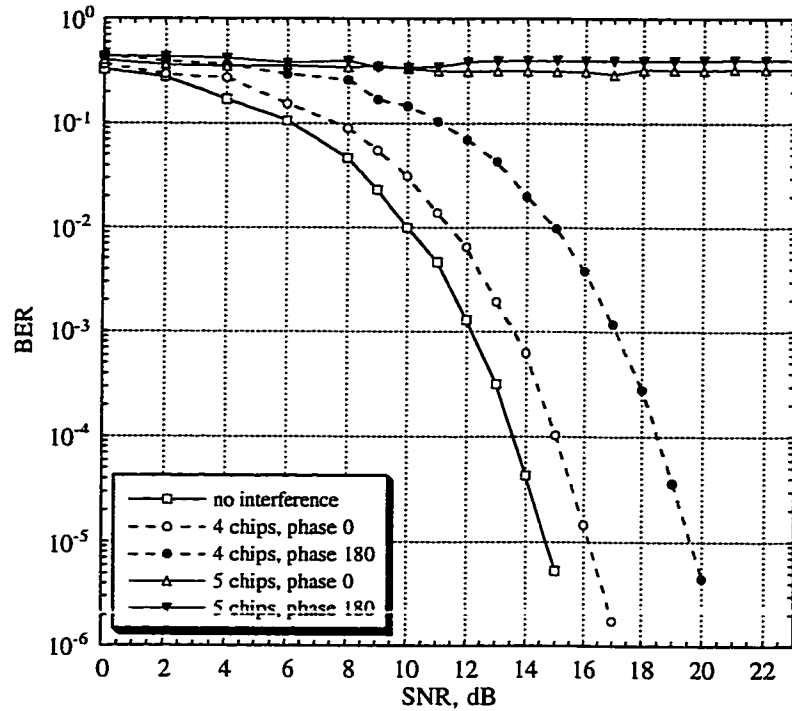


Fig 6.3.1-1 The BER for the $M = 2$ Wi-LAN/CSK over the multipath channel

A Matlab™ program has been written to simulate the $M = 2$ Wi-LAN/CSK system over the multipath channel. The results are plotted in Fig 6.3.1-1. The BER for the $M = 2$ Wi-LAN/CSK system over an AWGN channel is also plotted on the same graph for comparison. Again, two types of multipath channels have been simulated. They are the multipath channels with 4 and 5 chips delay. The complex gain $ae^{j\theta}$ of the multipath components have values of $a = 0.99$ and $\theta = 0^\circ$ and 180° .

In this case, the BER for the Wi-LAN/CSK system with multipath delayed by 4 chips and phase $\theta = 0^\circ$ is about 1.5 dB worse than that over an AWGN channel while the BER with phase $\theta = 180^\circ$ is about 5 dB worse than that over an AWGN channel. The second case may need a RAKE receiver or equalizer at the receiving end.

Recall that the two Wi-LAN Codes $\{\bar{C}_1, \bar{C}_2\}$ used are 10 chip long and can be divided into two subcodes $\bar{C}_{1,1} = [c_1 \ c_2 \ c_3 \ c_4 \ c_5]$ and $\bar{C}_{1,2} = [c_6 \ c_7 \ c_8 \ c_9 \ c_{10}]$.

The two Wi-LAN Codes $\{\bar{C}_1, \bar{C}_2\}$ are identical except that the second halves are of opposite polarity. Moreover, the two subcodes have the same pattern and the chips within $\bar{C}_{1,1}$ and $\bar{C}_{1,2}$ are different by $-j$ or $-\pi/2$. It is illustrated as follows:

$$\begin{aligned} \bar{C}_{1,1} &= [1 \ -1 \ 1 \ 1 \ 1] \\ \bar{C}_{1,2} &= -j \times \bar{C}_{1,1} = [-j \ j \ -j \ -j \ -j] \end{aligned} \quad \text{where } j = \sqrt{-1} \quad (6.2)$$

This explains why the peak cross-correlation values $|R_{i,j}(k)| = N$ occurs at $k = 5$, $\pm(N+5)$, $\pm(2N+5)$, ... etc.. When the multipath is delayed by 5 chips, the attenuated multipath components corrupt the received signal completely. Hence, the BER for the Wi-LAN/CSK system with multipath delayed by 5 chips stays constant even with increasing SNR. Obviously, a RAKE receiver or an equalizer is required.

6.3.2 M = 16 Wi-LAN Codes

The performance of the M = 16 Wi-LAN/CSK system over an AWGN channel has been discussed in Chapter 4. Its performance over a multipath channel is considered now. Since the N = 20 chip spreading sequences used in the M = 16 Wi-LAN/CSK system are made up of the N = 10 chip Wi-LAN Codes, both Wi-LAN Codes have similar cross-correlation. The M = 16 Wi-LAN Codes have peak cross-correlation values $|R_{i,j}(k)| = N$ at $k = \pm 5, \pm 10, \pm 15, \pm(N+5), \dots$. This means that this CSK system requires a RAKE receiver or an equalizer at these particular values of k . The performances of the CSK

system with a RAKE receiver and an equalizer implemented will be discussed in the next chapter.

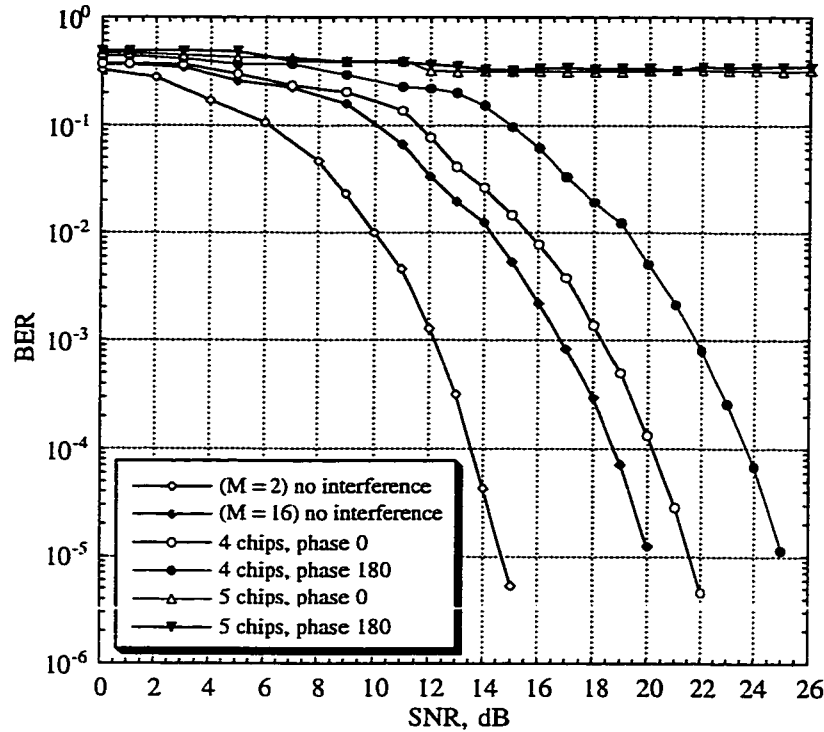


Fig 6.3.2-1 The BER for the $M = 16$ Wi-LAN/CSK over the multipath channel

A Matlab™ program has been written to simulate the $M = 16$ Wi-LAN/CSK system over multipath channels where the multipaths are delayed by 4 and 5 chips. Again, the complex gain $ae^{j\theta}$ of the multipath components have values of $a = 0.99$ and $\theta = 0^\circ$ and 180° . The results are plotted in Fig 6.3.2-1. The BERs for the $M = 2$ and the $M = 16$ Wi-LAN/CSK systems over an AWGN channel are also plotted there for comparison.

When the multipath is delayed by 4 chips with phase $\theta = 0^\circ$ and 180° , the BER for the $M = 16$ Wi-LAN/CSK system is about 1.5 dB and 5 dB worse than that over the AWGN channel, respectively. The second case may need a RAKE receiver or an equalizer. When the multipath is delayed by 5 chips with phase $\theta = 0^\circ$ and 180° , the BER is constant

against SNR. In this case, it is impossible to extract the data from the received signal without a RAKE receiver or an equalizer.

6.4 CSK System using TRLabs Codes

The TRLabs Codes are also $N = 10$ chips long. However, their cross-correlations are periodic, but not symmetric. Each correlation value $|R_{i,j}(k)|$ has a different magnitude. The largest and smallest cross-correlation values $|R_{i,j}(k)|$ are 4.4721 and 0, respectively. Thus, there are large differences between the system BERs with various multipath delay. A Matlab™ program was written to simulate the TRLabs/CSK system over various multipath channels. Again, the complex gain $ae^{j\theta}$ of the multipath components have values $a = 0.99$ and $\theta = 0^\circ$ and 180° . The simulation results are plotted in Fig 6.4-1 and Fig 6.4-2.

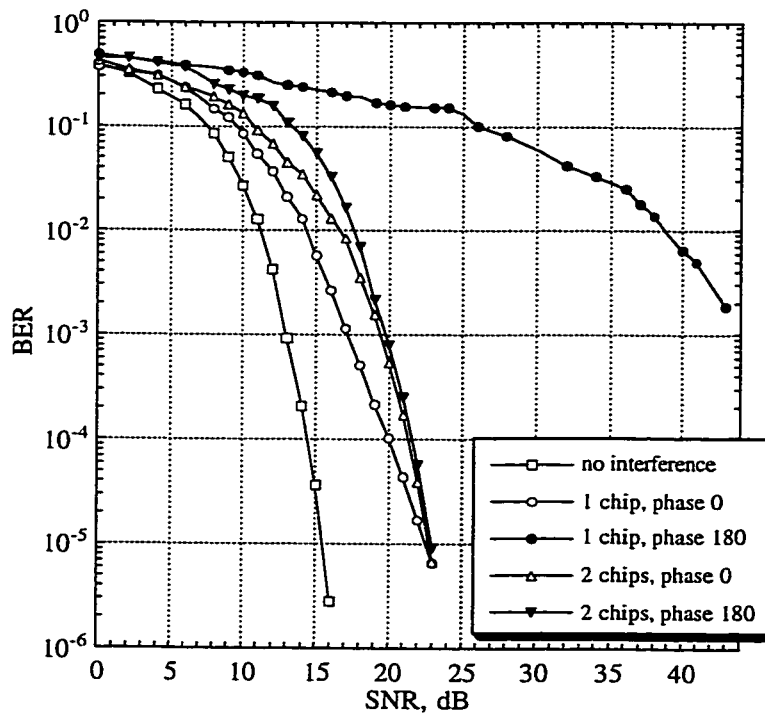


Fig 6.4-1 The BER for the TRLabs/CSK over the multipath channel (1 and 2 chips delay)

In Fig 6.4-1, the BERs for the TRLabs/CSK system over an AWGN channel and two-multipath channels with multipath delayed by 1 and 2 chips are plotted. It is noticed that when the multipath is delayed by 1 chip with phase $\theta = 180^\circ$, the BER is very poor compared to that with phase $\theta = 0^\circ$. Besides, when the multipath is delayed by 2 chips, the BER is about 7 dB worse than that over AWGN channel for both phases. Thus, it is definitely necessary to have a RAKE receiver or an equalizer at the receiving end when the multipath is delayed by 1 chip with phase $\theta = 180^\circ$.

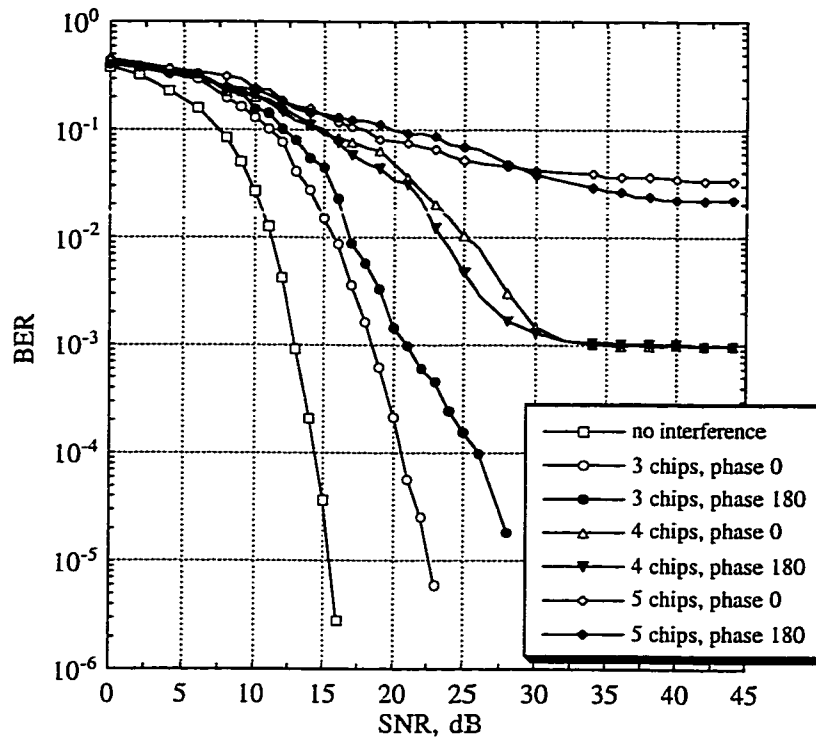


Fig 6.4-2 The BER for the TRLabs/CSK over the multipath channel (3 to 5 chips delay)

In Fig 6.4-2, the BERs for the TRLabs/CSK system over an AWGN channel and two-multipath channels with multipath delayed by 3, 4 and 5 chips are plotted. It can be seen that the BERs for the multipath channel with 3 chip delay are very different for the two phases $\theta = 0^\circ$ and 180° . When the multipath is delayed by 4 chips, the BER curves for

both phases are leveling off at about 30 dB. On the other hand, when the multipath is delayed by 5 chips, the BER curves have similar values for both phases. They decrease slowly with increasing SNR until SNR \approx 35 dB. Then, the BERs stay almost constant regardless of the increasing SNR. For both cases, the BER cannot be reduced further by increasing the SNR. This happens because the interference caused by the multipath components is so high that even in the absence of channel noise, there is a non-zero probability of error. Clearly, the TRLabs/CSK system requires a RAKE receiver or an equalizer at the receiving end when the multipath channels are delayed by 4 and 5 chips.

The performances of the DSSS system using the Barker Codes, the CSK systems using the Wi-LAN Codes and the TRLabs Codes over two multipath channels have been investigated. Some of the BERs of these systems for the investigated multipath channels are unacceptable and either a RAKE receiver or an equalizer are necessary to maintain a satisfactory performance. Both the RAKE receiver and the equalizer are discussed in the next chapter.

Chapter 7

Improve the Performance of a CSK System Over the Multipath Channel using Different Algorithms in the Receiver

In addition to noise, communications through multipath channels are subject to multipath fading and ISI. Up to now, several techniques have been developed to avoid such degradations such as equalization and frequency diversity. DSSS is resistant to multipath because of its inherent frequency diversity. A correlation receiver can separate the contribution of each path, and the peaks corresponding to the different channel paths can be readily detected and diversity combined to improve reception. This can be achieved with a RAKE receiver. Thus, the structures of a Decision-Feedback-Equalizer (DFE) and a RAKE receiver are discussed in Section 7.1 and 7.2 respectively. Moreover, Viterbi Algorithm is also considered in Section 7.3 for further improving the performance of the SS systems over multipath channels. Following the description of the above techniques, computer simulation results for the DSSS and CSK systems are presented.

7.1 Decision-Feedback-Equalizer (DFE)

7.1.1 Background

Wireless communication channels have time-variant frequency responses. Thus, it is impossible to design an optimum fixed demodulation filters. Channel distortion induced by the multipath channel, which is not known a priori, and AWGN, results in ISI. If the ISI is left uncompensated, it causes high error rates. The solution to the ISI problem is to design

a receiver that employs a means for compensating or reducing the ISI in the received signal. The compensator for the ISI is called an equalizer.

An equalization method that exploits the use of previously detected symbols to suppress the ISI in the present symbol being detected is called DFE [9]. In general, the DFE consists of two filters, a feedforward filter (FFF) and a feedback filter (FBF). Both filters have taps spaced at the chip interval T_c as SS signals are used here. The structure of a DFE is shown in Fig 7.1.1-1 on the next page [8]. The DFE has N_1+N_2+1 taps in the FFF and N_3 taps in the FBF, and its output can be expressed as:

$$\hat{d}_k = \sum_{n=-N_1}^{N_2} C_n^* \cdot y_{k-n} + \sum_{i=1}^{N_3} F_i^* \cdot d_{k-i} \quad (7.1)$$

where C_n^* and y_n are tap gains and the inputs, respectively, to the forward filter, F_i^* are tap gains for the feedback filter, and d_i ($i < k$) is the previous decision made on the detected signal. It should be observed that the DFE is nonlinear because the feedback filter contains previously detected symbols $\{d_i\}$.

Since the first incoming signal has been assumed to be the strongest signal, and the system is locked onto it during the synchronization process, ISI only induces feedback terms on the received signal over the multipath channel. Thus, the FFF can be ignored in the computer simulations.

The FBF has as its input a sequence of previously detected symbols. Functionally, the feedback filter is used to remove that part of the ISI from the present estimate caused by previously detected symbols. The values of the feedback coefficients result in complete

elimination of ISI from previously detected symbols provided that previous decisions are correct and that $N_3 \geq L$ where L is the number of multipath components.

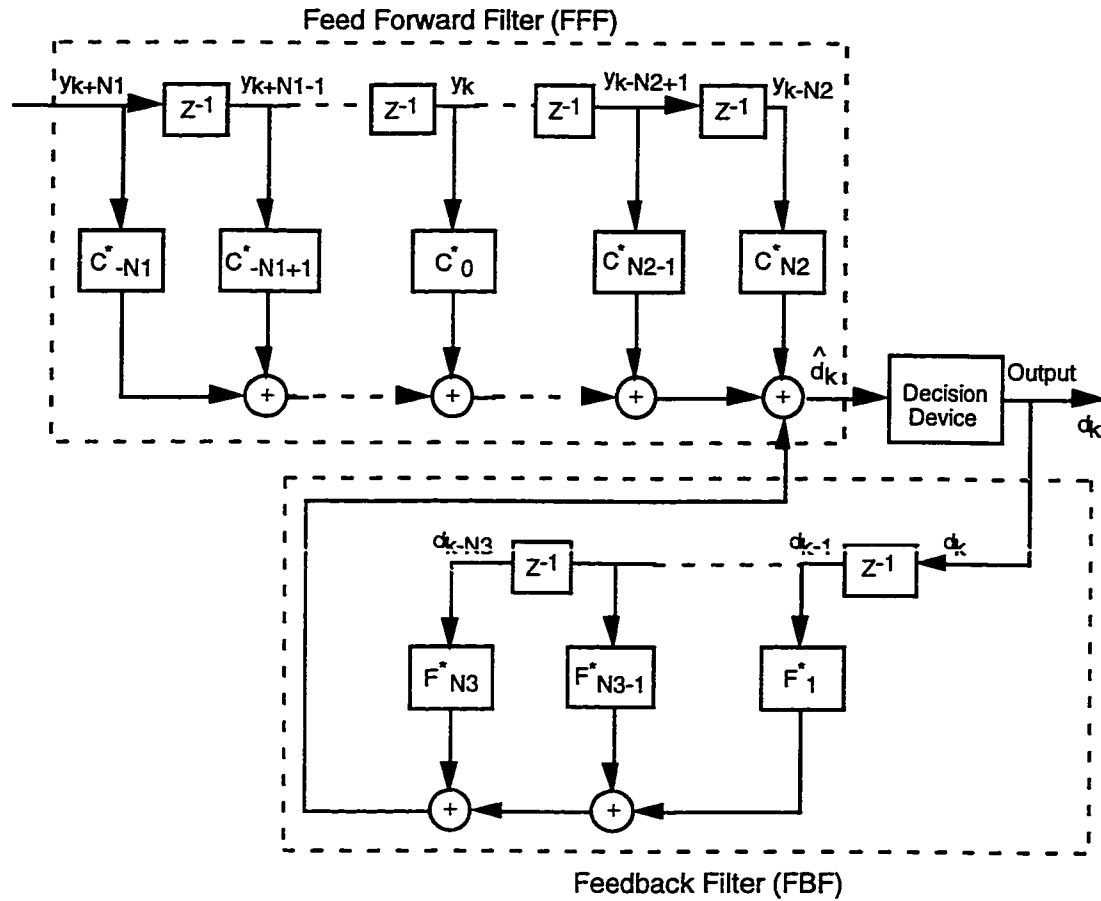


Fig 7.1.1-1 The structure of a Decision-Feedback Equalizer (DFE) [8]

7.1.2 Simulations and Results

First of all, the performance of the Barker/DSSS system with a DFE implemented in the receiver is considered. A Matlab™ program has been written to simulate the BER performance. Recall that the complex gain of the multipath channel has value $a = 0.99$ and phase $\theta = 0^\circ$ and 180° .

Since Barker Codes have a very low auto-correlation between successive chips such that $R_{i,i}(k) = -1$ only for $k \neq 0, \pm N, \dots$, propagation delay spread in the channel merely provides multiple versions of the transmitted signal at the receiver. If these multipath components are delayed in time by more than a chip duration, they appear like uncorrelated noise at the receiver, and equalization is not required. However, when these multipath components are delayed in time by multiples of N chips, they corrupt the received signal totally, and equalization is necessary. Therefore, the Barker/DSSS system using DFE is simulated for 11 chips multipath delay only.

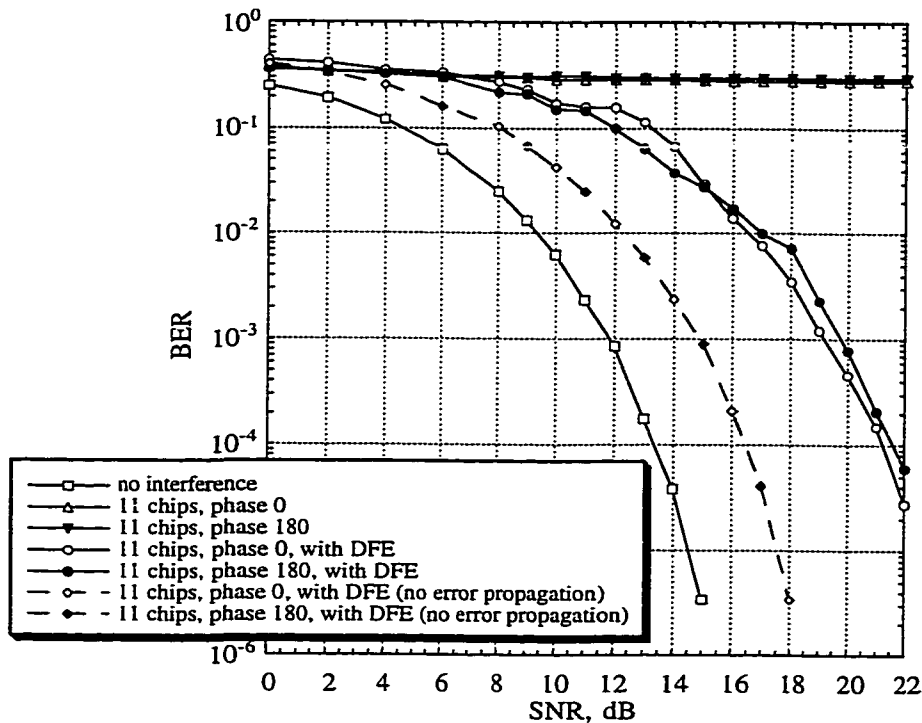


Fig 7.1.2-1 The BER for the Barker/DSSS using DFE over the multipath channel

According to Fig 7.1.2-1, the BER for Barker/DSSS system with the multipath component delayed by 11 chips is significantly improved when a DFE is implemented. However, its SNR is still about 8 dB worse than that without any interference. There are two reasons for the degradation of the BER performance: error propagation exists when the

previously detected symbol is wrong, and the multipath component which is carrying the desired information is removed from the current received signal instead of combined to the current signal. Fig 7.1.2-1 also shows that the Barker/DSSS system with DFE and without error propagation has only 3 dB loss in SNR for multipath channel over AWGN channel. This is expected. The performance of the DSSS system can be improved if the multipath components can be used as a form of diversity.

Secondly, the performance of the $M = 2$ and $M = 16$ Wi-LAN/CSK systems with DFE in the receiver are examined. Again, Matlab™ programs were developed to simulate the BER performance over a multipath channel. For the same reason mentioned previously, the $M = 2$ and $M = 16$ Wi-LAN/CSK systems using DFE are simulated for 5 chips multipath delay only. The results are plotted in Fig 7.1.2-2 and Fig 7.1.2-3.

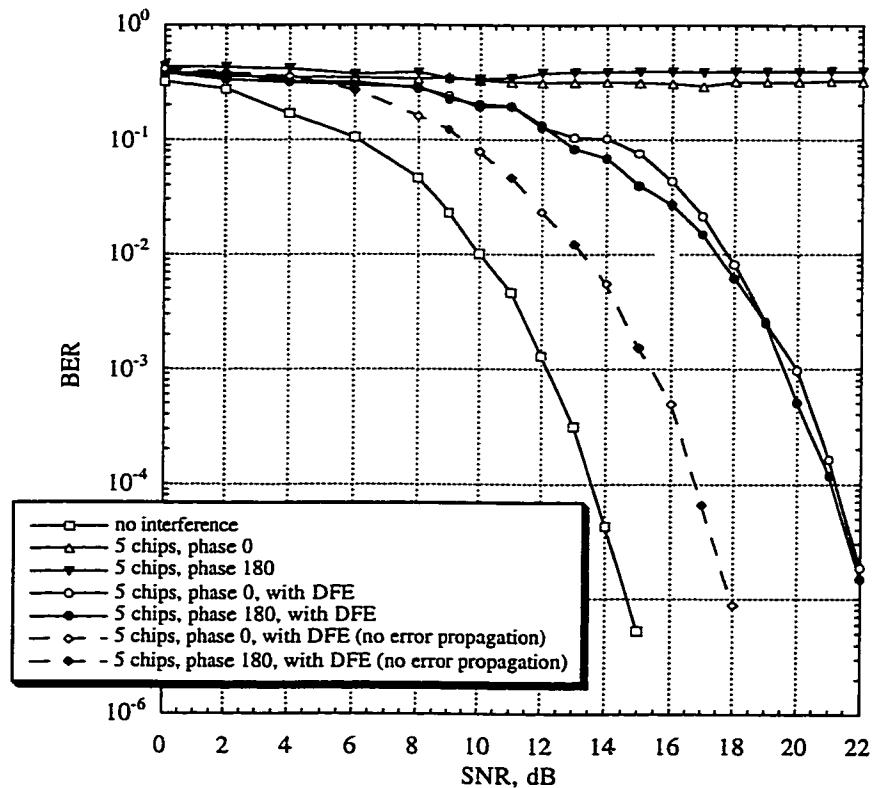


Fig 7.1.2-2 The BER for the $M = 2$ Wi-LAN/CSK using DFE over the multipath channel

Fig 7.1.2-2 shows that the BER for the $M = 2$ Wi-LAN/CSK system with the multipath component delayed by 5 chips is greatly improved when DFE is implemented. The loss in SNR is about 7.5 dB for DFE implemented in the receiver compared to AWGN. Again, the loss in SNR is only 3 dB when using the DFE without error propagation.

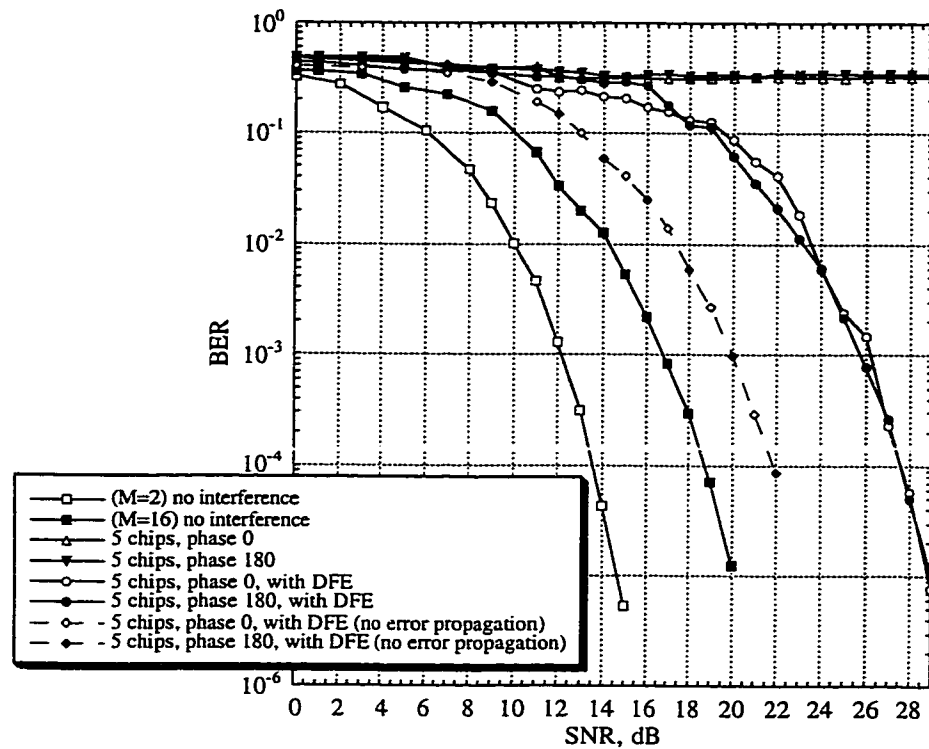


Fig 7.1.2-3 The BER for the $M = 16$ Wi-LAN/CSK using DFE over the multipath channel

Fig 7.1.2-3 shows the BER for $M = 16$ Wi-LAN/CSK system with the multipath component delayed by 5 chips. Its BER is again greatly improved when the DFE is implemented. It is about 9 dB worse than that over an AWGN channel. As mentioned above, the loss in SNR is only 3 dB when using the DFE without error propagation. The error propagation in DFE for the $M = 16$ Wi-LAN/CSK system causes larger degradation in BER. Since this CSK system has three modulation levels, an error occurring in the lowest modulation level usually causes errors in the upper modulation levels. Therefore, this CSK system experiences a larger loss in SNR over the multipath channel.

Finally, the performance of the TRLabs/CSK system over the multipath channel with a DFE implemented in the receiver is considered. Since some auto- and cross-correlation values of the TRLabs Codes $|R_{i,j}(k)|$ for $k \neq 0, \pm N, \dots$, are large enough to affect its BER performance, the TRLabs/CSK system using DFE is simulated with m chips multipath delay, where m is ranging from 1 to 5. The simulation results show that the DFE is effective in BER improvement over the multipath channel. See Fig 7.1.2-4 to Fig 7.1.2-8.

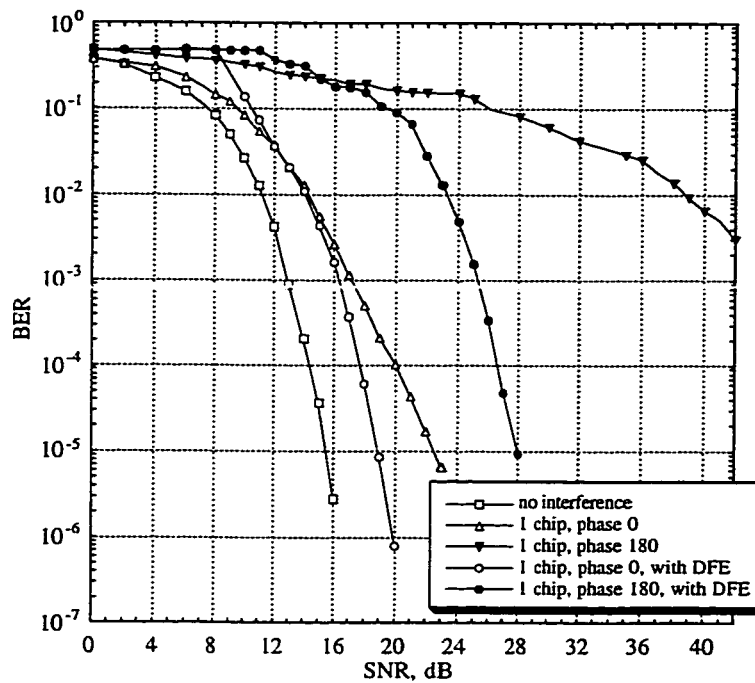


Fig 7.1.2-4 The BER for the TRLabs/CSK using DFE over the multipath channel (1 chip)

Fig 7.1.2-4 shows the BER for TRLabs/CSK system with the multipath component delayed by 1 chip. When DFE is implemented, its BER is greatly improved. The BERs are about 3.5 dB and 12 dB worse than that over an AWGN with phase $\theta = 0^\circ$ and 180° respectively. Since the cross-correlation between the desired received signal and its time-shifted version is not exactly zero, the components are either added up constructively or destructively at the receiver. Also, the DFE only removes the previously detected signal

from the current one. Thus, the non-zero cross-correlation values result in a big difference in BER performance for the TRLabs/CSK system between $\theta = 0^\circ$ and 180° .

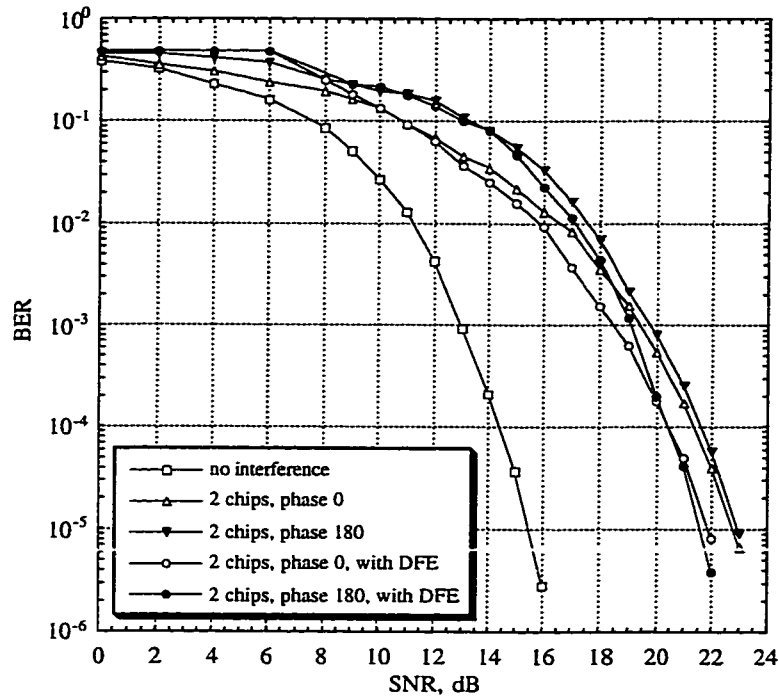


Fig 7.1.2-5 The BER for the TRLabs/CSK using DFE over the multipath channel (2 chips)

Fig 7.1.2-5 shows the BER for TRLabs/CSK system with the multipath component delayed by 2 chips. With the DFE implemented in the receiver, the improvement in BER is about 1 dB for the multipath channel.

The BERs for the TRLabs/CSK system with multipath delayed by 3 chips are shown in Fig 7.1.2-6 on the next page. For phase $\theta = 180^\circ$, the BER decreases slowly with increasing SNR. However, when the DFE is implemented in the receiver, the BER curves for both phases have a waterfall shape. The BERs are about 3 dB and 4 dB worse than that over AWGN for phases $\theta = 0^\circ$ and 180° respectively.

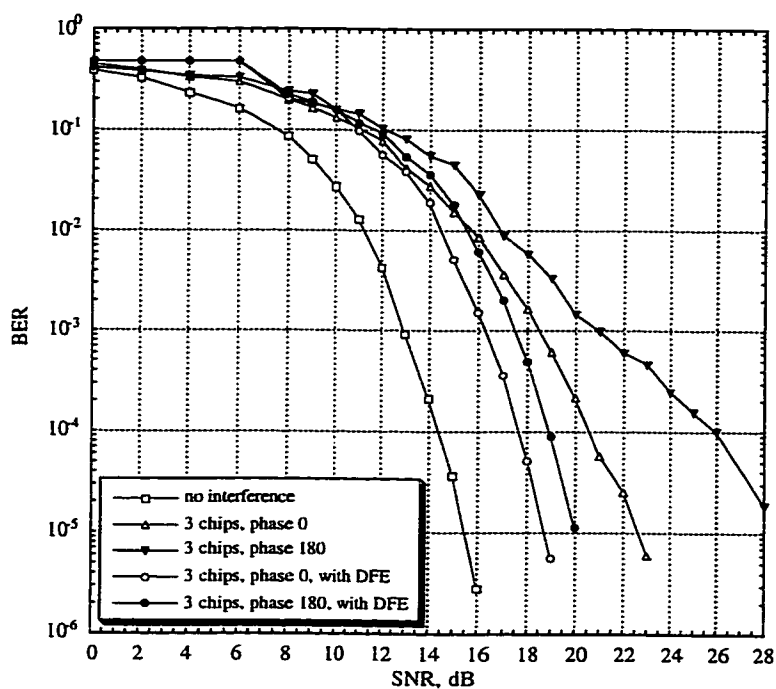


Fig 7.1.2-6 The BER for the TRLabs/CSK using DFE over the multipath channel (3 chips)

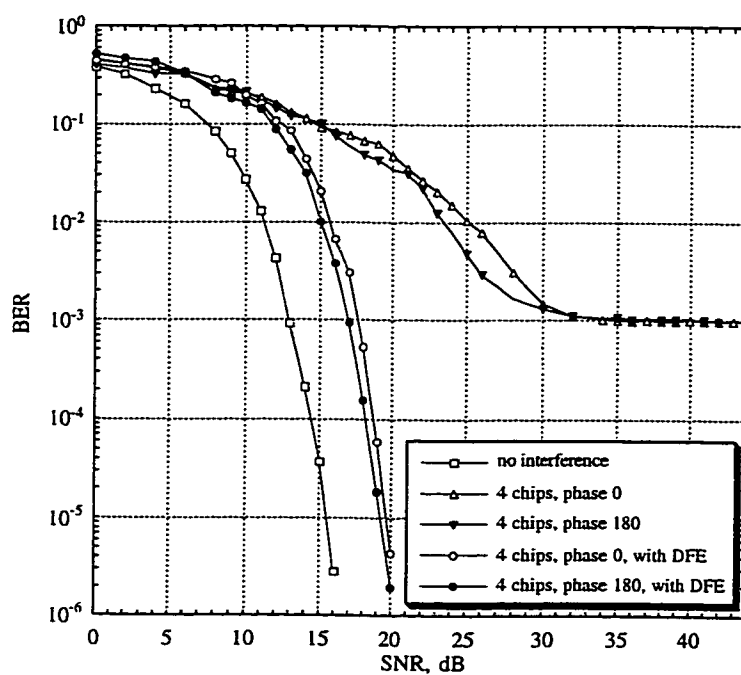


Fig 7.1.2-7 The BER for the TRLabs/CSK using DFE over the multipath channel (4 chips)

Fig 7.1.2-7 shows the BER for the TRLabs/CSK system with the multipath component delayed by 4 chips. As it is presented previously, the interference caused by the non-zero cross-correlation between codes is responsible for the leveling off of the BER curves at approximate 10^{-3} . However, when the DFE is used, the BER curves are significantly improved. They are only about 4 dB worse than that without interference.

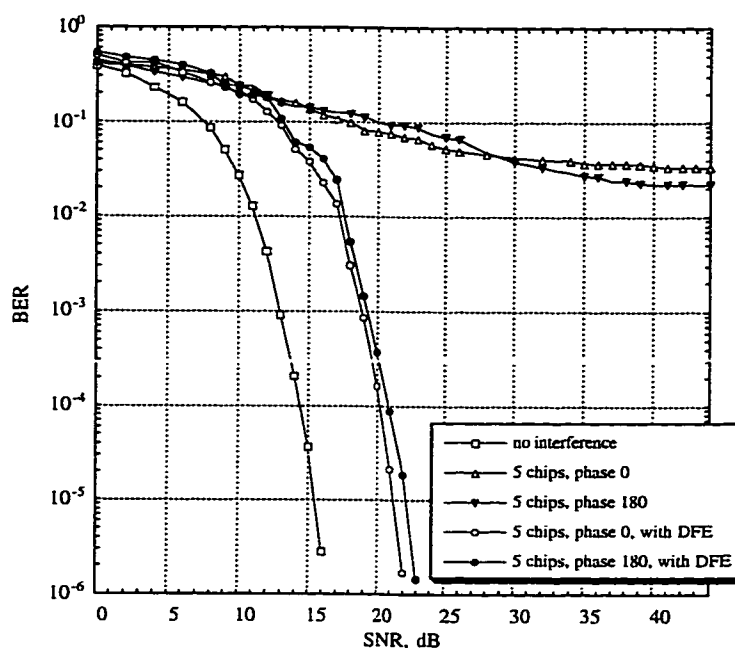


Fig 7.1.2-8 The BER for the TRLabs/CSK using DFE over the multipath channel (5 chips)

Finally, the BERs for the TRLabs/CSK system using the DFE with the multipath component delayed by 5 chips are simulated. The simulation results are shown in Fig 7.1.2-8. Again, the BER curves are leveling off at approximate 2×10^{-2} without DFE. The BERs with DFE are about 6 dB worse than that without interference now.

The DFE gets rid of the multipath components that are carrying desired information. This causes degradation in performance. If the multipath components can be combined properly in the receiver, the BER performance can be improved by 3 dB.

7.2 RAKE Receiver

7.2.1 Background

Spreading codes of a SS system are designed to provide very low correlation between successive chips. Multipath channels provide the time-shifted versions of the transmitted signal at the receiver. Thus, SS systems are not only resistant to multipath fading, but they can also exploit the multipath components to improve the performance of the system. This can be done using a RAKE receiver which combines the information obtained from several resolvable multipath components. A RAKE receiver consists of a bank of correlators, each of which correlates to a particular multipath component of the desired signal. The correlator outputs may be weighted according to their relative strengths, co-phased and summed to obtain the final signal estimate. [10]

The RAKE receiver for DQPSK signals, shown in Fig 7.2.1-1, utilizes multiple correlators to separately detect the L strongest multipath components. The outputs of each tap correlator are weighted to provide a better estimate of the transmitted signal than is provided by a single component. Demodulation and bit decisions are then based on the weighted outputs of the L correlators. Since the multipath model used in this thesis has one multipath component only, the RAKE receiver is implemented with $L = 2$ tap correlators.

The RAKE receiver shown consists of two main parts: the tap correlator (tapped delay line) and the demodulator. The correlator is made up of a tapped delay line which the multipath signal propagates through and its outputs are correlated with the despreading PN sequence. The main purpose of this operation is that if the cross-correlation between the desired received signal and its time-shifted versions is very low, then the output from each

correlator stage will come mainly from only one path corresponding to the desired signal. The tap delays are equal to multiples of T_c (a chip duration). This allows the RAKE receiver to distinguish multipath signals which are separated in time by multiples of T_c . Paths which are closer together are treated as a single path.

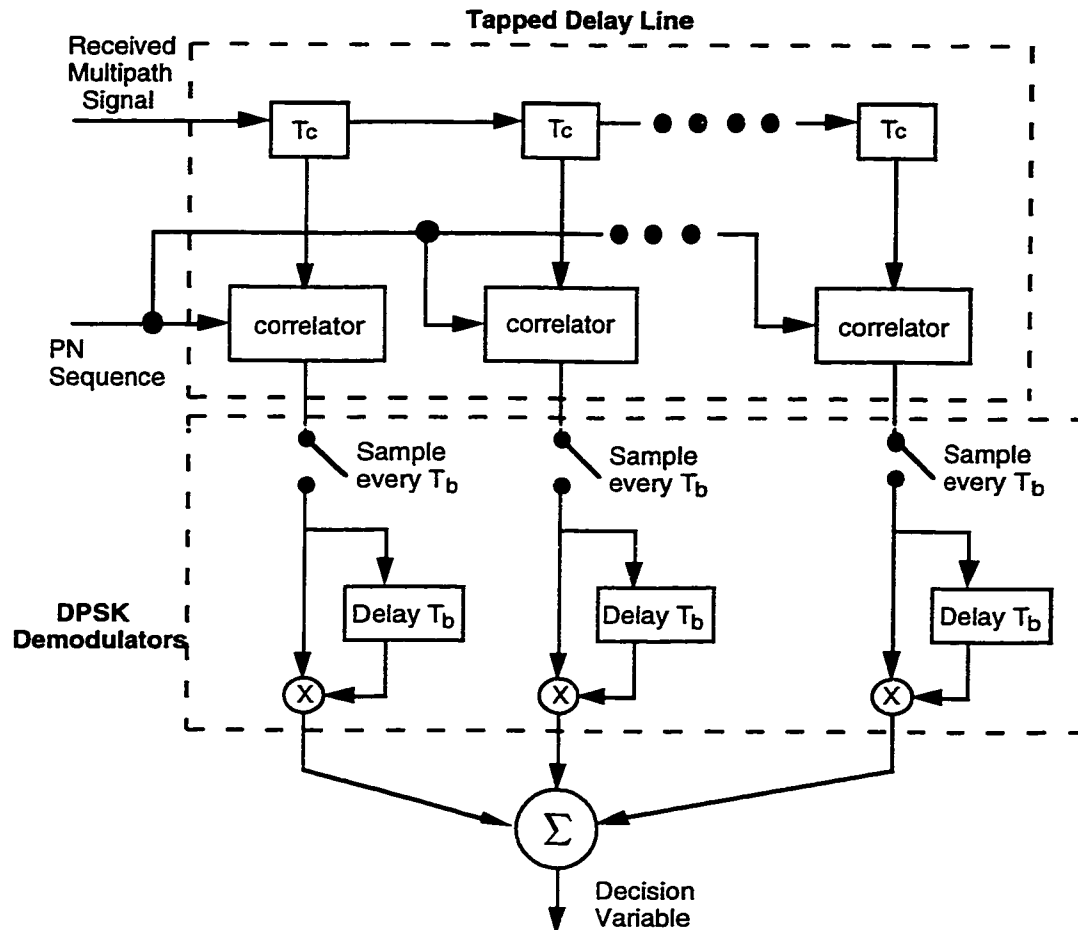


Fig 7.2.1-1 A RAKE demodulator for DPSK signals

The demodulator section consists of the DPSK demodulators. Each delay is equal to T_b (a symbol duration). This allows the demodulators to extract the differential phases between the current and previously received signals. There are an equal number of tap correlators and demodulators in the RAKE receiver. The outputs of the demodulators are combined with equal weighting here. Finally, the result is passed into the decision device.

Note that if only a single correlator is used in the receiver, once the output of the single correlator is corrupted by fading, the receiver cannot correct the value. Bit decisions based on only a single correlation may produce a large bit error rate. On the other hand, when the RAKE receiver has perfect (noiseless) estimates of the channel tap weights, it will achieve the performance of an equivalent maximal ratio combiner in a communication system with L th-order diversity.

The RAKE receiver operates in an optimum manner when a signal component is present at each delay. If that is not the case, its performance will be degraded, since some of the tap correlators will contribute only noise [11]. Under such conditions, the low level, noise-only contributions from the tap correlators should be excluded from the combiner.

The BERs are collected by simulating the DSSS and CSK systems over different multipath channels. The results are shown in the following section.

7.2.2 Simulations and Results

First of all, the performance of the Barker/DSSS system with a 2-tap RAKE receiver implemented is considered. Again, a Matlab™ program has been developed to simulate its BER performance over the multipath channel. The RAKE receiver exploits the multipath components to improve the system performance, provided that the cross-correlations between the desired received signal and its time-shifted versions are low. Otherwise, the output of the tap correlators contains the desired signal as well as the interference. Hence, the Barker/DSSS system can improve its performance with a RAKE receiver when the multipath component is delayed by less than 11 chips.

Fig 7.2.2-1 on the next page shows the BER for Barker/DSSS using a RAKE receiver with the multipath component delayed by 4 chips. It is clear that the differences in BERs are less than 1 dB for the RAKE receiver over the multipath channel compared to the AWGN channel. It is also observed that the BER for the DSSS system with a 4 chip delay and a phase $\theta = 180^\circ$ is even lower than for the AWGN channel. This is because the auto-correlation between the desired received signal and its time-shifted version is not exactly zero, in such a way that the components are added up constructively at the tap correlators. Since the final output of the RAKE receiver has a larger value than the desired received signal alone (see the following equations), its BER is thus lower than for the AWGN channel.

$$\text{Auto-correlations } R_{i,i}(k) \neq 0 \text{ (current situation): } \begin{cases} R_{i,i}(0) = 11 \\ R_{i,i}(4) = R_{i,i}(7) = -1 \\ ae^{j\theta} = 0.99e^{j\pi} \end{cases}$$

$$\begin{aligned} \text{Output of correlators} &= \text{RAKE arm \#1 output} + \text{RAKE arm \#2 output} \\ &= \left| R_{i,i}(0) + ae^{j\theta} \cdot R_{i,i}(4) \right| + \left| ae^{j\theta} \cdot R_{i,i}(0) + R_{i,i}(7) \right| \\ &= \left| 11 + 0.99e^{j\pi} \cdot (-1) \right| + \left| 0.99e^{j\pi} \cdot 11 + (-1) \right| \\ &= 23.88 \end{aligned} \quad (7.2)$$

$$\text{Auto-correlations } R_{i,i}(k) = 0 \text{ (Ideal condition): } \begin{cases} R_{i,i}(0) = 11 \\ R_{i,i}(4) = R_{i,i}(7) = 0 \\ ae^{j\theta} = 0.99e^{j\pi} \end{cases}$$

$$\begin{aligned} \text{Output of correlators} &= \text{RAKE arm \#1 output} + \text{RAKE arm \#2 output} \\ &= \left| R_{i,i}(0) + ae^{j\theta} \cdot R_{i,i}(4) \right| + \left| ae^{j\theta} \cdot R_{i,i}(0) + R_{i,i}(7) \right| \\ &= \left| 11 + 0.99e^{j\pi} \cdot (0) \right| + \left| 0.99e^{j\pi} \cdot 11 + (0) \right| \\ &= 21.89 \end{aligned} \quad (7.3)$$

Secondly, the performance of the $M = 2$ Wi-LAN/CSK system with a RAKE receiver is also examined. The simulation results for the $M = 2$ Wi-LAN/CSK system with the multipath component delayed by 4 chips are plotted in Fig 7.2.2-2 on the next page. The differences in BERs are less than 1 dB over the multipath channel with RAKE reception

compared to the AWGN case again. In this case, the BER for 4 chips delay and phase $\theta = 0^\circ$ is lower than for the AWGN channel for the same reason mentioned previously.

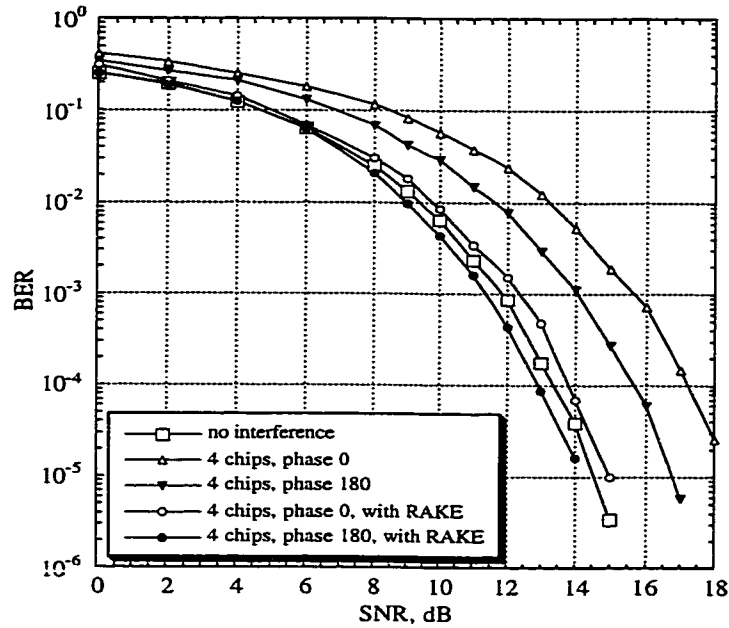


Fig 7.2.2-1 The BER for the Barker/DSSS using a RAKE receiver over the multipath channel

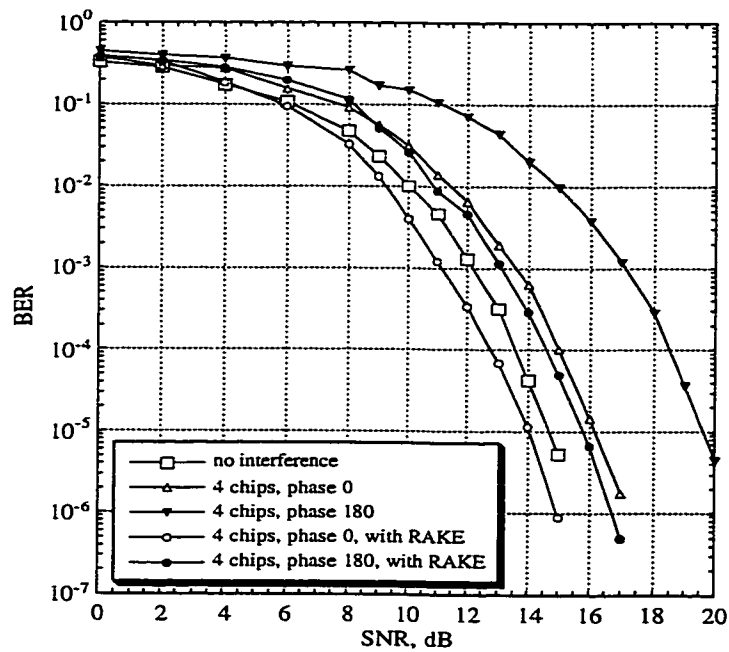


Fig 7.2.2-2 The BER for the M=2 Wi-LAN/CSK using a RAKE receiver over the multipath channel

Finally, the performance of the TRLabs/CSK system over the multipath channel with a RAKE receiver is investigated. First of all, the TRLabs/CSK system with the multipath component delayed by 1 chip is simulated. The simulation results are plotted in Fig 7.2.2-3 and Fig 7.2.2-4 corresponding to phase $\theta = 0^\circ$ and 180° respectively.

For the case with phase $\theta = 0^\circ$, Fig 7.2.2-3 shows the improvement in BER to be about 3 dB for a RAKE receiver compared to a DFE. The system performance over the multipath channel is now comparable to that over the AWGN channel.

For the case with phase $\theta = 180^\circ$, Fig 7.2.2-4 shows that the BER for the TRLabs/CSK system with a RAKE receiver does not have a 3 dB improvement in SNR over the DFE. In theory, the RAKE should offer a 3 dB improvement in SNR over the DFE provided that there is no ISI in the received signal and the cross-correlation between the desired received signal and its time-shifted version is low. However, ISI is present in this case. Also, the maximum cross-correlation value of the TRLabs Codes is ~ 4.47 . As a result, the output from each correlator tap of the RAKE not only contains the desired signal, but also the interference. To solve this problem, a modified RAKE receiver having a DFE after each tap correlator is used. The DFE removes the ISI from the received signal at each tap, then the RAKE combines the resulting signals. Fig 7.2.2-4 shows that the BER for the TRLabs/CSK system with the modified RAKE is improved by about 3 dB compared to the DFE without error propagation.

Fig 7.2.2-5 shows the BER for the TRLabs/CSK system with the multipath component delayed by 2 chips. The BER with a RAKE is about 5 dB and 4 dB better than for the DFE with $\theta = 0^\circ$ and 180° respectively. The losses in BERs are within 2 dB for the RAKE receiver compared to the AWGN case.

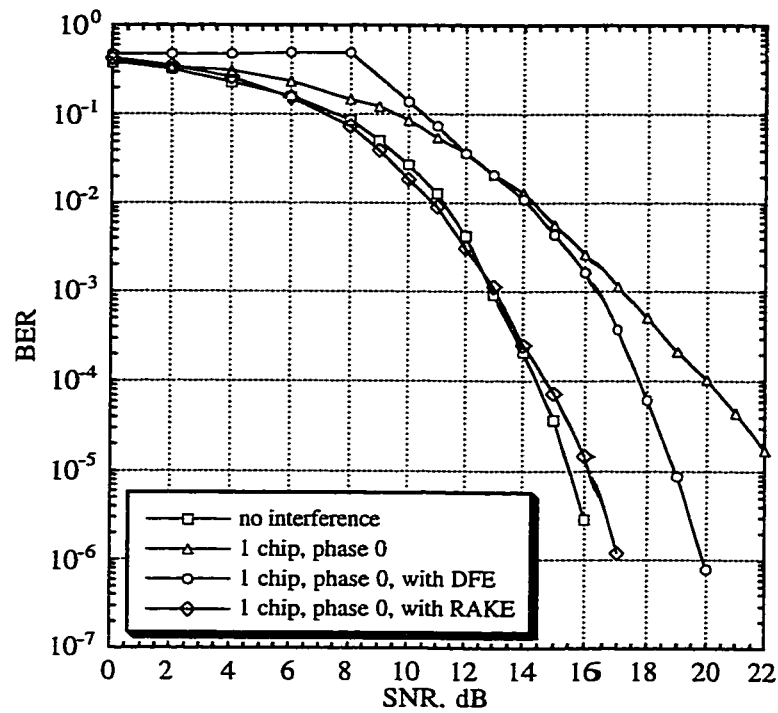


Fig 7.2.2-3 The BER for the TRLabs/CSK with a RAKE receiver over the multipath channel (1 chip, phase 0)

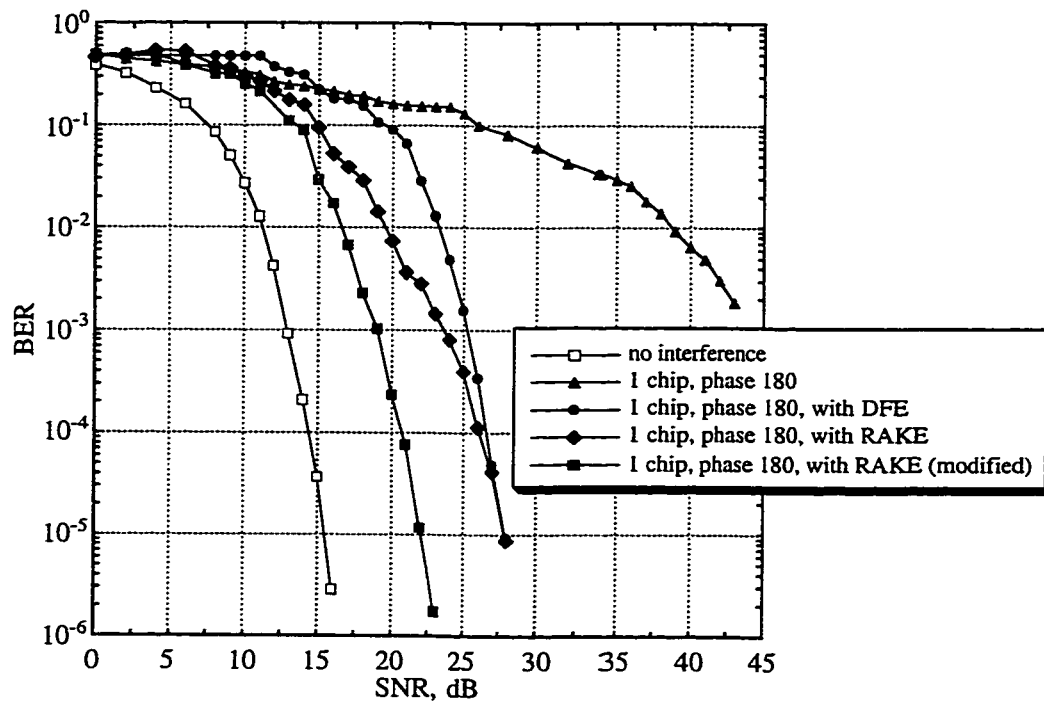


Fig 7.2.2-4 The BER for the TRLabs/CSK with a RAKE receiver over the multipath channel (1 chip, phase 180)

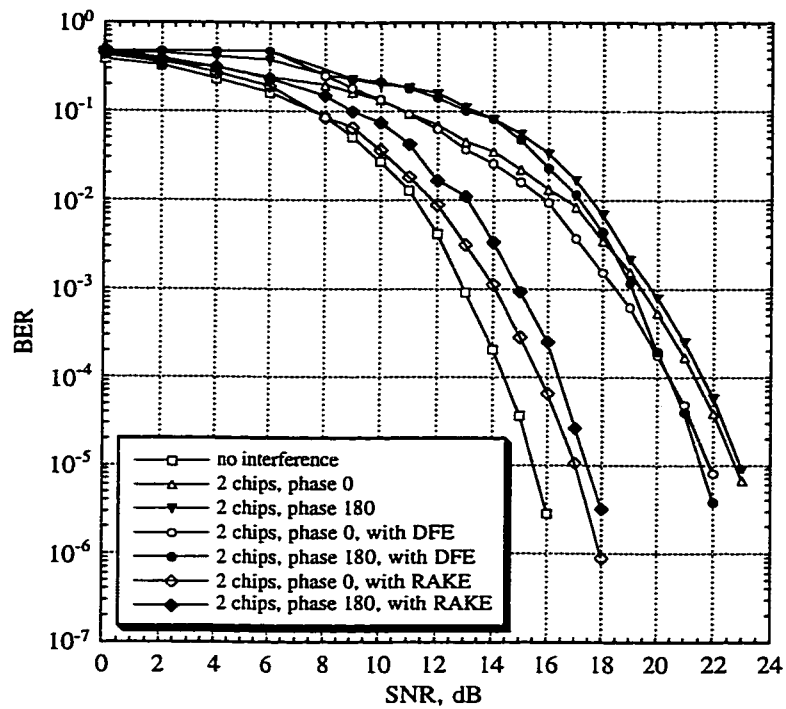


Fig 7.2.2-5 The BER for the TRLabs/CSK with a RAKE receiver over the multipath channel (2 chips)

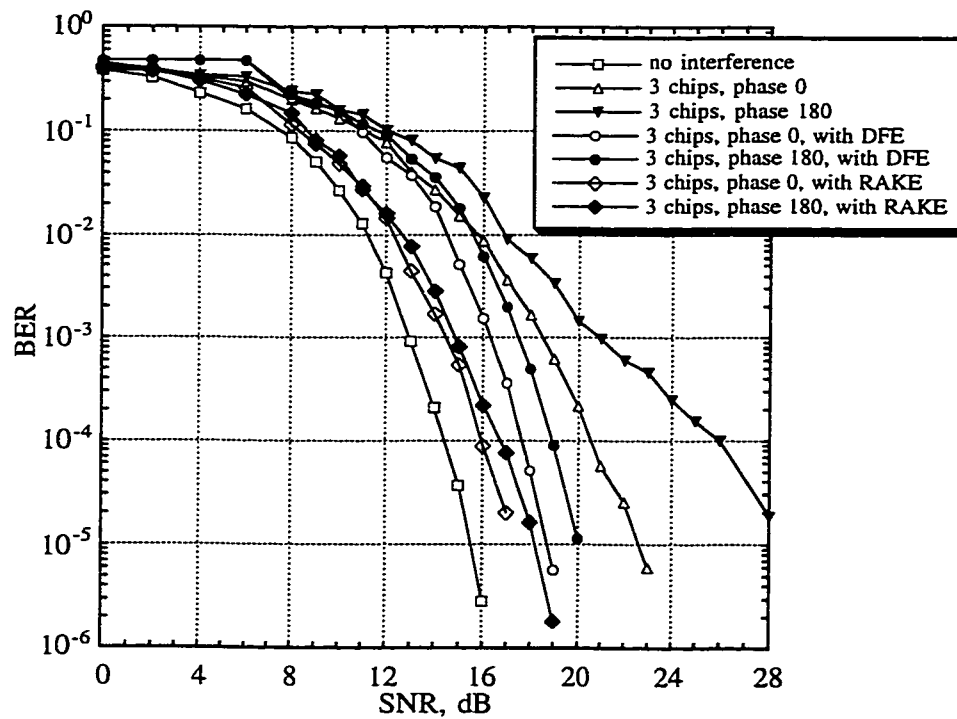


Fig 7.2.2-6 The BER for the TRLabs/CSK with a RAKE receiver over the multipath channel (3 chips)

The BERs for the TRLabs/CSK system with the multipath component delayed by 3 chips are plotted in Fig 7.2.2-6. The improvement in BER for both phases is about 2 dB for the RAKE receiver over the DFE. The BERs for the RAKE receiver are only 2 dB and 3 dB worse than that over the AWGN channel for $\theta = 0^\circ$ and 180° respectively.

Similarly, the BER curves for the TRLabs/CSK system with 4 chip multipath delay are plotted in Fig 7.2.2-7. The modified RAKE receiver can further improve the BER by 2 - 3 dB over the DFE. The losses in BER are about 2.5 dB over this multipath channel with RAKE reception compared to the AWGN channel.

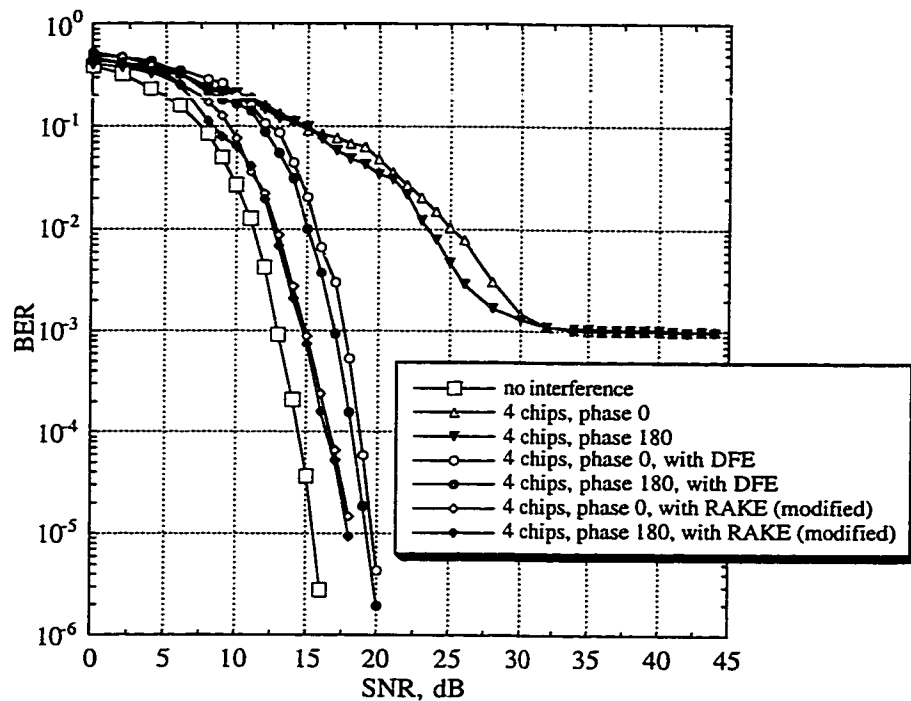


Fig 7.2.2-7 The BER for the TRLabs/CSK with a RAKE receiver over the multipath channel (4 chips)

Finally, the BER curves for the TRLabs/CSK system with the multipath component delayed by 5 chips are plotted in Fig 7.2.2-8. When the SNR is low ($\text{SNR} < 18 \text{ dB}$), the improvement in BER is 2 dB for the TRLabs/CSK system with modified RAKE compared

to the one with DFE for phase $\theta = 0^\circ$. However, when the SNR is high ($\text{SNR} \geq 18 \text{ dB}$), the DFE works better than the modified RAKE receiver. This is clearly observed for the case with phase $\theta = 180^\circ$. The RAKE receiver operates in an optimum manner provided that the cross-correlation between the desired received signal and its time-shifted versions is low. Otherwise, the system performance is degraded, since some of the tap correlators contribute both to the desired signal as well as to the interference. That is what happened for the TRLabs/CSK system using a RAKE receiver over the multipath channel with 5 chips delay.

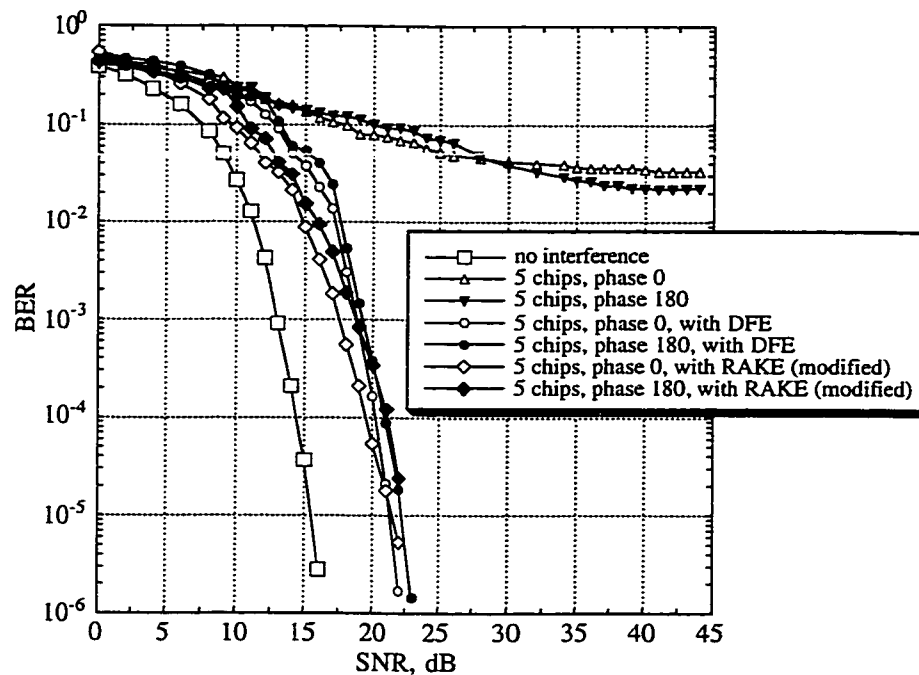


Fig 7.2.2-8 The BER for the TRLabs/CSK with a RAKE receiver over the multipath channel (5 chips)

According to the above simulation results, the performance of the DSSS and the CSK systems over the multipath channel can be improved further by implementing the RAKE receiver. Alternatively, the Viterbi Algorithm is considered as an optimal solution to the multipath channel as long as the channel is properly characterized.

7.3 Viterbi Algorithm (VA)

7.3.1 Background

The Viterbi Algorithm (VA) is a sequential trellis search algorithm for performing a Maximum-Likelihood (ML) sequence detection. To do this, the Euclidean distances between the received symbol and each possible transmitted symbol in the trellis are calculated. The value is called a branch metric or Euclidean distance metric. For the DQPSK data signal, the size of the symbol alphabet is $M = 4$. Since the multipath model used in this thesis has two multipath components, the number of interfering symbols contributing to the ISI is $L = 1$. Thus, the VA has M^L nodes at each stage. Each stage has $M = 4$ signal paths entering and $M = 4$ signal paths leaving each node. Hence the VA computes $M^{L+1} = 16$ metrics for each new received symbol. Then, the VA compares these metrics and discards $M-1 = 3$ paths having the larger metrics entering each node. The path with the lower metric is saved and is called the survivor. Thus, each stage of the VA has $M = 4$ survivors. The four survivor paths are then extended forward to the next stage. Therefore, the number of paths searched in the trellis is reduced by a factor of four at each stage. Fig 7.3.1-1 shows one stage of the trellis diagram for $M = 4$ symbol alphabet signal.

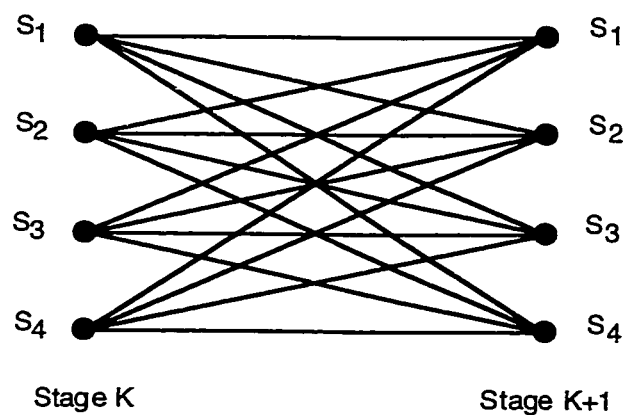


Fig 7.3.1-1 One stage of trellis diagram for a $M = 4$ symbol alphabet signal

In an ideal Viterbi decoder, the path metrics would be kept in memory until all surviving paths merge into one. However, the computational complexity grows exponentially with the length of the channel time dispersion. In practice, such a large computational complexity is prohibitively expensive to implement. Also, the decoding delay is too long for most practical applications.

If we advance to some stage, say K , where $K \gg L$ in the trellis, and we compare the surviving sequences, we shall find that with probability approaching one all surviving sequences will be identical in bit (or symbol) positions $K - 5L$ and less. In a practical implementation of the VA, decisions on each information bit (or symbol) are forced after a delay of $5L$ bits (or symbols), and hence, the surviving sequences are truncated to the $5L$ most recent bits (or symbols). The loss in performance resulting from the suboptimum detection procedure is negligible if the delay is at least $5L$ [12]. The amount of delay is set equal to 10 in the computer simulation in this thesis.

DPSK signals can be detected either by a differential detector or a coherent detector with differential decoding. Differential detection (DD) does not require a carrier recovery circuit as does coherent detection (CD), so the detector structure is much simpler than with CD. In addition, it has been found that Viterbi-decoding DD yields significantly improved BER performance with an SNR loss of only around 0.15 dB at $\text{BER} = 10^{-3}$ compared to coherent detection with differential decoding for a 2DPSK over AWGN. Viterbi-decoding DD can be also applied to any multilevel DPSK system [13]. Thus, DD based on MLSE is used in the VA in this thesis.

The multipath channel parameters ' a ' and ' θ ' are assumed to be perfectly estimated in the computer simulation. The performance of the VA is the main concern here.

7.3.2 Simulations and Results

First of all, the performance of the Barker/DSSS system using the $\pi/4$ QPSK modulation and a coherent receiver over an AWGN channel and a multipath channel are simulated. Fig 7.3.2-1 shows several BER curves for the DSSS system. The multipath channel has values $\alpha = 0.99$ and $\theta = 0^\circ$. The BER of the DSSS system over the multipath channel is constant with increasing SNR. The DFE yields significantly improved BER performance with an SNR loss of only ~ 3.5 dB over the multipath channel compared to that over an AWGN channel. The figure also shows the error propagation in the DFE is responsible for a loss of ~ 0.5 dB in SNR. When the VA is used in the receiver, the BER is further improved by ~ 3 dB over the DFE.

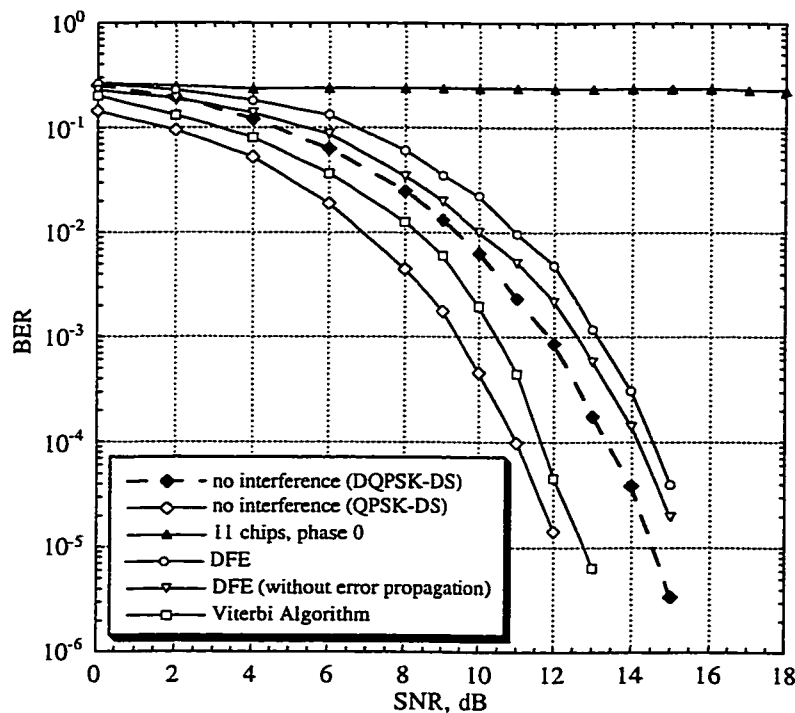


Fig 7.3.2-1 The BER for the Barker/DSSS system over an AWGN channel and the multipath channel ($\pi/4$ QPSK, coherent detection)

Secondly, the performance of the SS system with $\pi/4$ DQPSK and a differential detector is investigated. A Matlab™ program was written to simulate the BER performance for the Barker/DSSS system over a multipath channel with VA implemented in the receiver. The multipath delay is set to 11 chips, and the complex gain $ae^{j\theta}$ has values $a = 0.99$ and $\theta = 0^\circ$ and 180° . The simulation results are shown in Fig 7.3.2-2. The figure shows that the VA improves the system performance by about 3 dB compared to the DFE.

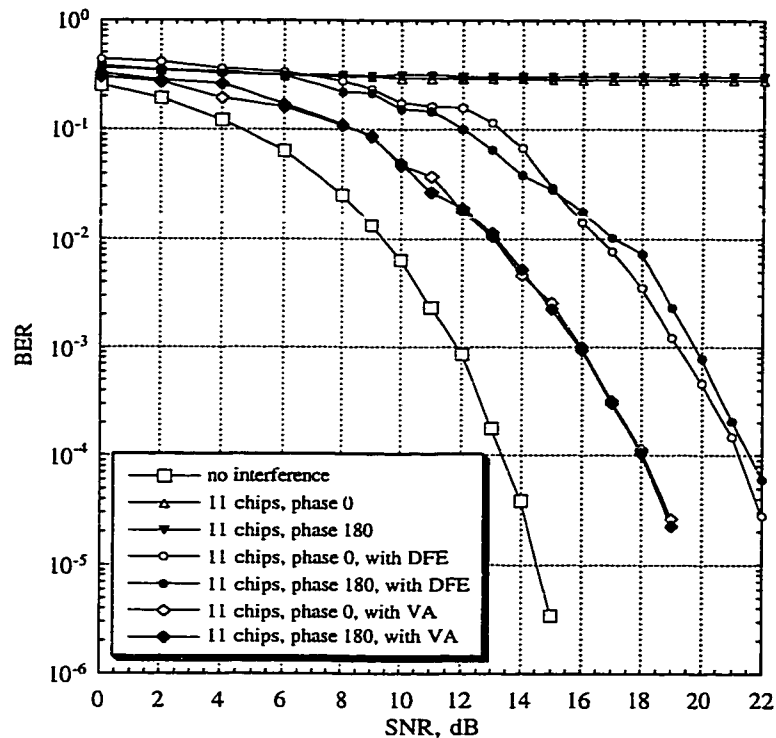


Fig 7.3.2-2 The BER for the Barker/DSSS using VA over the multipath channel

Another Matlab™ program has been developed to simulate the BER performance for the $M = 2$ Wi-LAN/CSK system over the multipath channel. In this case, the multipath delay is set to 5 chips. The simulation results are plotted in Fig 7.3.2-3. The results show that the improvement in BER is about 2 dB for the VA compared to the DFE.

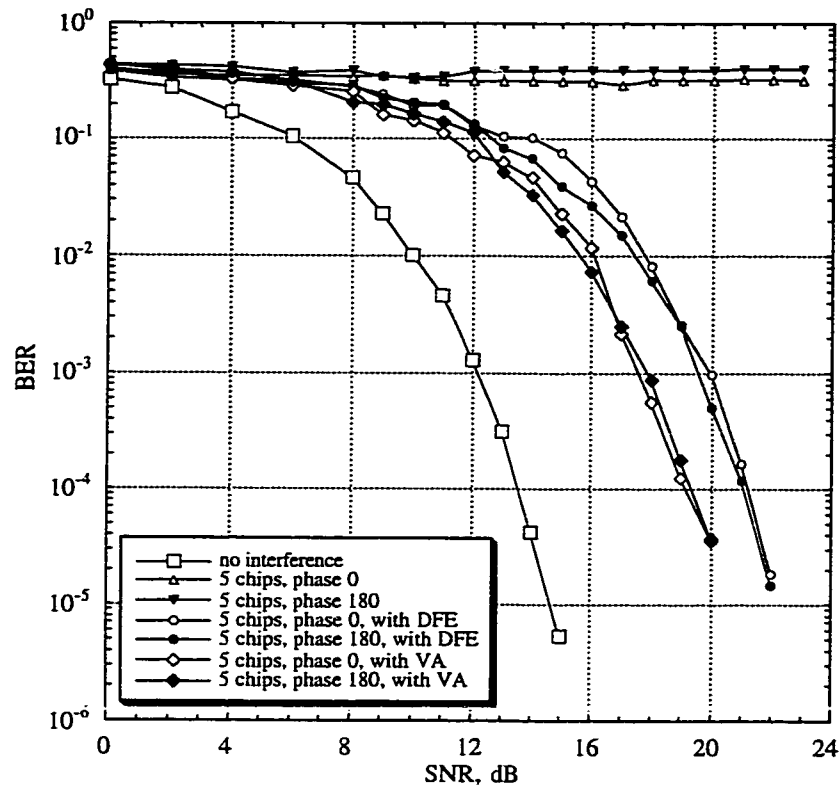


Fig 7.3.2-3 The BER for the $M = 2$ Wi-LAN/CSK using VA over the multipath channel

In this chapter, three techniques have been investigated in order to avoid degradation in system performance caused by the multipath fading and ISI. These techniques are the DFE, the RAKE receiver and the VA. They require a large amount of computations in the receiver, however, without changing the system architecture where only one N-chip correlator is ever required in the receiver.

Chapter 8

Conclusion and Future Work

8.1 Conclusion

A new low complexity CSK system has been presented in this thesis. This proposed CSK system can increase the net throughput of the conventional DSSS system over the wireless channel. In contrast to the DSSS system which uses only one PN sequence for spreading the data signal, the CSK system chooses one out of M possible PN sequences from a pre-selected set for spreading the data signal. Extra bits are thus transmitted over the same bandwidth to the receiver through the selection of the spreading codes, hence, the system bit rate is increased over the conventional DSSS system.

The low complexity CSK system also offers significant savings in receiver complexity compared to the classical CSK system where M correlators are required. The low complexity CSK system requires only one N chip correlator in the receiver regardless of the number of possible spreading sequences in the set. This can be achieved through the design of proper spreading codes for the CSK system such as the Wi-LAN Codes. Another new class of spreading codes for the low complexity CSK system has been found and it is referred to as the TRLabs Codes.

The Barker/DSSS system uses an 11 chip Barker Code as the spreading sequence and the $\pi/4$ DQPSK as the modulation scheme. On the other hand, the Wi-LAN/CSK system and the TRLabs/CSK system consist of two levels of modulation. They use the $\pi/4$ DQPSK in the first level of modulation and the DBPSK in the second level of modulation.

The performance of these systems has been investigated through computer simulations. According to the simulation results, it is found that almost all of the errors encountered are originating from the detection of the DQPSK symbol between adjacent received signals rather than from the DBPSK symbol. This important characteristic can be manipulated to transmit more important bits of information through the DBPSK symbols while transmitting less important bits through the DQPSK symbols. In addition, the bit rate of a CSK system can be increased using higher levels of modulation.

Although the low complexity CSK system can reduce its receiver complexity over the conventional DSSS system, this is achieved at the expense of system performance. Thus, a longer spreading sequence results in a larger processing gain which can be used to improve the performance of a CSK system. This was demonstrated by computer simulation over an AWGN channel in Chapter 5.

In addition to noise, communication through the multipath channel is subject to multipath fading and ISI. The effect of the multipath channel on the DSSS system and on the CSK system was discussed in Chapter 6. In Chapter 7, three techniques were considered in order to avoid such a degradation in system performance. These techniques are the DFE, the RAKE receiver and the VA.

The DFE exploits the use of previously detected symbols to suppress the ISI in the present symbol being detected. Thus, the CSK system can still maintain an acceptable reception under severe ISI conditions.

On the other hand, the RAKE receiver takes advantage of the implicit diversity of the multipath components in the received signals to further improve the system performance.

When the output of one or more correlators are corrupted by fading, the RAKE receiver can still correct the final value effectively by adjusting the weighting at each output of the demodulator.

The two reasons causing the degradation in performance for a DFE are error propagation and removal of useful multipath components. The VA based on ML sequence detection can avoid both degradations and thus is considered as an alternative to the DFE in improving the system performance over the multipath channel.

Following the description of these techniques, computer simulations on BER performance are performed over the multipath channel. The results are as previously predicted.

In conclusion, one can say that the low complexity CSK system using the TRLabs Codes can increase the bit rate of a conventional DSSS system. It requires a receiver complexity comparable to the one used for the DSSS system. It has a comparable performance to the DSSS system over an AWGN channel. It also has a comparable performance to the DSSS system over the multipath channel with an equalizer, a RAKE receiver or the Viterbi Algorithm at the receiving end.

8.2 Future Work

The future work would be to find other new spreading codes for the low complexity CSK system which can increase the net throughput of a conventional DSSS system and has reduced receiver complexity with the same performance as DSSS system over the wireless channel.

References

- [1] J. G. Proakis, "Digital Communications", Third Edition, International Editions, McGraw-Hill, 1995, pp. 695-698.
- [2] D. P. Whipple, "North American Cellular CDMA", Hewlett-Packard Journal, December 1993, pp. 90-97.
- [3] M. Fattouche, "Low Complexity Code Shift Keying over the Wireless Channel", Wi-LAN Inc., 1995.
- [4] W. F. Caton, FCC, "Amendment of Parts 2 and 15 of the Commission's Rules Regarding Spread Spectrum Transmitters", Washington, Internet, April 10, 1997.
- [5] J. G. Proakis, "Digital Communications", Third Edition, International Editions, McGraw-Hill, 1995, pp. 273-278.
- [6] J. G. Proakis, "Digital Communications", Third Edition, International Editions, McGraw-Hill, 1995, pp. 279-282.
- [7] B. Sklar, "Digital Communications - Fundamentals and Applications", Prentice Hall, pp.463.
- [8] T. S. Rappaport, "Wireless Communications - Principles & Practice", Prentice Hall, 1996, pp. 313-314.
- [9] J. G. Proakis, "Digital Communications", Third Edition, International Editions, McGraw-Hill, 1995, pp. 583-584, pp. 621-622.
- [10] T. S. Rappaport, "Wireless Communications - Principles & Practice", Prentice Hall, 1996, pp. 336-337.
- [11] T. Miyatam and Y. Araiwa, "A SS Communication System without reference signal for Frequency-Selective Fading channel", 43rd IEEE, Veh. Tech. Conference, Secaucus, N. J., May 18-20, 1993, pp. 835-838.
- [12] J. G. Proakis, "Digital Communications", Third Edition, International Editions, McGraw-Hill, 1995, pp. 483-486.
- [13] F. Adachi and M. Sawahashi, "Viterbi-Decoding differential detection of DPSK", Electronics letters, Vol.28, No.23, Nov. 5, 1992, pp.2196-2198

Appendix A

TRLabs Codes Generation and C Programs

A1 TRLabs Codes Generation

The C codes for generating all the TRLabs codes of length $N = 10$ are given as `search.cpp`, `funcs.cpp` and `code.h`. The method used to generate the TRLabs codes has been outlined in Chapter 4. Since a binary constant energy SS signal is preferred, the elements of the TRLabs code must be from the set $\{ 1, -1, j, -j \}$ only. Thus, the C programs search over all possible combination of these elements for the TRLabs codes.

```
/* filename: code.h */  
/* date: Sept 19, 1997 */
```

```
#include <stdio.h>  
#include <math.h>
```

```
typedef struct {                // complex number  
    int re;  
    int im;  
} complex;
```

```
void work(struct complex *code, int* count1 , float *automin, float*crossmin ,  
struct complex* mincode);
```

```
void loop(int index, struct complex* code, struct complex* bit, int* count, float* automin,  
float* crossmin, struct complex* mincode);
```

```
float maxcorr(struct complex *a, struct complex *b, char c);
```

```
float largest(float *num, int n);
```

```
struct complex mult(struct complex num1, struct complex num2);
```

```
void print_code(struct complex *a, int n);
```

```

/* filename: search.cpp */
/* date : Sept 19, 1997 */

```

```

#include <stdio.h>
#include <math.h>
#include "code.h"

```

```

void main()
{

```

```

    struct complex    code[10], mincode[10], bit[4];    // Initialize variables
    float              automin, crossmin;
    int                count, m, n, i;

```

```

    for(i=0; i<10; i++)    // Create codeword
    {
        code[i].re = 0;    // Starts with all -j
        code[i].im = -1;
    }

```

```

    bit[0].re = 0; bit[0].im = -1;    // bit 0 : -j
    bit[1].re = 0; bit[1].im = 1;    // bit 1 : j
    bit[2].re = -1; bit[2].im = 0;    // bit 2 : -1
    bit[3].re = 1; bit[3].im = 0;    // bit 3 : 1

```

```

    automin = 11.0;
    crossmin = 11.0;
    mincode = code;
    count = 0;

```

```

    work(code,&count,&automin,&crossmin,mincode);

```

```

    for(n=1; n<=10; n++)    // Double loop :
    {                        // test all possible combination
        for(m=2; m<=4; m++) // of codewords
        {

```

```

            code[n-1] = bit[m-1];
            if (n > 1)
                loop(n-1,code,bit,&count,&automin,&crossmin,mincode);
            else
                work(code,&count,&automin,&crossmin,mincode);    // Testing
        }

```

```

        printf("\nn = %d\n",n);    // Output
        printf("automin = %6.4f\n",automin);
        printf("crossmin = %6.4f\n",crossmin);
        printf("mincode = ");
        print_code(mincode,10);
        printf("\n\n");
    }

```

```

}

```

A2 Auto- and Cross-Correlations Between Spreading Codes

The `funs.cpp` contains several functions which are used to find the maximum auto- and cross-correlations between spreading codes. The functions account for the specified time shifts of a chip time between each pair of spreading codes according to the two constraints listed in Chapter 4.

```

/* filename: funs.cpp */
/* date: Sept 19, 1997 */

```

```

#include <stdio.h>
#include "code.h"

```

// try all possible combination of bits

```

void loop(int index, struct complex code[], struct complex bit[], int* count, float* automin,
float* crossmin, struct complex *mincode)

```

```

{
    int i;

    for(i=0; i<4; i++)
    {
        code[index-1] = bit[i];
        if (index != 1)
            loop(index-1,code,bit,count,automin,crossmin,mincode);
        else
            work(code,count,automin,crossmin,mincode);
    }
}

```

// check the auto and cross-correlations of each codeword

```

void work(struct complex code[], int* count, float* automin, float* crossmin, struct
complex *mincode)

```

```

{
    int i;
    float maxA[4], maxC[6], max_auto, max_cross;
    struct complex code2[10], code3[10], code4[10];

    ++*count;

    for(i=7; i<10; i++)
    {
        code2[i].re = code[i].re;
        code2[i].im = code[i].im;
        code3[i].re = code[i].re * -1;
        code3[i].im = code[i].im * -1;
        code4[i].re = code[i].re * -1;
        code4[i].im = code[i].im * -1;
    }

    for(i=3; i<7; i++)
    {
        code2[i].re = code[i].re * -1;
        code2[i].im = code[i].im * -1;
        code3[i].re = code[i].re;
        code3[i].im = code[i].im;
        code4[i].re = code[i].re * -1;
        code4[i].im = code[i].im * -1;
    }
}

```

```

// code1: [+++  +++++  +++]
// code2: [+++  ----  +++]
// code3: [+++  +++++  ---]
// code4: [+++  ----  ---]

```

```

for(i=0; i<3; i++)
{
    code3[i].re = code[i].re;
    code3[i].im = code[i].im;
    code2[i].re = code[i].re;
    code2[i].im = code[i].im;
    code4[i].re = code[i].re;
    code4[i].im = code[i].im;
}

maxA[0] = maxcorr(code,code,'a');
maxA[1] = maxcorr(code2,code2,'a');
maxA[2] = maxcorr(code3,code3,'a');
maxA[3] = maxcorr(code4,code4,'a');

max_auto = largest(maxA,4);

maxC[0] = maxcorr(code,code2,'c');
maxC[1] = maxcorr(code,code3,'c');
maxC[2] = maxcorr(code,code4,'c');
maxC[3] = maxcorr(code2,code3,'c');
maxC[4] = maxcorr(code2,code4,'c');
maxC[5] = maxcorr(code3,code4,'c');

max_cross = largest(maxC,6);

if( (max_cross <= *crossmin) )
{
    *crossmin = max_cross;

    if (max_auto <= *automin)
    {
        *automin = max_auto;
        for(i=0; i<10; i++)
        {
            mincode[i].re = code[i].re;
            mincode[i].im = code[i].im;
        }

        printf("both -- Automin = %6.4f , Crossmin = %6.4f, mincode=[" ,*automin,
        *crossmin);
        print_code(mincode,10);
        printf("]\n");
    }
}
}

```

// Check the auto-correlations

// Record the max auto-correlation

// Check the cross-correlations

// Record the max cross-correlation

// Output results

// valid spreading codes

// find out the largest value in the array num[]

```
float largest(float num[], int n)
{
    int    i;
    float  maximum;

    maximum = num[0];

    for(i=1; i<n; i++)
    {
        if(num[i] > maximum)
            maximum = num[i];
    }

    return maximum;
}
```

// complex number multiplication

```
struct complex mult(struct complex num1, struct complex num2)
{
    struct complex product;

    num2.im = -num2.im;                // complex conjugate
    if(num1.re != 0)
    {
        product.re = num1.re * num2.re;
        product.im = num1.re * num2.im;
    }
    else
    {
        product.re = -num1.im * num2.im;
        product.im = num1.im * num2.re;
    }
    return product;
}
```

// find the maximum auto- & cross- correlation value

```
float maxcorr(struct complex a[], struct complex b[], char c)
{
    int          i, j, k, Vreal, Vim, n_init, n_end;
    struct complex value;

    if(c == 'a')                // Auto-correlation
    {
        n_init = 1;
        n_end = 9;
    }
    else                        // Cross-correlation
    {
        n_init = -4;
        n_end = 4;
    }
}
```

```

float R[n_end-n_init+1];
k = 0;
for(i=n_init; i<=n_end; i++)
{
    R[k] = 0.0;
    Vreal = 0;
    Vim = 0;
    value.re = 0;
    value.im = 0;

    for(j=0; j<10; j++)
    {
        value = mult(a[j],b[(j+i+10)%10]);
        Vreal += value.re;
        Vim += value.im;
    }
    R[k++] = sqrt(Vreal*Vreal + Vim*Vim);
}
return largest(R,n_end-n_init+1);           // return max R
}

// print results
void print_code(struct complex a[], int n)
{
    int i;

    for(i=n-1; i>=0; i--)
    {
        if( (a[i].re == 0) && (a[i].im == 1) )
            printf(" j ");
        else if(a[i].re == 0)
            printf("-j ");
        else
            printf("%2d ",a[i].re);
    }
}

```

A3 TRLabs Codes (N = 10)

Maximum auto-correlation, $\max_{1 \leq i \leq M} \{R_{i,i}(1), R_{i,i}(2), \dots, R_{i,i}(N-1)\} = 2.8284$

Maximum cross-correlation, $\max_{1 \leq i \neq j \leq M} \{R_{i,j}(0), R_{i,j}(1), \dots, R_{i,j}(4)\} = 4.4721$

-j	-j	-j	-1	1	-1	-1	-j	-j	j
-j	-j	-j	-1	1	-1	-1	j	j	-j
-j	-j	-j	1	-1	1	1	-j	-j	j
-j	-j	-j	1	-1	1	1	j	j	-j
-j	-j	j	-1	1	1	1	-j	j	-j
-j	-j	j	-1	1	1	1	j	-j	j
-j	-j	j	1	-1	-1	-1	-j	j	-j
-j	-j	j	1	-1	-1	-1	j	-j	j

-j	-j	-1	-j	1	-j	j	-j	1	j
-j	-j	-1	-j	1	-j	j	j	-1	-j
-j	-j	-1	j	-1	j	-j	-j	1	j
-j	-j	-1	j	-1	j	-j	j	-1	-j
-j	-j	-1	-1	-j	j	1	-j	-j	1
-j	-j	-1	-1	-j	j	1	j	j	-1
-j	-j	-1	1	j	-j	-1	-j	-j	1
-j	-j	-1	1	j	-j	-1	j	j	-1

-j	-j	1	-j	-1	-j	j	-j	-1	j
-j	-j	1	-j	-1	-j	j	j	1	-j
-j	-j	1	j	1	j	-j	-j	-1	j
-j	-j	1	j	1	j	-j	j	1	-j
-j	-j	1	-1	j	-j	1	-j	-j	-1
-j	-j	1	-1	j	-j	1	j	j	1
-j	-j	1	1	-j	j	-1	-j	-j	-1
-j	-j	1	1	-j	j	-1	j	j	1

-j	j	-j	-1	-1	-1	1	-j	j	j
-j	j	-j	-1	-1	-1	1	j	-j	-j
-j	j	-j	1	1	1	-1	-j	j	j
-j	j	-j	1	1	1	-1	j	-j	-j
-j	j	j	-1	-1	1	-1	-j	-j	-j
-j	j	j	-1	-1	1	-1	j	j	j
-j	j	j	1	1	-1	1	-j	-j	-j
-j	j	j	1	1	-1	1	j	j	j

-j j -1	-j -1 -j -j	-j -1 j
-j j -1	-j -1 -j -j	j 1 -j
-j j -1	j 1 j j	-j -1 j
-j j -1	j 1 j j	j 1 -j
-j j -1	-1 j j -1	-j j 1
-j j -1	-1 j j -1	j -j -1
-j j -1	1 -j -j 1	-j j 1
-j j -1	1 -j -j 1	j -j -1

-j j 1	-j 1 -j -j	-j 1 j
-j j 1	-j 1 -j -j	j -1 -j
-j j 1	j -1 j j	-j 1 j
-j j 1	j -1 j j	j -1 -j
-j j 1	-1 -j -j -1	-j j -1
-j j 1	-1 -j -j -1	j -j 1
-j j 1	1 j j 1	-j j -1
-j j 1	1 j j 1	j -j 1

-j -1 j	-j -j 1 -j	-1 -j j
-j -1 j	-j -j 1 -j	-1 1 j
-j -1 j	-j -j 1 -j	1 j -j
-j -1 j	-j -j 1 -j	1 -1 -j
-j -1 j	-j j -1 j	-1 -j -j
-j -1 j	-j j -1 j	-1 -1 -j
-j -1 j	-j j -1 j	1 j j
-j -1 j	-j j -1 j	1 1 j

-j -1 j	j -j 1 -j	-1 -j -j
-j -1 j	j -j 1 -j	-1 -1 -j
-j -1 j	j -j 1 -j	1 j j
-j -1 j	j -j 1 -j	1 1 j
-j -1 j	j j -1 j	-1 -j j
-j -1 j	j j -1 j	-1 1 j
-j -1 j	j j -1 j	1 j -j
-j -1 j	j j -1 j	1 -1 -j

-j -1 -1	-j 1 -j j	-j 1 j
-j -1 -1	-j 1 -j j	j -1 -j
-j -1 -1	-j 1 -1 j	-j 1 1
-j -1 -1	-j 1 -1 j	j -1 -1
-j -1 -1	j -1 j -j	-j 1 j
-j -1 -1	j -1 j -j	j -1 -j
-j -1 -1	j -1 1 -j	-j 1 1
-j -1 -1	j -1 1 -j	j -1 -1

-j	-1	1	-j	1	-j	-j	-j	1	j
-j	-1	1	-j	1	-j	-j	j	-1	-j
-j	-1	1	-j	1	1	-j	-j	1	-1
-j	-1	1	-j	1	1	-j	j	-1	1
-j	-1	1	j	-1	j	j	-j	1	j
-j	-1	1	j	-1	j	j	j	-1	-j
-j	-1	1	j	-1	-1	j	-j	1	-1
-j	-1	1	j	-1	-1	j	j	-1	1

-j	1	j	-j	-j	-1	-j	-1	j	-j
-j	1	j	-j	-j	-1	-j	-1	1	-j
-j	1	j	-j	-j	-1	-j	1	-j	j
-j	1	j	-j	-j	-1	-j	1	-1	j
-j	1	j	-j	j	1	j	-1	j	j
-j	1	j	-j	j	1	j	-1	-1	j
-j	1	j	-j	j	1	j	1	-j	-j
-j	1	j	-j	j	1	j	1	1	-j

-j	1	j	j	-j	-1	-j	-1	j	j
-j	1	j	j	-j	-1	-j	-1	-1	j
-j	1	j	j	-j	-1	-j	1	-j	-j
-j	1	j	j	-j	-1	-j	1	1	-j
-j	1	j	j	j	1	j	-1	j	-j
-j	1	j	j	j	1	j	-1	1	-j
-j	1	j	j	j	1	j	1	-j	j
-j	1	j	j	j	1	j	1	-1	j

-j	1	-1	-j	-1	-j	-j	-j	-1	j
-j	1	-1	-j	-1	-j	-j	j	1	-j
-j	1	-1	-j	-1	-1	-j	-j	-1	1
-j	1	-1	-j	-1	-1	-j	j	1	-1
-j	1	-1	j	1	j	j	-j	-1	j
-j	1	-1	j	1	j	j	j	1	-j
-j	1	-1	j	1	1	j	-j	-1	1
-j	1	-1	j	1	1	j	j	1	-1

-j	1	1	-j	-1	-j	j	-j	-1	j
-j	1	1	-j	-1	-j	j	j	1	-j
-j	1	1	-j	-1	1	j	-j	-1	-1
-j	1	1	-j	-1	1	j	j	1	1
-j	1	1	j	1	j	-j	-j	-1	j
-j	1	1	j	1	j	-j	j	1	-j
-j	1	1	j	1	-1	-j	-j	-1	-1
-j	1	1	j	1	-1	-j	j	1	1

j-j-j	-1-1-1-1	-j-j-j
j-j-j	-1-1-1-1	j-j-j
j-j-j	1-1-1-1	-j-j-j
j-j-j	1-1-1-1	j-j-j

j-j-j	-1-1-1-1	-j-j-j
j-j-j	-1-1-1-1	j-j-j
j-j-j	1-1-1-1	-j-j-j
j-j-j	1-1-1-1	j-j-j

j-j-1	-j-1-j-j	-j-1-j
j-j-1	-j-1-j-j	j-1-j
j-j-1	j-1-j-j	-j-1-j
j-j-1	j-1-j-j	j-1-j
j-j-1	-1-j-j-1	-j-j-1
j-j-1	-1-j-j-1	j-j-1
j-j-1	1-j-j-1	-j-j-1
j-j-1	1-j-j-1	j-j-1

j-j-1	-j-1-j-j	-j-1-j
j-j-1	-j-1-j-j	j-1-j
j-j-1	j-1-j-j	-j-1-j
j-j-1	j-1-j-j	j-1-j
j-j-1	-1-j-j-1	-j-j-1
j-j-1	-1-j-j-1	j-j-1
j-j-1	1-j-j-1	-j-j-1
j-j-1	1-j-j-1	j-j-1

j-j-j	-1-1-1-1	-j-j-j
j-j-j	-1-1-1-1	j-j-j
j-j-j	1-1-1-1	-j-j-j
j-j-j	1-1-1-1	j-j-j

j-j-j	-1-1-1-1	-j-j-j
j-j-j	-1-1-1-1	j-j-j
j-j-j	1-1-1-1	-j-j-j
j-j-j	1-1-1-1	j-j-j

j-j-1	-j-1-j-j	-j-1-j
j-j-1	-j-1-j-j	j-1-j
j-j-1	j-1-j-j	-j-1-j
j-j-1	j-1-j-j	j-1-j
j-j-1	-1-j-j-1	-j-j-1
j-j-1	-1-j-j-1	j-j-1
j-j-1	1-j-j-1	-j-j-1
j-j-1	1-j-j-1	j-j-1

j	j	1	-j	1	-j	j	-j	1	j
j	j	1	-j	1	-j	j	j	-1	-j
j	j	1	j	-1	j	-j	-j	1	j
j	j	1	j	-1	j	-j	j	-1	-j
j	j	1	-1	-j	j	1	-j	-j	1
j	j	1	-1	-j	j	1	j	j	-1
j	j	1	1	j	-j	-1	-j	-j	1
j	j	1	1	j	-j	-1	j	j	-1

j	-1	-j	-j	-j	-1	-j	-1	j	-j
j	-1	-j	-j	-j	-1	-j	-1	1	-j
j	-1	-j	-j	-j	-1	-j	1	-j	j
j	-1	-j	-j	-j	-1	-j	1	-1	j
j	-1	-j	-j	j	1	j	-1	j	j
j	-1	-j	-j	j	1	j	-1	-1	j
j	-1	-j	-j	j	1	j	1	-j	-j
j	-1	-j	-j	j	1	j	1	1	-j

j	-1	-j	j	-j	-1	-j	-1	j	j
j	-1	-j	j	-j	-1	-j	-1	-1	j
j	-1	-j	j	-j	-1	-j	1	-j	-j
j	-1	-j	j	-j	-1	-j	1	1	-j
j	-1	-j	j	j	1	j	-1	j	-j
j	-1	-j	j	j	1	j	-1	1	-j
j	-1	-j	j	j	1	j	1	-j	j
j	-1	-j	j	j	1	j	1	-1	j

j	-1	-1	-j	-1	-j	j	-j	-1	j
j	-1	-1	-j	-1	-j	j	j	1	-j
j	-1	-1	-j	-1	1	j	-j	-1	-1
j	-1	-1	-j	-1	1	j	j	1	1
j	-1	-1	j	1	j	-j	-j	-1	j
j	-1	-1	j	1	j	-j	j	1	-j
j	-1	-1	j	1	-1	-j	-j	-1	-1
j	-1	-1	j	1	-1	-j	j	1	1

j	-1	1	-j	-1	-j	-j	-j	-1	j
j	-1	1	-j	-1	-j	-j	j	1	-j
j	-1	1	-j	-1	-1	-j	-j	-1	1
j	-1	1	-j	-1	-1	-j	j	1	-1
j	-1	1	j	1	j	j	-j	-1	j
j	-1	1	j	1	j	j	j	1	-j
j	-1	1	j	1	1	j	-j	-1	1
j	-1	1	j	1	1	j	j	1	-1

j	1-j	-j-j	1-j	-1-j	j	
j	1-j	-j-j	1-j	-1	1-j	
j	1-j	-j-j	1-j	1	j-j	
j	1-j	-j-j	1-j	1-1	-j	
j	1-j	-j	j-1	j	-1-j-j	
j	1-j	-j	j-1	j	-1-1-j	
j	1-j	-j	j-1	j	1-j-j	
j	1-j	-j	j-1	j	1	1-j

j	1-j	j-j	1-j	-1-j-j
j	1-j	j-j	1-j	-1-1-j
j	1-j	j-j	1-j	1 j j
j	1-j	j-j	1-j	1 1 j
j	1-j	j	j-1 j	-1-j j
j	1-j	j	j-1 j	-1 1 j
j	1-j	j	j-1 j	1 j-j
j	1-j	j	j-1 j	1-1-j

j	1-1	-j	1-j-j	-j	1-j			
j	1-1	-j	1-j-j	j	-1-j			
j	1-1	-j	1	1-j	-j	1-1		
j	1-1	-j	1	1-j	j	-1	1	
j	1-1	j	-1	j	j	-j	1	j
j	1-1	j	-1	j	j	j	-1	-j
j	1-1	j	-1	-1	j	-j	1	-1
j	1-1	j	-1	-1	j	j	-1	1

j	1	1	-j	1	-j	j	-j	1	j
j	1	1	-j	1	-j	j	j	-1	-j
j	1	1	-j	1	-1	j	-j	1	1
j	1	1	-j	1	-1	j	j	-1	-1
j	1	1	j	-1	j	-j	-j	1	j
j	1	1	j	-1	j	-j	j	-1	-j
j	1	1	j	-1	1	-j	-j	1	1
j	1	1	j	-1	1	-j	j	-1	-1

-1-j-j	-1-j-j	1	-1-j-j
-1-j-j	-1-j-j	1	1-j-j
-1-j-j	-1-j	-1-1	-1-j-1
-1-j-j	-1-j	-1-1	1-j-1
-1-j-j	1-j	j-1	-1-j-j
-1-j-j	1-j	j-1	1-j-j
-1-j-j	1-j	1-1	-1-j-1
-1-j-j	1-j	1-1	1-j-1

-1-j j	-1 j j-1	-1 j-j
-1-j j	-1 j j-1	1-j j
-1-j j	-1 j-1-1	-1 j 1
-1-j j	-1 j-1-1	1-j-1
-1-j j	1-j-j 1	-1 j-j
-1-j j	1-j-j 1	1-j j
-1-j j	1-j 1 1	-1 j 1
-1-j j	1-j 1 1	1-j-1

-1-j 1	-1-1 j-1	-j j 1
-1-j 1	-1-1 j-1	-j-1 1
-1-j 1	-1-1 j-1	j-j-1
-1-j 1	-1-1 j-1	j 1-1
-1-j 1	-1 1-j 1	-j-j-1
-1-j 1	-1 1-j 1	-j-1-1
-1-j 1	-1 1-j 1	j j 1
-1-j 1	-1 1-j 1	j 1 1

-1-j 1	1-1 j-1	-j-j-1
-1-j 1	1-1 j-1	-j-1-1
-1-j 1	1-1 j-1	j j 1
-1-j 1	1-1 j-1	j 1 1
-1-j 1	1 1-j 1	-j j 1
-1-j 1	1 1-j 1	-j-1 1
-1-j 1	1 1-j 1	j-j-1
-1-j 1	1 1-j 1	j 1-1

-1 j-j	-1-j-j-1	-1-j j
-1 j-j	-1-j-j-1	1 j-j
-1 j-j	-1-j-1-1	-1-j 1
-1 j-j	-1-j-1-1	1 j-1
-1 j-j	1 j j 1	-1-j j
-1 j-j	1 j j 1	1 j-j
-1 j-j	1 j 1 1	-1-j 1
-1 j-j	1 j 1 1	1 j-1

-1 j j	-1-j j 1	-1-j-j
-1 j j	-1-j j 1	1 j j
-1 j j	-1-j-1 1	-1-j 1
-1 j j	-1-j-1 1	1 j-1
-1 j j	1 j-j-1	-1-j-j
-1 j j	1 j-j-1	1 j j
-1 j j	1 j 1-1	-1-j 1
-1 j j	1 j 1-1	1 j-1

-1	j	1	-1	-1	-j	-1	-j	j	-1
-1	j	1	-1	-1	-j	-1	-j	1	-1
-1	j	1	-1	-1	-j	-1	j	-j	1
-1	j	1	-1	-1	-j	-1	j	-1	1
-1	j	1	-1	1	j	1	-j	-j	1
-1	j	1	-1	1	j	1	-j	1	1
-1	j	1	-1	1	j	1	j	j	-1
-1	j	1	-1	1	j	1	j	-1	-1

-1	j	1	1	-1	-j	-1	-j	-j	1
-1	j	1	1	-1	-j	-1	-j	1	1
-1	j	1	1	-1	-j	-1	j	j	-1
-1	j	1	1	-1	-j	-1	j	-1	-1
-1	j	1	1	1	j	1	-j	j	-1
-1	j	1	1	1	j	1	-j	1	-1
-1	j	1	1	1	j	1	j	-j	1
-1	j	1	1	1	j	1	j	-1	1

-1	-1	-j	-j	-1	1	j	-1	-1	j
-1	-1	-j	-j	-1	1	j	1	1	-j
-1	-1	-j	j	1	-1	-j	-1	-1	j
-1	-1	-j	j	1	-1	-j	1	1	-j
-1	-1	-j	-1	j	-1	1	-1	j	1
-1	-1	-j	-1	j	-1	1	1	-j	-1
-1	-1	-j	1	-j	1	-1	-1	j	1
-1	-1	-j	1	-j	1	-1	1	-j	-1

-1	-1	j	-j	1	-1	j	-1	-1	-j
-1	-1	j	-j	1	-1	j	1	1	j
-1	-1	j	j	-1	1	-j	-1	-1	-j
-1	-1	j	j	-1	1	-j	1	1	j
-1	-1	j	-1	-j	-1	1	-1	-j	1
-1	-1	j	-1	-j	-1	1	1	j	-1
-1	-1	j	1	j	1	-1	-1	-j	1
-1	-1	j	1	j	1	-1	1	j	-1

-1	-1	-1	-j	j	-j	-j	-1	-1	1
-1	-1	-1	-j	j	-j	-j	1	1	-1
-1	-1	-1	j	-j	j	j	-1	-1	1
-1	-1	-1	j	-j	j	j	1	1	-1

-1	-1	1	-j	j	j	j	-1	1	-1
-1	-1	1	-j	j	j	j	1	-1	1
-1	-1	1	j	-j	-j	-j	-1	1	-1
-1	-1	1	j	-j	-j	-j	1	-1	1

-1	1	-j	-j	1	1	-j	-1	1	j
-1	1	-j	-j	1	1	-j	1	-1	-j
-1	1	-j	j	-1	-1	j	-1	1	j
-1	1	-j	j	-1	-1	j	1	-1	-j
-1	1	-j	-1	-j	-1	-1	-1	-j	1
-1	1	-j	-1	-j	-1	-1	1	j	-1
-1	1	-j	1	j	1	1	-1	-j	1
-1	1	-j	1	j	1	1	1	j	-1

-1	1	j	-j	-1	-1	-j	-1	1	-j
-1	1	j	-j	-1	-1	-j	1	-1	j
-1	1	j	j	1	1	j	-1	1	-j
-1	1	j	j	1	1	j	1	-1	j
-1	1	j	-1	j	-1	-1	-1	j	1
-1	1	j	-1	j	-1	-1	1	-j	-1
-1	1	j	1	-j	1	1	-1	j	1
-1	1	j	1	-j	1	1	1	-j	-1

-1	1	-1	-j	-j	-j	j	-1	1	1
-1	1	-1	-j	-j	-j	j	1	-1	-1
-1	1	-1	j	j	j	-j	-1	1	1
-1	1	-1	j	j	j	-j	1	-1	-1

-1	1	1	-j	-j	j	-j	-1	-1	-1
-1	1	1	-j	-j	j	-j	1	1	1
-1	1	1	j	j	-j	j	-1	-1	-1
-1	1	1	j	j	-j	j	1	1	1

1	-j	-j	-1	-j	j	1	-1	-j	-j
1	-j	-j	-1	-j	j	1	1	j	j
1	-j	-j	-1	-j	-1	1	-1	-j	1
1	-j	-j	-1	-j	-1	1	1	j	-1
1	-j	-j	1	j	-j	-1	-1	-j	-j
1	-j	-j	1	j	-j	-1	1	j	j
1	-j	-j	1	j	1	-1	-1	-j	1
1	-j	-j	1	j	1	-1	1	j	-1

1	-j	j	-1	-j	-j	-1	-1	-j	j
1	-j	j	-1	-j	-j	-1	1	j	-j
1	-j	j	-1	-j	-1	-1	-1	-j	1
1	-j	j	-1	-j	-1	-1	1	j	-1
1	-j	j	1	j	j	1	-1	-j	j
1	-j	j	1	j	j	1	1	j	-j
1	-j	j	1	j	1	1	-1	-j	1
1	-j	j	1	j	1	1	1	j	-1

1-j-1	-1-1-j-1	-j j-1
1-j-1	-1-1-j-1	-j 1-1
1-j-1	-1-1-j-1	j-j 1
1-j-1	-1-1-j-1	j-1 1
1-j-1	-1 1 j 1	-j-j 1
1-j-1	-1 1 j 1	-j 1 1
1-j-1	-1 1 j 1	j j-1
1-j-1	-1 1 j 1	j-1-1
1-j-1	1-1-j-1	-j-j 1
1-j-1	1-1-j-1	-j 1 1
1-j-1	1-1-j-1	j j-1
1-j-1	1-1-j-1	j-1-1
1-j-1	1 1 j 1	-j j-1
1-j-1	1 1 j 1	-j 1-1
1-j-1	1 1 j 1	j-j 1
1-j-1	1 1 j 1	j-1 1

1 j-j	-1 j j-1	-1 j-j
1 j-j	-1 j j-1	1-j j
1 j-j	-1 j-1-1	-1 j 1
1 j-j	-1 j-1-1	1-j-1
1 j-j	1-j-j 1	-1 j-j
1 j-j	1-j-j 1	1-j j
1 j-j	1-j 1 1	-1 j 1
1 j-j	1-j 1 1	1-j-1

1 j j	-1 j-j 1	-1 j j
1 j j	-1 j-j 1	1-j-j
1 j j	-1 j-1 1	-1 j 1
1 j j	-1 j-1 1	1-j-1
1 j j	1-j j-1	-1 j j
1 j j	1-j j-1	1-j-j
1 j j	1-j 1-1	-1 j 1
1 j j	1-j 1-1	1-j-1

1 j-1	-1-1 j-1	-j j 1
1 j-1	-1-1 j-1	-j-1 1
1 j-1	-1-1 j-1	j-j-1
1 j-1	-1-1 j-1	j 1-1
1 j-1	-1 1-j 1	-j-j-1
1 j-1	-1 1-j 1	-j-1-1
1 j-1	-1 1-j 1	j j 1
1 j-1	-1 1-j 1	j 1 1
1 j-1	1-1 j-1	-j-j-1
1 j-1	1-1 j-1	-j-1-1
1 j-1	1-1 j-1	j j 1
1 j-1	1-1 j-1	j 1 1

1 j -1	1 1 -j 1	-j j 1
1 j -1	1 1 -j 1	-j -1 1
1 j -1	1 1 -j 1	j -j -1
1 j -1	1 1 -j 1	j 1 -1

1 -1 -j	-j -1 -1 -j	-1 1 -j
1 -1 -j	-j -1 -1 -j	1 -1 j
1 -1 -j	j 1 1 j	-1 1 -j
1 -1 -j	j 1 1 j	1 -1 j
1 -1 -j	-1 j -1 -1	-1 j 1
1 -1 -j	-1 j -1 -1	1 -j -1
1 -1 -j	1 -j 1 1	-1 j 1
1 -1 -j	1 -j 1 1	1 -j -1

1 -1 j	-j 1 1 -j	-1 1 j
1 -1 j	-j 1 1 -j	1 -1 -j
1 -1 j	j -1 -1 j	-1 1 j
1 -1 j	j -1 -1 j	1 -1 -j
1 -1 j	-1 -j -1 -1	-1 -j 1
1 -1 j	-1 -j -1 -1	1 j -1
1 -1 j	1 j 1 1	-1 -j 1
1 -1 j	1 j 1 1	1 j -1

1 -1 -1	-j -j j -j	-1 -1 -1
1 -1 -1	-j -j j -j	1 1 1
1 -1 -1	j j -j j	-1 -1 -1
1 -1 -1	j j -j j	1 1 1

1 -1 1	-j -j -j j	-1 1 1
1 -1 1	-j -j -j j	1 -1 -1
1 -1 1	j j j -j	-1 1 1
1 -1 1	j j j -j	1 -1 -1

1 1 -j	-j 1 -1 j	-1 -1 -j
1 1 -j	-j 1 -1 j	1 1 j
1 1 -j	j -1 1 -j	-1 -1 -j
1 1 -j	j -1 1 -j	1 1 j
1 1 -j	-1 -j -1 1	-1 -j 1
1 1 -j	-1 -j -1 1	1 j -1
1 1 -j	1 j 1 -1	-1 -j 1
1 1 -j	1 j 1 -1	1 j -1

1	1	j	-j	-1	1	j	-1	-1	j
1	1	j	-j	-1	1	j	1	1	-j
1	1	j	j	1	-1	-j	-1	-1	j
1	1	j	j	1	-1	-j	1	1	-j
1	1	j	-1	j	-1	1	-1	j	1
1	1	j	-1	j	-1	1	1	-j	-1
1	1	j	1	-j	1	-1	-1	j	1
1	1	j	1	-j	1	-1	1	-j	-1

1	1	-1	-j	j	j	j	-1	1	-1
1	1	-1	-j	j	j	j	1	-1	1
1	1	-1	j	-j	-j	-j	-1	1	-1
1	1	-1	j	-j	-j	-j	1	-1	1

1	1	1	-j	j	-j	-j	-1	-1	1
1	1	1	-j	j	-j	-j	1	1	-1
1	1	1	j	-j	j	j	-1	-1	1
1	1	1	j	-j	j	j	1	1	-1